Dual transcriptome analysis of *Toxoplasma gondii* infected mice leads to the investigation of Z-DNA binding protein-1 involvement during infection.

By

Kelly Pittman

A dissertation submitted in partial fulfillment of the requirements for the degree of
Doctor of Philosophy

Cellular and Molecular Biology

At the

University of Wisconsin-Madison
2015

Date of final oral examination: 8/26/15

The dissertation is approved by the following members of the Final Oral Committee:

Laura J. Knoll, Associate Professor, Medical Microbiology and Immunology

Christina M. Hull, Associate Professor, Bimolecular Chemistry

William M. Bement, Associate Professor, Cellular and Molecular Biology

Colin N. Dewey, Associate Professor, Biostatistics and Medical Informatics

Timothy P. Yoshino, Associate Professor, Pathobiological Sciences

Table of Contents

Appendix B

List of Tables and Figures

Chapter 1

Chapter 2

Chapter 3

Appendix A

Appendix B

Acknowledgements

There are so many people who have helped me get to where I am today. First off, I want to thank my parents. They taught me that all great things are worth working hard for and to never, never, never give up. My parents, somehow, put up with me through my rebellious teenage years, which lasted from age 15 to 25. I am grateful for every sacrifice they have made to help me achieve all of my goals.

I also want to thank my advisor Dr. Laura Knoll. She took a huge risk in taking me on. I was a third year graduate student who wanted a complete change in my field of research. I have grown so much as a scientist because of this and I will forever be thankful for her. She has not only mentored me as a scientist, she has also been a great "science mom" to me (Laura is only 3 years younger than my mother). Anytime I have had an issue with my apartment or timing of a lease, Laura has offered her basement or cabin for me to stay in without hesitation. Though I have never taken her up on this, the fact that she cares so much for my well-being means a great deal to me. I also want to extend a huge thank you to all the past and present members of the Knoll lab. Christine Hsiao, Erik Settles, Lindsey Moser, Kyle Bolden, Amanda (Ocho) Payne, Lori Neal, Crystal Tobin, Emily Wilson, Sarah Wilson, and Will Olson have all influenced me in many ways over the years and have helped keep me sane.

Lastly, I want to thank my best friend and soon to be husband, Nate. He is the best thing that has ever happened to me. He has stuck with me through all my science highs and lows and has encouraged me to keep going. I would not be here without his love and support. Oh, and I can't forget to thank my dog Gus. His adorable face and wagging, whip like tail that greets me after a long day of work melts my heart every single day.

Dissertation Abstract

Dual transcriptome analysis of *Toxoplasma gondii* infected mice leads to the investigation of Z-DNA binding protein-1 involvement during infection.

Kelly Pittman

Under the supervision of Associate Professor Dr. Laura J. Knoll

At the University of Wisconsin-Madison

T. gondii is one of the most successful parasites in the world with approximately 30 percent of the population infected. The abundance of this parasitic infection is due to the ability of *T. gondii* to remain infectious in all life stages. During acute infection, the asexual tachyzoite rapidly disseminates throughout the host through invasion of migratory immune cells such as macrophages and dendritic cells. Once *T. gondii* invades these cells, the parasite manipulates their function to gain access to immunoprivileged areas of the body, like the brain. Pressure from the immune system, along with other unknown factors, triggers tachyzoite differentiation into the slower growing, encysted bradyzoite form. The bradyzoite persists for the lifetime of the host as intracellular cysts present in striated muscle and the central nervous system.

T. gondii has developed a multitude of strategies to evade the host immune response. One pathway of particular interest to our laboratory is the ability of *T. gondii* to block parasite degradation by nitric oxide (NO) production in activated macrophages. In this thesis an RNAseq approach was used to study both host and parasite interactions during acute and chronic *T. gondii*

infection. The goal of this analysis was to elucidate *T. gondii* specific elements that contribute to establishment and maintenance of a life-long infection as well as identify host factors that aid in parasite survival. From this dataset, the host specific gene Z-DNA binding protein-1 (*ZBP1)* was highly expressed in the forebrains of mice during acute and chronic infection. ZBP1 was initially identified as a product of IFN-γ stimulation in activated macrophages, but the function has yet to be elucidated. In recent studies we have identified ZBP1 as a new host target that *T. gondii* down regulates during infection. We have described a novel role for ZBP1 in the degradation of *T. gondii* through nitric oxide production in activated macrophages. We have also determined absence of ZBP1 in activated macrophages leads to a defect in parasite degradation. In the future, we will determine whether ZBP1 is involved in regulation of iNOS on the protein level. We will also focus on elucidating the interaction between ZBP1 and production of nitric oxide in activated macrophages as well as determining the contributions of ZBP1 during chronic infection.

Chapter 1

Introduction

Long-term relationships: The complicated interplay between the host and the developmental stages of *Toxoplasma gondii* during acute and chronic infection

Kelly J. Pittman and Laura J. Knoll

Department of Medical Microbiology and Immunology, University of Wisconsin - Madison, 1550 Linden Drive, Madison, WI 53706

This chapter was accepted for publication in Microbiology and Molecular Biology Reviews (MMBR) on July 26th, 2015.

Summary

Toxoplasma gondii is one of the most common parasitic infections in the world. The asexual cycle can occur within any warm-blooded animal, but the sexual cycle is restricted to the feline intestinal epithelium. *T. gondii* is acquired through consumption of tissue cysts in undercooked meat and food and water contaminated with oocysts. Once ingested, it differentiates into a rapidly replicating asexual form and disseminates throughout the body during acute infection. After stimulation of the host immune response, *T. gondii* differentiates into a slow growing, asexual cyst form that is the hallmark of chronic infection. One-third of the human

population is chronically infected with *T. gondii* cysts, which can reactivate and are especially dangerous to individuals with reduced immune surveillance. Serious complications can also occur in healthy individuals if infected with certain *T. gondii* strains or if infection is acquired congenitally. No drugs are available to clear the cyst form during the chronic stages of infection. This therapeutic gap is due in part to an incomplete understanding of both host and pathogen responses during the progression of *T. gondii* infection. While many individual aspects of *T. gondii* infection are well understood, viewing the interconnections between host and parasite during acute and chronic infection may lead to better approaches for future treatment. The aim of this review is to provide an overview of what is known and unknown about the complex relationship between the host and parasite during the progression of *T. gondii* infection, with the ultimate goal of bridging these events.

Introduction

Toxoplasma gondii is an obligate intracellular parasite that has been shown to infect a wide variety of warm-blooded animals (1). While the asexual cycle can likely occur in any warm-blooded host, the *T. gondii* sexual cycle only occurs in feline intestinal epithelial cells (2). Within intermediate hosts two distinct asexual forms of *T. gondii* exist. During acute infection the rapidly diving tachyzoite disseminates throughout the host until pressure from the immune system, and other unknown factors, trigger differentiation to the slower growing encysted bradyzoite. Formation of cysts containing bradyzoites occurs within cells of the central nervous system and striated muscle (3). Bradyzoite cysts can persist for the lifetime of the host and are infectious if consumed. *T. gondii* infection is typically asymptomatic, but does present issues in the immune compromised and unborn fetuses when acquired congenitally. In humans, ingestion

of undercooked meat containing bradyzoite cysts is considered the primary route of exposure to *T. gondii* (4, 5), but antibodies have been detected against oocyst stages, which suggests oocyst contamination of food and water is also a major source of infection (4, 6).

Prevalence and Disease

T. gondii is one of the most successful parasites worldwide, with upwards of 30% of the human population infected. *T. gondii* infection is usually asymptomatic in healthy individuals. Prevalence rates among humans vary greatly from country to country and range from 5-80% (7). This variation is based on differences in cultural practices as well as environmental conditions that favor stability of oocysts in soil and water. Although prevalence rates in the United States are significantly lower than most European countries (7), *T. gondii* is considered the second leading cause of foodborne related deaths in the United States (8). The high occurrence of *T. gondii* infection worldwide is attributed to its ability to be infectious in its sexual and asexual forms, establish a chronic infection in any warm-blooded animal, and remain infectious for the lifetime of that host. While *T. gondii* infection in immunocompetent individuals is usually asymptomatic, flu-like symptoms can occur. If passed from mother to fetus more extreme outcomes may occur, such as hydrocephaly and death (9-12). Infection with *T. gondii* is more detrimental in immune compromised individuals, such as those with HIV, patients receiving organ transplants or undergoing cancer treatment, developing fetuses, and the elderly (13-17). In these individuals, either primary infection with *T. gondii* or reactivation of latent bradyzoite cysts cannot be controlled, resulting in encephalitis and pulmonary toxoplasmosis.

Sexual Cycle

The sexual cycle of *T. gondii* is restricted to the feline intestine. First, the ingested bradyzoites or oocysts are released by pepsin and acid digestion in the stomach. Bradyzoites or sporozoites then invade the feline intestinal epithelium and differentiate into five morphologically distinct asexual types of schizonts, designated A through E (18) (Figure 1). Within two days in the feline intestine, *T. gondii* progresses through all five stages of schizonts and develops into merozoites, the first sexual stage. Merozoites undergo a limited proliferation of two to four doublings before they differentiate into macrogametes and microgametes. The macro- and microgametes fuse to produce diploid oocysts, which develop thick impermeable walls and are shed in the feces (Figure 1). Cats excrete between 2-20 million oocysts per day in their feces and shed 3-10 days post-infection. In ambient air and temperature, oocysts sporulate by undergoing mitosis and meiosis until they produce eight haploid sporozoites encased within the oocyst wall. *T. gondii* oocysts are stable for over a year in a variety of environmental conditions and are most stable when stored in 2% sulfuric acid (19, 20).

Many details about sexual development of *T. gondii* remain unanswered, including how such distinct host specificity developed. Knowledge of the sexual cycle has largely come from electron microscopic examination of infected feline intestinal cells. The lack of a tissue culture model for studying the sexual development of *T. gondii* has caused a dearth in molecular analysis of the parasite. Recently the application of RNA sequencing technology (RNAseq) of infected feline tissue has allowed the first transcriptome analysis of the sexual stages (21). Further RNAseq of infected feline epithelial cells as well as the development of a stable feline intestinal epithelial cell line will be necessary to address the many questions surrounding *T. gondii* sexual development.

Asexual Cycle

The ability of *T. gondii* to establish bradyzoite cysts that persist for the lifetime of the host while maintaining infectivity if consumed is likely a major factor in the global success of this parasite. This development allows the parasite to circumvent the sexual cycle and still be transmittable to another host upon ingestion. Within intermediate hosts infected with oocysts, excysted sporozoites are detectable in epithelial cells of the small intestines within 2 hours post-inoculation (22). By 12 hours post inoculation, sporozoites have differentiated into tachyzoites in the intestinal epithelium, and by 48 hours rapid replication has occurred (23). Consumption of encysted bradyzoites in infected tissue is another leading cause of infection (Figure 2). When mice are inoculated with bradyzoites, parasites disseminate faster compared to mice fed oocysts (24). One hour post inoculation bradyzoites are detected in the intestinal epithelium and differentiation into tachyzoites occurs within 2 hours (24). By 48 hours tachyzoites are detected in the lymph nodes. Once tachyzoites infect migratory cells, such as macrophages and dendritic cells (DCs), they can rapidly disseminate throughout the host (25). Eventually pressure from the immune system and other unknown factors induce conversion to the bradyzoite, the asexual stage associated with chronic infection. Cysts containing bradyzoites can persist for decades within striated muscle and tissue of the central nervous system (3). The sexual cycle of *T. gondii* is perpetuated when uninfected felids consume chronically infected intermediate hosts.

Tissue Culture Bradyzoite Development

The development of tissue culture conditions that mimic bradyzoite formation in animals has greatly aided analyses of the asexual cycle. The transition from the rapidly replicating tachyzoite to the slow growing bradyzoite is a stress response to immunological, metabolic, and

chemical exposure. During such stresses, the growth of the parasite slows, bradyzoite-specific markers are expressed, and a cyst wall is formed. Many exogenous stresses independent of the host immune system contribute to tachyzoite to bradyzoite differentiation. Bradyzoite differentiation can be chemically induced in vitro through exposure to high pH (8.0-8.2), addition of sodium arsenite to culture media, or shifting to higher temperatures (37°C shifted to 43°C) (26). These tissue culture conditions for bradyzoite development have greatly advanced the molecular analysis of the bradyzoite stage.

Acute *T. gondii* infection

Virulence in Mice Associate with Different Strain Types

Many factors influence severity of infection including environmental, host genetics, strain of *T. gondii*, stage of the parasite during inoculation and route of infection. While divergent strains of *T. gondii* do exist, the predominant strains in Europe and North America are classified as types I, II and III (27-29). *T. gondii* strains from South America have been found to lack a clonal population structure and can be clustered into haplogroups 4 to 15 (30-33). Phenotypically the lineages vary in virulence, growth rate, and cyst burdens in the host. Lineages are classified as type I, known for its high virulence in mice, type II, responsible for the majority of human infections in Europe and North America, and type III, an avirulent lineage uncommon in humans (34, 35). While infection in immunocompetent individuals is usually asymptomatic, recent epidemiological studies of *T. gondii* outbreaks in different regions have identified outlier strains to the traditional classification (36). These “atypical” strains can cause severe symptoms including fever, headaches, vomiting, and malaise in healthy individuals (29). There are instances of ocular toxoplasmosis associated with type-I strains, or atypical strains having

similarities to type-I parasites, which account for a large proportion of retinal infections leading to blindness in otherwise healthy people (27, 28). It is important to note that not all atypical strains cause more severe disease in immune competent people, but instead that more severe disease is associated with atypical strains.

Establishment of acute infection via oral transmission

The most common routes of *T. gondii* infection are ingestion of sporulated oocysts, the products of sexual development, or ingestion of bradyzoites, the encysted asexual form (Figure 2A). After digestion of the oocyst or tissue cyst wall, the parasites are released into the lumen of the small intestine. Sporozoites or bradyzoites invade the enterocytes in the small intestine where they differentiate to the tachyzoites, rapidly replicate and by 48 hours post infection, tachyzoites can be seen in the majority of cell types within the lamina propria (37) (Figure 2B-E). The host immune response to *T. gondii* begins as soon as sporozoites or bradyzoites invade enterocytes. Multitudes of chemokines are secreted by infected enterocytes, resulting in the recruitment of a variety of leukocytes in response to parasitic infection (38-41). These chemokines are essential for the recruitment of leukocytes to the lamina propria (42, 43). Once *T. gondii* reaches the lamina propria, the parasites encounter both resident and recruited immune cells that aid in parasite clearance, cytokine production, and antigen presentation (44) (Figure 2F-G).

An interesting interplay occurs between *T. gondii* and intestinal bacteria during oral infection. The gut commensal bacteria act as molecular adjuvants to provide protective immunostimulation against *T. gondii* (45). In contrast, *T. gondii* infection results in elimination of Paneth cells, which are the main generators of antimicrobial peptides in the intestine, leading to a microbial imbalance in the intestine (46). Further investigations of the gut microbiome,

including bacteria, fungi, viruses and other parasites, will help elucidate how *T. gondii* establishes intestinal infection.

Key cytokines during *T. gondii* infection

Interleukin 12

Interleukin-12 (IL-12) has a variety of affects on cells during innate immunity including production of interferon-gamma (IFN-γ), cell mediated cytotoxicity, cell proliferation and differentiation (47-49). Production of IL-12 is critical during the first few days post-*T. gondii* infection, as mice supplemented with exogenous IL-12 show enhanced survival to lethal doses of parasites and decreased survival when treated with antibodies blocking IL-12 (50, 51). Production of IL-12 is dependent on the recruitment of the proper circulating immune cells. Upon *T. gondii* infection, epithelial cells and resident immune cells secrete potent chemokines such as monocyte chemotactic protein-1 (MCP-1/CCL2) and macrophage inflammatory protein-2 (MIP-2/CXCL8), which attract circulating immune cells to the site of infection (52-54) (Figure 3A). Neutrophils and inflammatory monocytes are among the first detectable cells that translocate to the lumen of the small intestine of infected mice (55-57). At the site of infection, inflammatory monocytes may differentiate into macrophages or dendritic cells (DCs) (58) (Figure 3B). These recruited cells aid in parasite clearance by phagocytosis, recruitment and stimulation of other immune cells, and antigen presentation (56, 59-64). The ability of cells to produce IL-12 during *T. gondii* infection is dependent on activation of the adaptor molecule myeloid differentiation factor 88 (MyD88) (65). MyD88 is recruited to Toll-like Receptors (TLRs) in response to pathogen specific molecule binding to multiple host TLRs (66, 67). Mice lacking MyD88 are unable to produce IL-12 and thus cannot control acute *T. gondii* infection

(65). The importance of TLRs/MyD88 during innate immunity have been extensively reviewed elsewhere (68).

Many cell types produce IL-12 after exposure to *T. gondii* in vitro, but elucidating the essential producers in vivo is challenging. Studies using Batf$^{-/-}$ mice, which lack CD8α^{+} DCs, have shown an essential role for these cells in the production of IL-12. Batf$^{-/-}$ mice rapidly succumb to sub-lethal doses of *T. gondii* and display decreased levels of both IL-12 and IFN-γ (69). Survival of Batf$^{-/-}$ mice infected with *T. gondii* was restored after administration of exogenous IL-12. Studies affecting the recruitment of inflammatory monocytes to the site of infection using both CCR2 and MCP-1 knockout mice and antibody neutralization of inflammatory monocytes revealed an essential role for these cells in surviving acute *T. gondii* infection (53, 70). However, mice lacking normal levels of monocytes still produce high levels of IL-12 and IFN-γ (53, 70). This result suggests that while the role of inflammatory monocytes in immunity against *T. gondii* is critical, they are not associated with induction of the Th1 cytokine response. Neutrophils are another important cell type, but whether they are essential sources of IL-12 remains controversial. Mice depleted of neutrophils produce statistically lower levels of IL-12, but do not succumb to *T. gondii* infection at an accelerated rate (70). Other studies have shown that neutrophil depletion leads to premature death and increased pathology after *T. gondii* infection (59, 71). These differences are likely due to the antibodies used for depletion. RB6-8C5 depletes both Ly6C^{hi} inflammatory monocytes and Ly6C^{int} Ly6G^{+} neutrophils (59, 71), and the anti-Ly6G antibody 1A8 depletes neutrophils only (70). Regardless, neutrophils are a major source of IL-12 during *T. gondii* infection.

IL-12 is also critical in the maintenance of a persistent chronic *T. gondii* infection. While IL-12 knockout mice die during acute *T. gondii* infection, they can be rescued if exogenous IL-

12 is administered (72). If these mice stop receiving exogenous IL-12 after the establishment of chronic *T. gondii* infection, they display higher cyst burdens and succumb to Toxoplasmic Encephalitis (TE) (72). These results suggest an important role for IL-12 in the control of latent *T. gondii* infections. The necessity for IL-12 during chronic infection is associated with its role in maintaining production of IFN-γ (72). Without continued production of IFN-γ during chronic infection reactivation of bradyzoites cysts cannot be controlled in the brain (73).

Interferon gamma

IL-12 and IFN-γ are essential for the Th1 cell mediated immunity response that controls progression of *T. gondii* infection. Much like loss of IL-12, mice lacking the IFN-γ gene or the receptor, as well as mice treated with an antibody against IFN-γ, rapidly succumb to *T. gondii* infection (74-76). T cells, NK cells and potentially neutrophils are important initial producers of IFN-γ during acute *T. gondii* infection (77-79) (Figure 3C). IL-12 is critical for triggering production of IFN-γ in NK cells, as animals treated with anti-IL-12 antibodies after exposure to tachyzoites display severely decreased IFN-γ production (77).

The importance of IFN-γ is linked to its downstream effects, primarily through the stimulation of hundreds of genes in mice (80). These genes initiate a multitude of host responses necessary for control of the parasite including immune cell proliferation, differentiation, and destruction of infected cells. Both hemopoietic and nonhemopoietic cells serve important roles during IFN-γ dependent host immunity to *T. gondii* infection (81). Guanylate-binding proteins (GBPs) and immunity related GTPases (IRGs) are two major families of GTPases expressed in response to IFN-γ stimulation (82, 83). They are expressed in most cell types and aid in control of parasite replication by localizing to the parasitophorous vacuole (84, 85) (Figure 4A). At the

parasitophorous vacuole, IRGs disrupt the integrity of the membrane and cause release of the parasites into the host cell cytoplasm where they are destroyed (86). While there are 23 different IRG genes in rodents, there are only two IRG genes present in humans (87). GBPs are expressed in a wide host range and in response to *T. gondii* induced IFN-γ, they localize to the parasitophorous vacuole (88, 89). GBPs help control parasite burden, but the exact mechanism of action is not understood. IFN-γ also controls parasite replication by cell mediated nutrient starvation. *T. gondii* is an obligate intracellular parasite and relies on the host cell for multiple resources it is unable to synthesize, such as tryptophan. IFN-γ induces indoleamine 2,3-dioxygenase production, which converts tryptophan into an unusable form for the parasite and is able to limit its growth (90, 91).

In macrophages, a major function of IFN-γ during *T. gondii* infection is the production of reactive oxygen species (ROS) and reactive nitrogen species (RNS), which have potent antimicrobial activity (92). Nitric oxide (NO) is a well studied RNS that is synthesized by inducible nitric oxide synthase (iNOS) in activated macrophages using L-arginine as the substrate (93) (Figure 4B). During infection, L-arginine is rapidly consumed to provide abundant levels of intracellular NO to combat parasite growth. A balance of NO needs to be maintained, as too much NO can cause massive host cell destruction and even death. As a way to regulate the level of NO synthesis in the host IL-4 and IL-13 trigger production of arginase-1 which degrades L-arginine thus making it unavailable for NO production (94). Reactive oxygen species have independent antimicrobial functions to RNS, but can also act synergistically to create toxic intermediates to intracellular *T. gondii* (95, 96). Over time a robust immune response to combat *T. gondii* leads to a decrease in intracellular parasite replication and eventual differentiation to the bradyzoite form, the hallmark of chronic infection.

IFN-γ is not only critical for clearance of tachyzoites during acute infection, but affects the development of TE caused by reactivation of bradyzoites during chronic infection. Mice treated with antibodies to IFN-γ show reactivation and development of TE (73). IL-6 may be a leading contributor to IFN-γ production during chronic infection as IL-6 is significantly up-regulated in the brains of mice during onset of TE (97). IL-6 deficient mice infected with *T. gondii* have increased incidences of TE, more severe tissue damage in the brain, higher cyst burdens, and decreased levels of IFN-γ (98). In humans, uncontrolled IL-6 production contributes to the development of various autoimmune diseases. Treatment of such autoimmune diseases now includes tocilizumab, an antibody that blocks IL-6 production. Given the high seroprevalence rates in humans, whether or not tocilizumab treatment can predispose *T. gondii* positive patients to adverse reactivation is an important future clinical question.

It is unclear which cell types are important sources of IFN-γ during chronic infection, but data suggests NK cells are critical because high transcript abundance of players in the cytotoxic NK cell pathway are present during chronic infection in the forebrains of mice (99). IFN-γ production by T cells is critical to control of chronic infection, as depletion of both $CD4^+$ and $CD8^+$ T cells results in reactivation of latent cysts (100). As molecular analysis of *T. gondii* advances, a theme has emerged demonstrating the continuation of acute infection immune responses to maintain latent chronic infection.

Tumor Necrosis Factor Alpha

TNF-α was originally identified as a cytokine essential to macrophage targeted cytotoxicity of tumor cells (101). TNF-α alone has no effect on growth of *T. gondii* in macrophages that have not been previously primed (102). Once macrophages have been activated by IFN-γ and then exposed to TNF-α they experience enhanced antimicrobial affects

including inhibition of intracellular *T. gondii* growth (103). TNF-α decreases intracellular levels of *T. gondii* in primed macrophages by inducing lysosomal fusion of the parasitophorous vacuole and subsequent degradation (104). Macrophages treated 24 hours prior to *T. gondii* infection with recombinant IFN-γ and an antibody against TNF-α displayed higher rates of *T. gondii* growth compared to macrophages treated with IFN-γ alone (105). This suggests that, upon exposure to IFN-γ, macrophages produce TNF-α to enhance the antimicrobial effects of the cell population.

TNF-α generally acts as a co-stimulatory molecule. In NK cells, TNF-α serves an important role in production of IFN-γ. While NK cells exposed to tachyzoites, parasite extracts, or TNF-α alone are unable to produce IFN-γ, parasite antigens and TNF-α together cause NK cells to secrete IFN-γ (106). Another example of TNF-α co-stimulation can be found during the generation of reactive nitrogen intermediates in macrophages (107). Treatment of macrophages with anti-TNF-α antibodies drastically reduces production of reactive nitrogen intermediates after recombinant IFN-γ stimulation (105). Treatment of macrophages with TNF-α alone does not have any inhibitory effects on *T. gondii* proliferation or clearance, suggesting it is dependent on co-stimulation.

TNF-α has an important, but nonessential role during acute infection, as mice lacking the receptors that recognize TNF-α do not die during early stages of *T. gondii* infection (108). Interestingly, three to four weeks post infection these mice prematurely die of encephalitis and have higher cyst burdens, which signifies that TNF-α plays an essential role during later stages of infection (108). The role for the cytokine throughout infection demonstrates the complex nature of immune signaling during *T. gondii* infection. The necessity for a co-stimulatory signal

is thought to contribute to specificity of the host response to extracellular targets versus intracellular targets, such as tumorigenic cells.

Interleukin-10

Host cell mechanisms to dampen the immune response are just as essential to host survival as triggering the initial response to infection. While rapid response to infection is crucial for survival of the host, an overabundant response can be detrimental. During lethal challenge with *T. gondii*, mice do not succumb due to parasitemia, but from tissue damage associated with an excessive antimicrobial response. IL-10 is a critical cytokine necessary to prevent tissue damage associated with a robust Th1 cytokine response. IL-10 is able to prevent IL-12 production, and thus decreases the amount of IFN-γ produced by lymphocytes (51, 109). In mice deficient in IL-10, high levels of IL-12 and IFN-γ are found in serum as compared to wild type mice, while parasitemia is similar or lower (110). Mice lacking IL-10 die during acute infection, not from *T. gondii* itself, but from tissue damage associated with an over production of cytokines (110). IL-10 knockout mice can survive to chronic infection if treated with sulfadiazine (111), but when sulfadiazine treatment is stopped, IL-10 knockout mice eventually succumb to chronic infection (111). These data demonstrate the essential role of IL-10 during acute and chronic infection.

IL-4 and IL-13 serve a similar role as IL-10, but instead of controlling IFN-γ they regulate NO production. As previously stated, too much NO can cause detrimental host cell destruction. As a way to balance the level of NO synthesis in the host, IL-4 and IL-13 trigger production of arginase-1 that degrades L-arginine, the substrate for NO synthesis, making it

unavailable for NO production (94). These examples highlight the delicate balance necessary to maintain host survival during infection.

T. gondii manipulation of host response

NF-κB response

T. gondii has developed a multitude of strategies to evade the host immune response. One pathway *T. gondii* interferes with is the MyD88 dependent production of IL-12 and subsequent expression of IFN-γ. The downstream effector of the MyD88 pathway that triggers IL-12 transcription is NF-κB. NF-κB must translocate from the cytoplasm to the nucleus upon TLR stimulation to initiate transcription of IL-12. Type I and III strains of *T. gondii* have developed the ability to block the translocation of NF-κB to the nucleus upon TLR recognition of parasite antigens (112-114). Type II strains have an opposite effect on NF-κB and promote expression and translocation to the nucleus via secretion of GRA15 (115). The promotion of pro-inflammatory signal would seem detrimental to the parasite, but stimulation of this mechanism may be adapted by the parasite to ensure survival of the host, establishment of a stable chronic infection and subsequent persistence of the parasite.

NO production

Another interesting example of *T. gondii* modulation of host cell responses lies in the ability of *T. gondii* to block degradation in activated macrophages (112, 116). At least part of this block is due to the ability of *T. gondii* to suppress NO production by limiting the availability of intracellular arginine (116-118). Type I strain parasites initiate arginine starvation by secreting ROP16, a kinase that activates STAT6 resulting in expression of host arginase-1(116). As

discussed previously, arginase-1 degrades available host cell arginine thus limiting the availability for NO (92). A decrease in NO synthesis would appear to be beneficial to the parasite, but *T. gondii* is an arginine auxotroph and exhibits decreased growth in media lacking arginine (116). This is another example of *T. gondii* triggering a response that leads to reduction in parasite growth for the purpose of long-term survival of the parasite within the host.

A library of insertional mutants was screened to identify parasites that were unable to suppress NO production from activated macrophages (119). A patatin-like phospholipase (TgPL1) was identified as essential to block NO production and subsequent parasite degradation in activated macrophages. TgPL1 changes localization from punctate vesicles within the parasite to the parasitophorous vacuole membrane during the stress of macrophage activation and bradyzoite development (119-121). While NO plays a role during acute infection, it is most important during chronic infection, as iNOS knockout mice succumb to *T. gondii* in the early stages of chronic infection (20-25 days) (122). C57BL/6 mice, which are susceptible to TE during chronic infection, have a decreased cytokine response by 8 weeks post-infection in response to wild type parasites. It is likely that this reduction in the pro-inflammatory response is the cause of reactivation and subsequent development of TE, as parasites lacking TgPL1 maintain high cytokine levels and do not display TE symptoms (121). The exact mechanism of how TgPL1 is modulating the cytokine response is currently unknown. TgPL1 does not have phospholipase activity with any of the substrates examined so far, likely because it is missing the critical active site serine seen in all other patatins (119-121). We hypothesize that TgPL1 is interacting with a host cell protein at the parasitophorous vacuole membrane to down regulate the immune response, as seen by both NO and cytokine production.

Inhibition of pro-inflammatory responses

As discussed previously, an over abundant Th1 cytokine response can cause detrimental host tissue damage, thus harming the host more than the pathogen itself. Because of this, the host will naturally produce anti-inflammatory molecules to lessen the affects of the initial response. To take advantage of this system, *T. gondii* has developed a strategy to manipulate these responses in order to decrease targeted destruction of the parasite as well increase host survival. *T. gondii* invasion of macrophages leads to the induction of suppressor of cytokine signaling protein 1 (SOCS1), a potent inhibitor of IFN-γ signaling, which aids the parasite in suppressing antimicrobial actions associated with the IFN-γ response (123). Another example of parasite driven modulation of host cell factors to restrict the Th1 response lies in the production of lipoxin A_4 (LXA_4). LXA_4 is an eicosanoid mediator that modulates anti-inflammatory processes through the down-regulation of IL-12 production by DCs (124). Mice infected with *T. gondii* have high levels of LXA_4 in their serum, although it has not been determined if this response is induced by *T. gondii* factors or is part of the progression the host anti-inflammatory response (125). *T. gondii* has evolved to decrease rapid replication and host cell damage in order to preserve the host's life and allow for future transmission. Collectively these data demonstrate the complexity of the interactions between host and pathogen during infection with *T. gondii*.

Chronic *T. gondii* infection

Establishment of Chronic Infection

After oral ingestion of *T. gondii,* parasites can be found in mesenteric lymph nodes as early as 18 hours post inoculation and circulating in the blood by 24 hours (126). The rapid dissemination of *T. gondii* throughout the body is credited to the ability of the parasite to actively migrate across epithelial barriers as well as invade migratory cells, such as DCs and

macrophages, and influence their migratory behavior (127-131) (Figure 5A). These observations are thought to be the mechanisms responsible for the ability of *T. gondii* to cross immunoprivileged biological barriers such as the blood-brain barrier, referred to as the Trojan Horse mechanism (132) (Figure 5B). Once *T. gondii* penetrates the blood-brain barrier tachyzoites invade resident brain cells and differentiate to bradyzoites (Figure 5C). It is understood that the tachyzoite to bradyzoite conversion is a stress-mediated response that corresponds to a slowing of growth of the parasite. As mentioned, bradyzoite differentiation can be mimicked in tissue culture by various stresses, but how development occurs in animals is still not well characterized.

Cell mediated immunity

Initiation of the adaptive immune response is key to triggering conversion to the bradyzoite form. Adaptive immunity relies heavily on antigen presenting cells (APCs), such as DCs, through their activation of T and B cells in secondary lymphoid organs. Although *T. gondii* activates a strong antibody response, cell mediated responses play the lead role in protective immunity (133-135). Activation of T and B cells requires both the migration of APCs from the site of infection to secondary lymphoid organs and the activation of resident APCs through exposure of *T. gondii* antigens. Once activated, B cells can act as APCs to stimulate $CD4^+$ T cells as well as secrete cytokines such as IL-12 and IFN-γ (136, 137). Activation of T cells drives immunity to *T. gondii* and can confer resistance to naive hosts when adoptively transferred (138). $CD4^+$ and $CD8^+$ T cells play a critical role during late infection and act synergistically to prevent reactivation of bradyzoite cysts in hosts (100). Once bradyzoite cysts have formed in the brain,

immunocompetent hosts have prolonged basal levels of cerebral inflammation, which is thought to be necessary for the control of chronic infection (139, 140).

Pioneering studies of chronic infection in mice used full genome microarrays to examine the host response up to 12 months post-infection, simulating middle to early elderly ages in humans (141). More recent studies have used RNAseq analysis to identify host and pathogen responses that may be important in the establishment and maintenance of chronic infection (99, 142). Using transcriptomic and proteomic analyses to address host and pathogen interplay at distinct time points may be the best way to further elucidate the many unknown factors that contribute to persistence of *T. gondii* infection. It is apparent that a delicate balance between pro- and anti-inflammatory signals must be involved, as mice rapidly succumb to chronic infection if either IFN-γ or IL-10 is blocked at later stages of infection (73, 143). The current gaps in knowledge of key host and pathogen contributors to maintenance of infection contribute to the lack of treatments available for chronic *T. gondii* infection.

Molecular analysis of bradyzoites

Most of what is currently known about bradyzoites has been done in tissue culture under stress conditions to induce differentiation. Morphologically bradyzoites look almost identical to tachyzoites making it difficult to distinguish between the two stages via light microscopy. Slight distinctions can be made by electron microscopy including a greater number of micronemes and amylopectin granules in bradyzoites as well as the posterior localization of the nucleus (144). Once conversion to the bradyzoite is initiated, a cyst wall forms that is composed of proteins and carbohydrates, which can be bound by Wheat germ agglutinin and Dolichos biflorus agglutinin (DBA) (145). While the exact make-up of the cyst wall has yet to be determined, the

glycoprotein that binds to DBA, called CST1, has been identified. Deletion strains of CST1 have a reduced cyst burden in mice suggesting it plays a critical role in conversion to or survival of the bradyzoite form (146). Similarly, *T. gondii* strains containing deletions in the nucleotide-sugar transporter (TgNST1) can no longer interact with lectins and display severe defects in persistence during chronic infection (147). Analysis of the bradyzoite transcriptome for potentially secreted proteins identified two proteins, bradyzoite pseudokinase 1 and microneme adhesive repeat domain-containing protein 4, which co-localize with DBA on the cyst wall (148-150). Glycomic and proteomic analysis of the cyst wall and the parasites within it would greatly enhance of understanding of bradyzoite biology.

Although tachyzoites and bradyzoites have similar size and shape, the development of genomic technologies has demonstrated the multitude of transcriptional differences between the two asexual forms. Microarray technology has been an excellent tool for characterizing transcriptomic differences between tachyzoites and bradyzoites in tissue culture (148-150). Studies of the transcriptome have also compared in vitro and in vivo samples with in vitro tachyzoites, in vivo bradyzoites, and feline derived oocysts, as well as tissue culture tachyzoites and bradyzoites, developing oocysts, and bradyzoites purified from mouse brains 21 days post-infection (148, 151). To gain more insight on in vivo development of *T. gondii,* host microarrays were performed on peritoneal-derived tachyzoites from different strain types of *T. gondii* from wild type and IFN-γ deleted mice (152-154). Similarly, transcriptional changes in the brains of mice were compared after infection with either type I or type II strains (152-154). These studies have been crucial to our understanding of asexual development of *T. gondii* within the intermediate host.

Depth of coverage and dynamic range of RNAseq makes it an excellent tool for in vivo analysis of *T. gondii* infection. RNAseq is ideal for in vivo studies because parasites do not need to be purified from host samples prior to analysis. This reduces changes to the transcriptome that occur during sample preparation and allows for simultaneous analysis of host and pathogen transcriptomes. Using RNAseq, studies have compared mouse brains that were uninfected or infected with *T. gondii* for 32 days (142). Another study performed a time course of the mouse forebrain infected with *T. gondii* for 10 days and 28 days post infection. This study utilized both host and pathogen information to analyze transcriptomic differences between the time points (99). Future temporal studies using different strain types will allow for an in depth analysis of host and parasite response throughout *T. gondii* infection.

Effects of chronic infection

Infection Induced Behavioral Changes

Within the rodent host, *T. gondii* has been shown to have several effects, both on behavior and immune response to co-infection. Mice chronically infected with *T. gondii* show an increase in general movement compared to controls (155, 156). This "hyperactivity" phenotype was also seen in *T. gondii* infected rats, including an enhanced susceptibility to be captured in baited traps (157). Changes in human behaviour have also been correlated with *T. gondii* infection (158); however, human behavioural studies are obviously difficult to control. As rodents are the key reservoir for this parasite, it is appropriate to investigate behavioural changes that would increase transmission. Increased activity and decreased avoidance of novel stimuli would raise transmission by increasing the chances of an infected animal being preyed upon. Specifically, chronic infection with *T. gondii* converted the aversion rodents have to feline urine

into attraction (159). While the mechanism of these behavioural changes is unknown, dopamine is a likely candidate. Infection with *T. gondii* causes increased host dopamine levels and treatment with dopamine receptor antagonists block the attraction of infected rats to cat urine (160-162). It is speculated that this increase in dopamine is directly carried out by the parasite through two aromatic amino acid hydrolases (AAH) encoded in the *T. gondii* genome. AAHs carry out the rate-limiting step in dopamine synthesis. However, deletion or overexpression of AAH2 in *T. gondii* does not change host dopamine levels, suggesting the increase in dopamine synthesis during *T. gondii* infection may be initiated by the host response (163).

Protection Against Lethal Co-Infection

The immune response associated with maintenance of a chronic *T. gondii* infection can also protect rodents against lethal co-infections with a wide variety of pathogens. Original studies of *T. gondii* acquired protection against co-infections include the bacteria *Listeria monocytogenes* and *Salmonella enterica* (164), Mengo virus (165), the fungus *Cryptococcus neoformans* (166), and other parasites such as *Schistosoma mansoni* (167, 168) and *Plasmodium yoelii* (167, 168). Protection was even observed nine months post-*T. gondii* infection. The mechanisms of *T. gondii* induced protection against other pathogens are mediated by the innate immune system, but vary based on the organism of co-infection. For instance in influenza virus, *T. gondii* induction of IFN-γ from NK cells was both necessary and sufficient for protection, even 4 months post initial *T. gondii* infection (169). NK cells likely play a role in maintenance of chronic infection as they are still found in significantly increased concentrations in the peritoneal cavity of mice six months after *T. gondii* infection (170). Similarly, *T. gondii* induced IL-12, or injection of recombinant IL-12, significantly decreased *Plasmodium berghei* parasitemia (171).

In the case of *L. monocytogenes, T. gondii* induced protection is IFN-γ dependent but IL-12 independent and reliant on inflammatory monocytes (172). While the evolutionary advantage for *T. gondii* to protect its host from lethal secondary infection is not immediately obvious, a healthier host has an increased chance of being consumed instead of dying from the secondary infection and decomposing.

Vaccine development

Benefits of *T. gondii* Vaccines

The Centers for Disease Control and Prevention (CDC) in the United States has recently placed *T. gondii* on its list of neglected parasitic infections. One of the goals for this listing is to prioritize disease prevention and vaccine development. There are multiple benefits to development of a vaccine to prevent *T. gondii* infection. 1) Health benefits associated with reduced transmission to humans and subsequent complications associated with infections in the immunocompromised and fetuses. 2) Reduction in economic burden associated with treatment of human disease. 3) Decrease in economic burden associated with loss of livestock from spontaneous abortions during congenital transmission. In the United States, *T. gondii* infection is the cause of approximately 300 deaths, over 4,000 hospitalizations annually, and 3 billion dollars in cost of treatment (8, 173). These numbers stress the need for prevention as well as treatment options. An animal vaccine would not only decrease livestock abortions but, if a non-persisting strain was used, would also eliminate the risk of human infection from consumption of contaminated meat. Vaccine use in domestic cats would decrease the amount of oocysts in the environment, and subsequent livestock and human infections. Currently, only one vaccine has been successfully developed for use in livestock, but only those animals not destined for human

consumption. The absence of an effective vaccine for prevention of *T. gondii* infection highlights the complexity of interplay between the parasite and the host immune response.

S48 Vaccine

Live attenuated parasites have been more effective than inactivated, subunit or DNA vaccines at stimulating an immune response that confers resistance. However, the development of a safe live parasite that cannot form infectious bradyzoite cysts or revert to virulent tachyzoites has been difficult. A stable attenuated strain, S48, was generated from prolonged and routine passaging through mice twice a week for 30 years. S48 is marketed as Toxovax and is licensed only for use in wool-producing sheep to prevent spontaneous abortion. It has yet to be determined if it is safe to use in livestock destined for human consumption. Toxovax provides immunity-based protection in sheep against congenital infection for up to 18 months post vaccination (174). At this point it has not been determined if Toxovax can provide resistance to establishment of a long-term infection when challenged with cyst stages of parasites.

Difficulties in *T. gondii* Vaccine Development

Many combinations of mutant strains, parasite extracts, recombinant proteins and DNA have been used with varying degrees of effectiveness. All of these trials have been previously summarized (1). Currently, none of these vaccines have eliminated the ability of the parasite to establish cysts in the brain or completely prevent congenital transmission. Previous studies determined that primary infection with one *T. gondii* strain type does not provide protection when challenged with differing strains or against the same strain containing variants of rhoptry proteins ROP5 and ROP18 (175, 176). This suggests long-term immunity relies on a multitude of

parasite factors. As *T. gondii* is represented by multiple strain types, is infectious during multiple life stages, and expresses different antigens at each stage, developing a comprehensive vaccine is extremely difficult. To confer life-long protection from all possible sources of infection, a vaccine will need to incorporate stage specific proteins from oocysts, tachyzoites and bradyzoites from the major strain types as well as stimulate the appropriate immune response for each stage. Nevertheless, the recent molecular advances in our understanding of the biology of *T. gondii* have led to optimism that an effective multi-stage vaccine can be developed.

Conclusions

In order to develop novel therapeutics and a safe vaccine for *T. gondii*, a better understanding of host and pathogen interplay during the progression from acute to chronic infection is required. A broader view of the commonalities between the innate and adaptive immune response as well as the *T. gondii* specific proteins required to stimulate these responses is key for development of future therapeutics and vaccines. The recent advances in tools to analyze host/parasite interactions at a molecular level will greatly enhance our understanding of *T. gondii* biology. As mentioned in this review, the use of RNAseq and proteomics to analyze parasites in vivo will give a more complete picture of *T. gondii* asexual development. The adaptation of CRISPER/Cas9 technology for rapid gene deletions in both host and parasite will allow for faster analysis of function for candidate genes identified from RNAseq and proteomic analyses (177, 178). Other tools such as parasites that express luciferase or fluorescent proteins combined with Cre-reporter mice will allow for specific monitoring of infected cells during animal infection (179). Future molecular analyses of *T. gondii* and host during in vivo infection

will allow discovery of new drug targets active against bradyzoites and vaccines effective against multiple stages and strains.

References

1. **Lindsay DS and Dubey JP.** 2014. Toxoplasmosis in wild and domestic animals. p.194-209. Edited by Weiss LM and Kim K. Toxoplasma gondii: the model apicomplexan. Int J Parasitol **34:**423-432.
2. **Frenkel JK, Dubey JP, Miller NL.** 1970. Toxoplasma gondii in cats: fecal stages identified as coccidian oocysts. Science **167:**893-896.
3. **Dubey JP, Lindsay DS, Speer CA.** 1998. Structures of Toxoplasma gondii tachyzoites, bradyzoites, and sporozoites and biology and development of tissue cysts. Clin Microbiol Rev **11:**267-299.
4. **Munoz-Zanzi CA, Fry P, Lesina B, Hill D.** 2010. Toxoplasma gondii oocyst-specific antibodies and source of infection. Emerg Infect Dis **16:**1591-1593.
5. **Cook AJ, Gilbert RE, Buffolano W, Zufferey J, Petersen E, Jenum PA, Foulon W, Semprini AE, Dunn DT.** 2000. Sources of toxoplasma infection in pregnant women: European multicentre case-control study. European Research Network on Congenital Toxoplasmosis. Bmj **321:**142-147.
6. **Boyer K, Hill D, Mui E, Wroblewski K, Karrison T, Dubey JP, Sautter M, Noble AG, Withers S, Swisher C, Heydemann P, Hosten T, Babiarz J, Lee D, Meier P, McLeod R, Toxoplasmosis Study G.** 2011. Unrecognized ingestion of Toxoplasma gondii oocysts leads to congenital toxoplasmosis and causes epidemics in North America. Clin Infect Dis **53:**1081-1089.
7. **Pappas G, Roussos N, Falagas ME.** 2009. Toxoplasmosis snapshots: global status of Toxoplasma gondii seroprevalence and implications for pregnancy and congenital toxoplasmosis. Int J Parasitol **39:**1385-1394.
8. **Scallan E, Hoekstra RM, Angulo FJ, Tauxe RV, Widdowson MA, Roy SL, Jones JL, Griffin PM.** 2011. Foodborne illness acquired in the United States--major pathogens. Emerg Infect Dis **17:**7-15.
9. **McAuley J, Boyer KM, Patel D, Mets M, Swisher C, Roizen N, Wolters C, Stein L, Stein M, Schey W, et al.** 1994. Early and longitudinal evaluations of treated infants and children and untreated historical patients with congenital toxoplasmosis: the Chicago Collaborative Treatment Trial. Clin Infect Dis **18:**38-72.
10. **Luft BJ, Remington JS.** 1992. Toxoplasmic encephalitis in AIDS. Clin Infect Dis **15:**211-222.
11. **Grigg ME, Ganatra J, Boothroyd JC, Margolis TP.** 2001. Unusual abundance of atypical strains associated with human ocular toxoplasmosis. J Infect Dis **184:**633-639.
12. **Montoya JG, Liesenfeld O.** 2004. Toxoplasmosis. Lancet **363:**1965-1976.
13. **Ong EL.** 2008. Common AIDS-associated opportunistic infections. Clin Med **8:**539-543.
14. **Chaudhry SA, Gad N, Koren G.** 2014. Toxoplasmosis and pregnancy. Can Fam Physician **60:**334-336.
15. **Barsoum RS.** 2006. Parasitic infections in transplant recipients. Nat Clin Pract Nephrol **2:**490-503.
16. **Israelski DM, Remington JS.** 1993. Toxoplasmosis in patients with cancer. Clin Infect Dis **17 Suppl 2:**S423-435.
17. **Derouin F, Pelloux H.** 2008. Prevention of toxoplasmosis in transplant patients. Clin Microbiol Infect **14:**1089-1101.

18. **Dubey JP, Frenkel JK.** 1972. Cyst-induced toxoplasmosis in cats. The Journal of protozoology **19:**155-177.
19. **Yilmaz SM, Hopkins SH.** 1972. Effects of different conditions on duration of infectivity of Toxoplasma gondii oocysts. J Parasitol **58:**938-939.
20. **Dubey JP, Miller NL, Frenkel JK.** 1970. The Toxoplasma gondii oocyst from cat feces. J Exp Med **132:**636-662.
21. **Hehl AB, Basso WU, Lippuner C, Ramakrishnan C, Okoniewski M, Walker RA, Grigg ME, Smith NC, Deplazes P.** 2015. Asexual expansion of Toxoplasma gondii merozoites is distinct from tachyzoites and entails expression of non-overlapping gene families to attach, invade, and replicate within feline enterocytes. BMC Genomics **16:**66.
22. **Speer CA, Dubey JP.** 1998. Ultrastructure of early stages of infections in mice fed Toxoplasma gondii oocysts. Parasitology **116 (Pt 1):**35-42.
23. **Dubey JP, Speer CA, Shen SK, Kwok OC, Blixt JA.** 1997. Oocyst-induced murine toxoplasmosis: life cycle, pathogenicity, and stage conversion in mice fed Toxoplasma gondii oocysts. J Parasitol **83:**870-882.
24. **Dubey JP.** 1997. Bradyzoite-induced murine toxoplasmosis: stage conversion, pathogenesis, and tissue cyst formation in mice fed bradyzoites of different strains of Toxoplasma gondii. J Eukaryot Microbiol **44:**592-602.
25. **Ueno N, Harker KS, Clarke EV, McWhorter FY, Liu WF, Tenner AJ, Lodoen MB.** 2014. Real-time imaging of Toxoplasma-infected human monocytes under fluidic shear stress reveals rapid translocation of intracellular parasites across endothelial barriers. Cell Microbiol **16:**580-595.
26. **Soete M, Camus D, Dubremetz JF.** 1994. Experimental induction of bradyzoite-specific antigen expression and cyst formation by the RH strain of Toxoplasma gondii in vitro. Exp Parasitol **78:**361-370.
27. **Grigg ME, Ganatra J, Boothroyd JC, Margolis TP.** 2001. Unusual abundance of atypical strains associated with human ocular toxoplasmosis. J Infect Dis **184:**633-639.
28. **McCannel CA, Holland GN, Helm CJ, Cornell PJ, Winston JV, Rimmer TG.** 1996. Causes of uveitis in the general practice of ophthalmology. UCLA Community-Based Uveitis Study Group. American journal of ophthalmology **121:**35-46.
29. **de Moura L, Bahia-Oliveira LM, Wada MY, Jones JL, Tuboi SH, Carmo EH, Ramalho WM, Camargo NJ, Trevisan R, Graca RM, da Silva AJ, Moura I, Dubey JP, Garrett DO.** 2006. Waterborne toxoplasmosis, Brazil, from field to gene. Emerg Infect Dis **12:**326-329.
30. **Rajendran C, Su C, Dubey JP.** 2012. Molecular genotyping of Toxoplasma gondii from Central and South America revealed high diversity within and between populations. Infection, genetics and evolution : journal of molecular epidemiology and evolutionary genetics in infectious diseases **12:**359-368.
31. **Minot S, Melo MB, Li F, Lu D, Niedelman W, Levine SS, Saeij JP.** 2012. Admixture and recombination among Toxoplasma gondii lineages explain global genome diversity. Proc Natl Acad Sci U S A **109:**13458-13463.
32. **Ferreira Ade M, Vitor RW, Gazzinelli RT, Melo MN.** 2006. Genetic analysis of natural recombinant Brazilian Toxoplasma gondii strains by multilocus PCR-RFLP. Infection, genetics and evolution : journal of molecular epidemiology and evolutionary genetics in infectious diseases **6:**22-31.

33. **Su C, Khan A, Zhou P, Majumdar D, Ajzenberg D, Darde ML, Zhu XQ, Ajioka JW, Rosenthal BM, Dubey JP, Sibley LD.** 2012. Globally diverse Toxoplasma gondii isolates comprise six major clades originating from a small number of distinct ancestral lineages. Proc Natl Acad Sci U S A **109:**5844-5849.
34. **Howe DK, Sibley LD.** 1995. Toxoplasma gondii comprises three clonal lineages: correlation of parasite genotype with human disease. J Infect Dis **172:**1561-1566.
35. **Howe DK, Honore S, Derouin F, Sibley LD.** 1997. Determination of genotypes of Toxoplasma gondii strains isolated from patients with toxoplasmosis. J Clin Microbiol **35:**1411-1414.
36. **Vaudaux JD, Muccioli C, James ER, Silveira C, Magargal SL, Jung C, Dubey JP, Jones JL, Doymaz MZ, Bruckner DA, Belfort R, Jr., Holland GN, Grigg ME.** 2010. Identification of an atypical strain of toxoplasma gondii as the cause of a waterborne outbreak of toxoplasmosis in Santa Isabel do Ivai, Brazil. J Infect Dis **202:**1226-1233.
37. **Speer CA, Dubey JP, Blixt JA, Prokop K.** 1997. Time lapse video microscopy and ultrastructure of penetrating sporozoites, types 1 and 2 parasitophorous vacuoles, and the transformation of sporozoites to tachyzoites of the VEG strain of Toxoplasma gondii. J Parasitol **83:**565-574.
38. **Buzoni-Gatel D, Debbabi H, Mennechet FJ, Martin V, Lepage AC, Schwartzman JD, Kasper LH.** 2001. Murine ileitis after intracellular parasite infection is controlled by TGF-beta-producing intraepithelial lymphocytes. Gastroenterology **120:**914-924.
39. **Egan CE, Craven MD, Leng J, Mack M, Simpson KW, Denkers EY.** 2009. CCR2-dependent intraepithelial lymphocytes mediate inflammatory gut pathology during Toxoplasma gondii infection. Mucosal immunology **2:**527-535.
40. **Laurent F, Eckmann L, Savidge TC, Morgan G, Theodos C, Naciri M, Kagnoff MF.** 1997. Cryptosporidium parvum infection of human intestinal epithelial cells induces the polarized secretion of C-X-C chemokines. Infect Immun **65:**5067-5073.
41. **Mennechet FJ, Kasper LH, Rachinel N, Li W, Vandewalle A, Buzoni-Gatel D.** 2002. Lamina propria CD4+ T lymphocytes synergize with murine intestinal epithelial cells to enhance proinflammatory response against an intracellular pathogen. J Immunol **168:**2988-2996.
42. **Shibahara T, Wilcox JN, Couse T, Madara JL.** 2001. Characterization of epithelial chemoattractants for human intestinal intraepithelial lymphocytes. Gastroenterology **120:**60-70.
43. **Buzoni-Gatel D, Debbabi H, Moretto M, Dimier-Poisson IH, Lepage AC, Bout DT, Kasper LH.** 1999. Intraepithelial lymphocytes traffic to the intestine and enhance resistance to Toxoplasma gondii oral infection. J Immunol **162:**5846-5852.
44. **Buzoni-Gatel D, Schulthess J, Menard LC, Kasper LH.** 2006. Mucosal defences against orally acquired protozoan parasites, emphasis on Toxoplasma gondii infections. Cell Microbiol **8:**535-544.
45. **Benson A, Pifer R, Behrendt CL, Hooper LV, Yarovinsky F.** 2009. Gut commensal bacteria direct a protective immune response against Toxoplasma gondii. Cell host & microbe **6:**187-196.
46. **Raetz M, Hwang SH, Wilhelm CL, Kirkland D, Benson A, Sturge CR, Mirpuri J, Vaishnava S, Hou B, Defranco AL, Gilpin CJ, Hooper LV, Yarovinsky F.** 2013. Parasite-induced TH1 cells and intestinal dysbiosis cooperate in IFN-gamma-dependent elimination of Paneth cells. Nature immunology **14:**136-142.

47. **Kobayashi M, Fitz L, Ryan M, Hewick RM, Clark SC, Chan S, Loudon R, Sherman F, Perussia B, Trinchieri G.** 1989. Identification and purification of natural killer cell stimulatory factor (NKSF), a cytokine with multiple biologic effects on human lymphocytes. J Exp Med **170:**827-845.
48. **Chan SH, Perussia B, Gupta JW, Kobayashi M, Pospisil M, Young HA, Wolf SF, Young D, Clark SC, Trinchieri G.** 1991. Induction of interferon gamma production by natural killer cell stimulatory factor: characterization of the responder cells and synergy with other inducers. J Exp Med **173:**869-879.
49. **O'Garra A.** 1998. Cytokines induce the development of functionally heterogeneous T helper cell subsets. Immunity **8:**275-283.
50. **Khan IA, Matsuura T, Kasper LH.** 1994. Interleukin-12 enhances murine survival against acute toxoplasmosis. Infect Immun **62:**1639-1642.
51. **Gazzinelli RT, Hayashi S, Wysocka M, Carrera L, Kuhn R, Muller W, Roberge F, Trinchieri G, Sher A.** 1994. Role of IL-12 in the initiation of cell mediated immunity by Toxoplasma gondii and its regulation by IL-10 and nitric oxide. J Eukaryot Microbiol **41:**9S.
52. **Brenier-Pinchart MP, Pelloux H, Simon J, Ricard J, Bosson JL, Ambroise-Thomas P.** 2000. Toxoplasma gondii induces the secretion of monocyte chemotactic protein-1 in human fibroblasts, in vitro. Molecular and cellular biochemistry **209:**79-87.
53. **Robben PM, LaRegina M, Kuziel WA, Sibley LD.** 2005. Recruitment of Gr-1+ monocytes is essential for control of acute toxoplasmosis. J Exp Med **201:**1761-1769.
54. **Ohtsuka Y, Lee J, Stamm DS, Sanderson IR.** 2001. MIP-2 secreted by epithelial cells increases neutrophil and lymphocyte recruitment in the mouse intestine. Gut **49:**526-533.
55. **Gregg B, Taylor BC, John B, Tait-Wojno ED, Girgis NM, Miller N, Wagage S, Roos DS, Hunter CA.** 2013. Replication and distribution of Toxoplasma gondii in the small intestine after oral infection with tissue cysts. Infect Immun **81:**1635-1643.
56. **Bliss SK, Butcher BA, Denkers EY.** 2000. Rapid recruitment of neutrophils containing prestored IL-12 during microbial infection. J Immunol **165:**4515-4521.
57. **Coombes JL, Charsar BA, Han SJ, Halkias J, Chan SW, Koshy AA, Striepen B, Robey EA.** 2013. Motile invaded neutrophils in the small intestine of Toxoplasma gondii-infected mice reveal a potential mechanism for parasite spread. Proc Natl Acad Sci U S A **110:**E1913-1922.
58. **Muller WA, Randolph GJ.** 1999. Migration of leukocytes across endothelium and beyond: molecules involved in the transmigration and fate of monocytes. Journal of leukocyte biology **66:**698-704.
59. **Sayles PC, Johnson LL.** 1996. Exacerbation of toxoplasmosis in neutrophil-depleted mice. Natural immunity **15:**249-258.
60. **Del Rio L, Bennouna S, Salinas J, Denkers EY.** 2001. CXCR2 deficiency confers impaired neutrophil recruitment and increased susceptibility during Toxoplasma gondii infection. J Immunol **167:**6503-6509.
61. **Bliss SK, Marshall AJ, Zhang Y, Denkers EY.** 1999. Human polymorphonuclear leukocytes produce IL-12, TNF-alpha, and the chemokines macrophage-inflammatory protein-1 alpha and -1 beta in response to Toxoplasma gondii antigens. J Immunol **162:**7369-7375.

62. **Bliss SK, Zhang Y, Denkers EY.** 1999. Murine neutrophil stimulation by Toxoplasma gondii antigen drives high level production of IFN-gamma-independent IL-12. J Immunol **163:**2081-2088.
63. **Robben PM, Mordue DG, Truscott SM, Takeda K, Akira S, Sibley LD.** 2004. Production of IL-12 by macrophages infected with Toxoplasma gondii depends on the parasite genotype. J Immunol **172:**3686-3694.
64. **Reis e Sousa C, Hieny S, Scharton-Kersten T, Jankovic D, Charest H, Germain RN, Sher A.** 1997. In vivo microbial stimulation induces rapid CD40 ligand-independent production of interleukin 12 by dendritic cells and their redistribution to T cell areas. J Exp Med **186:**1819-1829.
65. **Scanga CA, Aliberti J, Jankovic D, Tilloy F, Bennouna S, Denkers EY, Medzhitov R, Sher A.** 2002. Cutting edge: MyD88 is required for resistance to Toxoplasma gondii infection and regulates parasite-induced IL-12 production by dendritic cells. J Immunol **168:**5997-6001.
66. **Yarovinsky F, Zhang D, Andersen JF, Bannenberg GL, Serhan CN, Hayden MS, Hieny S, Sutterwala FS, Flavell RA, Ghosh S, Sher A.** 2005. TLR11 activation of dendritic cells by a protozoan profilin-like protein. Science **308:**1626-1629.
67. **Debierre-Grockiego F, Campos MA, Azzouz N, Schmidt J, Bieker U, Resende MG, Mansur DS, Weingart R, Schmidt RR, Golenbock DT, Gazzinelli RT, Schwarz RT.** 2007. Activation of TLR2 and TLR4 by glycosylphosphatidylinositols derived from Toxoplasma gondii. J Immunol **179:**1129-1137.
68. **Egan CE, Sukhumavasi W, Butcher BA, Denkers EY.** 2009. Functional aspects of Toll-like receptor/MyD88 signalling during protozoan infection: focus on Toxoplasma gondii. Clinical and experimental immunology **156:**17-24.
69. **Mashayekhi M, Sandau MM, Dunay IR, Frickel EM, Khan A, Goldszmid RS, Sher A, Ploegh HL, Murphy TL, Sibley LD, Murphy KM.** 2011. CD8alpha(+) dendritic cells are the critical source of interleukin-12 that controls acute infection by Toxoplasma gondii tachyzoites. Immunity **35:**249-259.
70. **Dunay IR, Fuchs A, Sibley LD.** 2010. Inflammatory monocytes but not neutrophils are necessary to control infection with Toxoplasma gondii in mice. Infect Immun **78:**1564-1570.
71. **Bliss SK, Gavrilescu LC, Alcaraz A, Denkers EY.** 2001. Neutrophil depletion during Toxoplasma gondii infection leads to impaired immunity and lethal systemic pathology. Infect Immun **69:**4898-4905.
72. **Yap G, Pesin M, Sher A.** 2000. Cutting edge: IL-12 is required for the maintenance of IFN-gamma production in T cells mediating chronic resistance to the intracellular pathogen, Toxoplasma gondii. J Immunol **165:**628-631.
73. **Suzuki Y, Joh K.** 1994. Effect of the strain of Toxoplasma gondii on the development of toxoplasmic encephalitis in mice treated with antibody to interferon-gamma. Parasitol Res **80:**125-130.
74. **Scharton-Kersten TM, Wynn TA, Denkers EY, Bala S, Grunvald E, Hieny S, Gazzinelli RT, Sher A.** 1996. In the absence of endogenous IFN-gamma, mice develop unimpaired IL-12 responses to Toxoplasma gondii while failing to control acute infection. J Immunol **157:**4045-4054.
75. **Deckert-Schluter M, Rang A, Weiner D, Huang S, Wiestler OD, Hof H, Schluter D.** 1996. Interferon-gamma receptor-deficiency renders mice highly susceptible to

toxoplasmosis by decreased macrophage activation. Laboratory investigation; a journal of technical methods and pathology **75:**827-841.

76. **Suzuki Y, Orellana MA, Schreiber RD, Remington JS.** 1988. Interferon-gamma: the major mediator of resistance against Toxoplasma gondii. Science **240:**516-518.
77. **Gazzinelli RT, Hieny S, Wynn TA, Wolf S, Sher A.** 1993. Interleukin 12 is required for the T-lymphocyte-independent induction of interferon gamma by an intracellular parasite and induces resistance in T-cell-deficient hosts. Proc Natl Acad Sci U S A **90:**6115-6119.
78. **Sturge CR, Benson A, Raetz M, Wilhelm CL, Mirpuri J, Vitetta ES, Yarovinsky F.** 2013. TLR-independent neutrophil-derived IFN-gamma is important for host resistance to intracellular pathogens. Proc Natl Acad Sci U S A **110:**10711-10716.
79. **Sher A, Oswald IP, Hieny S, Gazzinelli RT.** 1993. Toxoplasma gondii induces a T-independent IFN-gamma response in natural killer cells that requires both adherent accessory cells and tumor necrosis factor-alpha. J Immunol **150:**3982-3989.
80. **de Veer MJ, Holko M, Frevel M, Walker E, Der S, Paranjape JM, Silverman RH, Williams BR.** 2001. Functional classification of interferon-stimulated genes identified using microarrays. Journal of leukocyte biology **69:**912-920.
81. **Yap GS, Sher A.** 1999. Effector cells of both nonhemopoietic and hemopoietic origin are required for interferon (IFN)-gamma- and tumor necrosis factor (TNF)-alpha-dependent host resistance to the intracellular pathogen, Toxoplasma gondii. J Exp Med **189:**1083-1092.
82. **Cheng YS, Colonno RJ, Yin FH.** 1983. Interferon induction of fibroblast proteins with guanylate binding activity. J Biol Chem **258:**7746-7750.
83. **Boehm U, Guethlein L, Klamp T, Ozbek K, Schaub A, Futterer A, Pfeffer K, Howard JC.** 1998. Two families of GTPases dominate the complex cellular response to IFN-gamma. J Immunol **161:**6715-6723.
84. **Degrandi D, Kravets E, Konermann C, Beuter-Gunia C, Klumpers V, Lahme S, Wischmann E, Mausberg AK, Beer-Hammer S, Pfeffer K.** 2013. Murine guanylate binding protein 2 (mGBP2) controls Toxoplasma gondii replication. Proc Natl Acad Sci U S A **110:**294-299.
85. **Yamamoto M, Okuyama M, Ma JS, Kimura T, Kamiyama N, Saiga H, Ohshima J, Sasai M, Kayama H, Okamoto T, Huang DC, Soldati-Favre D, Horie K, Takeda J, Takeda K.** 2012. A cluster of interferon-gamma-inducible p65 GTPases plays a critical role in host defense against Toxoplasma gondii. Immunity **37:**302-313.
86. **Ling YM, Shaw MH, Ayala C, Coppens I, Taylor GA, Ferguson DJ, Yap GS.** 2006. Vacuolar and plasma membrane stripping and autophagic elimination of Toxoplasma gondii in primed effector macrophages. J Exp Med **203:**2063-2071.
87. **Bekpen C, Hunn JP, Rohde C, Parvanova I, Guethlein L, Dunn DM, Glowalla E, Leptin M, Howard JC.** 2005. The interferon-inducible p47 (IRG) GTPases in vertebrates: loss of the cell autonomous resistance mechanism in the human lineage. Genome Biol **6:**R92.
88. **Virreira Winter S, Niedelman W, Jensen KD, Rosowski EE, Julien L, Spooner E, Caradonna K, Burleigh BA, Saeij JP, Ploegh HL, Frickel EM.** 2011. Determinants of GBP recruitment to Toxoplasma gondii vacuoles and the parasitic factors that control it. PLoS One **6:**e24434.

89. **Kresse A, Konermann C, Degrandi D, Beuter-Gunia C, Wuerthner J, Pfeffer K, Beer S.** 2008. Analyses of murine GBP homology clusters based on in silico, in vitro and in vivo studies. BMC Genomics **9:**158.
90. **Pfefferkorn ER.** 1984. Interferon gamma blocks the growth of Toxoplasma gondii in human fibroblasts by inducing the host cells to degrade tryptophan. Proc Natl Acad Sci U S A **81:**908-912.
91. **Pfefferkorn ER, Rebhun S, Eckel M.** 1986. Characterization of an indoleamine 2,3-dioxygenase induced by gamma-interferon in cultured human fibroblasts. Journal of interferon research **6:**267-279.
92. **Green SJ, Mellouk S, Hoffman SL, Meltzer MS, Nacy CA.** 1990. Cellular mechanisms of nonspecific immunity to intracellular infection: cytokine-induced synthesis of toxic nitrogen oxides from L-arginine by macrophages and hepatocytes. Immunology letters **25:**15-19.
93. **Hibbs JB, Jr., Taintor RR, Vavrin Z, Rachlin EM.** 1988. Nitric oxide: a cytotoxic activated macrophage effector molecule. Biochemical and biophysical research communications **157:**87-94.
94. **Rutschman R, Lang R, Hesse M, Ihle JN, Wynn TA, Murray PJ.** 2001. Cutting edge: Stat6-dependent substrate depletion regulates nitric oxide production. J Immunol **166:**2173-2177.
95. **Nathan C, Shiloh MU.** 2000. Reactive oxygen and nitrogen intermediates in the relationship between mammalian hosts and microbial pathogens. Proc Natl Acad Sci U S A **97:**8841-8848.
96. **MacMicking JD.** 2012. Interferon-inducible effector mechanisms in cell-autonomous immunity. Nat Rev Immunol **12:**367-382.
97. **Hunter CA, Roberts CW, Murray M, Alexander J.** 1992. Detection of cytokine mRNA in the brains of mice with toxoplasmic encephalitis. Parasite immunology **14:**405-413.
98. **Suzuki Y, Rani S, Liesenfeld O, Kojima T, Lim S, Nguyen TA, Dalrymple SA, Murray R, Remington JS.** 1997. Impaired resistance to the development of toxoplasmic encephalitis in interleukin-6-deficient mice. Infect Immun **65:**2339-2345.
99. **Pittman KJ, Aliota MT, Knoll LJ.** 2014. Dual transcriptional profiling of mice and Toxoplasma gondii during acute and chronic infection. BMC Genomics **15:**806.
100. **Gazzinelli R, Xu Y, Hieny S, Cheever A, Sher A.** 1992. Simultaneous depletion of CD4+ and CD8+ T lymphocytes is required to reactivate chronic infection with Toxoplasma gondii. J Immunol **149:**175-180.
101. **Matthews N.** 1981. Production of an anti-tumour cytotoxin by human monocytes. Immunology **44:**135-142.
102. **De Titto EH, Catterall JR, Remington JS.** 1986. Activity of recombinant tumor necrosis factor on Toxoplasma gondii and Trypanosoma cruzi. J Immunol **137:**1342-1345.
103. **Sibley LD, Adams LB, Fukutomi Y, Krahenbuhl JL.** 1991. Tumor necrosis factor-alpha triggers antitoxoplasmal activity of IFN-gamma primed macrophages. J Immunol **147:**2340-2345.
104. **Andrade RM, Wessendarp M, Gubbels MJ, Striepen B, Subauste CS.** 2006. CD40 induces macrophage anti-Toxoplasma gondii activity by triggering autophagy-dependent

fusion of pathogen-containing vacuoles and lysosomes. The Journal of clinical investigation **116:**2366-2377.

105. **Langermans JA, Van der Hulst ME, Nibbering PH, Hiemstra PS, Fransen L, Van Furth R.** 1992. IFN-gamma-induced L-arginine-dependent toxoplasmastatic activity in murine peritoneal macrophages is mediated by endogenous tumor necrosis factor-alpha. J Immunol **148:**568-574.
106. **Sher A, Oswald IP, Hieny S, Gazzinelli RT.** 1993. Toxoplasma gondii induces a T-independent IFN-gamma response in natural killer cells that requires both adherent accessory cells and tumor necrosis factor-alpha. J Immunol **150:**3982-3989.
107. **Adams LB, Hibbs JB, Jr., Taintor RR, Krahenbuhl JL.** 1990. Microbiostatic effect of murine-activated macrophages for Toxoplasma gondii. Role for synthesis of inorganic nitrogen oxides from L-arginine. J Immunol **144:**2725-2729.
108. **Yap GS, Scharton-Kersten T, Charest H, Sher A.** 1998. Decreased resistance of TNF receptor p55- and p75-deficient mice to chronic toxoplasmosis despite normal activation of inducible nitric oxide synthase in vivo. J Immunol **160:**1340-1345.
109. **Khan IA, Matsuura T, Kasper LH.** 1995. IL-10 mediates immunosuppression following primary infection with Toxoplasma gondii in mice. Parasite immunology **17:**185-195.
110. **Gazzinelli RT, Wysocka M, Hieny S, Scharton-Kersten T, Cheever A, Kuhn R, Muller W, Trinchieri G, Sher A.** 1996. In the absence of endogenous IL-10, mice acutely infected with Toxoplasma gondii succumb to a lethal immune response dependent on CD4+ T cells and accompanied by overproduction of IL-12, IFN-gamma and TNF-alpha. J Immunol **157:**798-805.
111. **Wilson EH, Wille-Reece U, Dzierszinski F, Hunter CA.** 2005. A critical role for IL-10 in limiting inflammation during toxoplasmic encephalitis. J Neuroimmunol **165:**63-74.
112. **Butcher BA, Kim L, Johnson PF, Denkers EY.** 2001. Toxoplasma gondii tachyzoites inhibit proinflammatory cytokine induction in infected macrophages by preventing nuclear translocation of the transcription factor NF-kappa B. J Immunol **167:**2193-2201.
113. **Shapira S, Speirs K, Gerstein A, Caamano J, Hunter CA.** 2002. Suppression of NF-kappaB activation by infection with Toxoplasma gondii. J Infect Dis **185 Suppl 1:**S66-72.
114. **Shapira S, Harb OS, Margarit J, Matrajt M, Han J, Hoffmann A, Freedman B, May MJ, Roos DS, Hunter CA.** 2005. Initiation and termination of NF-kappaB signaling by the intracellular protozoan parasite Toxoplasma gondii. Journal of cell science **118:**3501-3508.
115. **Rosowski EE, Lu D, Julien L, Rodda L, Gaiser RA, Jensen KD, Saeij JP.** 2011. Strain-specific activation of the NF-kappaB pathway by GRA15, a novel Toxoplasma gondii dense granule protein. J Exp Med **208:**195-212.
116. **Butcher BA, Fox BA, Rommereim LM, Kim SG, Maurer KJ, Yarovinsky F, Herbert DR, Bzik DJ, Denkers EY.** 2011. Toxoplasma gondii rhoptry kinase ROP16 activates STAT3 and STAT6 resulting in cytokine inhibition and arginase-1-dependent growth control. PLoS Pathog **7:**e1002236.
117. **Chao CC, Anderson WR, Hu S, Gekker G, Martella A, Peterson PK.** 1993. Activated microglia inhibit multiplication of Toxoplasma gondii via a nitric oxide mechanism. Clinical immunology and immunopathology **67:**178-183.

118. **Peterson PK, Gekker G, Hu S, Chao CC.** 1995. Human astrocytes inhibit intracellular multiplication of Toxoplasma gondii by a nitric oxide-mediated mechanism. J Infect Dis **171:**516-518.
119. **Mordue DG, Scott-Weathers CF, Tobin CM, Knoll LJ.** 2007. A patatin-like protein protects Toxoplasma gondii from degradation in activated macrophages. Mol Microbiol **63:**482-496.
120. **Tobin CM, Knoll LJ.** 2012. A patatin-like protein protects Toxoplasma gondii from degradation in a nitric oxide-dependent manner. Infect Immun **80:**55-61.
121. **Tobin Magle C, Pittman KJ, Moser LA, Boldon KM, Knoll LJ.** 2014. A toxoplasma patatin-like protein changes localization and alters the cytokine response during toxoplasmic encephalitis. Infect Immun **82:**618-625.
122. **Scharton-Kersten TM, Yap G, Magram J, Sher A.** 1997. Inducible nitric oxide is essential for host control of persistent but not acute infection with the intracellular pathogen Toxoplasma gondii. J Exp Med **185:**1261-1273.
123. **Zimmermann S, Murray PJ, Heeg K, Dalpke AH.** 2006. Induction of suppressor of cytokine signaling-1 by Toxoplasma gondii contributes to immune evasion in macrophages by blocking IFN-gamma signaling. J Immunol **176:**1840-1847.
124. **Aliberti J, Hieny S, Reis e Sousa C, Serhan CN, Sher A.** 2002. Lipoxin-mediated inhibition of IL-12 production by DCs: a mechanism for regulation of microbial immunity. Nature immunology **3:**76-82.
125. **Aliberti J, Serhan C, Sher A.** 2002. Parasite-induced lipoxin A4 is an endogenous regulator of IL-12 production and immunopathology in Toxoplasma gondii infection. J Exp Med **196:**1253-1262.
126. **Dubey JP.** 1997. Bradyzoite-induced murine toxoplasmosis: Stage conversion, pathogenesis, and tissue cyst formation in mice fed bradyzoites of different strains of Toxoplasma gondii. Journal of Eukaryotic Microbiology **44:**592-602.
127. **Barragan A, Sibley LD.** 2002. Transepithelial migration of Toxoplasma gondii is linked to parasite motility and virulence. Journal of Experimental Medicine **195:**1625-1633.
128. **Barragan A, Brossier F, Sibley LD.** 2005. Transepithelial migration of Toxoplasma gondii involves an interaction of intercellular adhesion molecule 1 (ICAM-1) with the parasite adhesin MIC2. Cell Microbiol **7:**561-568.
129. **Lambert H, Hitziger N, Dellacasa I, Svensson M, Barragan A.** 2006. Induction of dendritic cell migration upon Toxoplasma gondii infection potentiates parasite dissemination. Cell Microbiol **8:**1611-1623.
130. **Da Gama LM, Ribeiro-Gomes FL, Guimaraes U, Arnholdt ACV.** 2004. Reduction in adhesiveness to extracellular matrix components, modulation of adhesion molecules and in vivo migration of murine macrophages infected with Toxoplasma gondii. Microbes and Infection **6:**1287-1296.
131. **Courret N, Darche S, Sonigo P, Milon G, Buzoni-Gatel D, Tardieux I.** 2006. CD11c- and CD11b-expressing mouse leukocytes transport single Toxoplasma gondii tachyzoites to the brain. Blood **107:**309-316.
132. **Feustel SM, Meissner M, Liesenfeld O.** 2012. Toxoplasma gondii and the blood-brain barrier. Virulence **3:**182-192.
133. **Takei Y, Miyagami T, Nagasawa H, Sasaki H, Kawakami T, Omata Y, Suzuki N.** 1981. Microbicidal activity of toxoplasma immune beagle plasma and lymphokines to toxoplasma multiplication in host cells. Zentralblatt fur Bakteriologie, Mikrobiologie und

Hygiene. 1. Abt. Originale A, Medizinische Mikrobiologie, Infektionskrankheiten und Parasitologie = International journal of microbiology and hygiene. A, Medical micro **250:**392-402.

134. **Li S, Maine G, Suzuki Y, Araujo FG, Galvan G, Remington JS, Parmley S.** 2000. Serodiagnosis of recently acquired Toxoplasma gondii infection with a recombinant antigen. J Clin Microbiol **38:**179-184.
135. **Sher A, Denkers EY, Gazzinelli RT.** 1995. Induction and regulation of host cell-mediated immunity by Toxoplasma gondii. Ciba Foundation symposium **195:**95-104; discussion 104-109.
136. **Harris DP, Haynes L, Sayles PC, Duso DK, Eaton SM, Lepak NM, Johnson LL, Swain SL, Lund FE.** 2000. Reciprocal regulation of polarized cytokine production by effector B and T cells. Nature immunology **1:**475-482.
137. **Harris DP, Goodrich S, Gerth AJ, Peng SL, Lund FE.** 2005. Regulation of IFN-gamma production by B effector 1 cells: essential roles for T-bet and the IFN-gamma receptor. J Immunol **174:**6781-6790.
138. **Khan IA, Ely KH, Kasper LH.** 1994. Antigen-specific CD8+ T cell clone protects against acute Toxoplasma gondii infection in mice. J Immunol **152:**1856-1860.
139. **Hermes G, Ajioka JW, Kelly KA, Mui E, Roberts F, Kasza K, Mayr T, Kirisits MJ, Wollmann R, Ferguson DJP, Roberts CW, Hwang JH, Trendler T, Kennan RP, Suzuki Y, Reardon C, Hickey WF, Chen LP, McLeod R.** 2008. Neurological and behavioral abnormalities, ventricular dilatation, altered cellular functions, inflammation, and neuronal injury in brains of mice due to common, persistent, parasitic infection. J Neuroinflamm **5**.
140. **Biswas A, Dunay IR.** 2014. Ly6Chi monocytes govern cerebral toxoplasmosis. J Neuroimmunol **275:**75-76.
141. **Hermes G, Ajioka JW, Kelly KA, Mui E, Roberts F, Kasza K, Mayr T, Kirisits MJ, Wollmann R, Ferguson DJ, Roberts CW, Hwang JH, Trendler T, Kennan RP, Suzuki Y, Reardon C, Hickey WF, Chen L, McLeod R.** 2008. Neurological and behavioral abnormalities, ventricular dilatation, altered cellular functions, inflammation, and neuronal injury in brains of mice due to common, persistent, parasitic infection. J Neuroinflammation **5:**48.
142. **Tanaka S, Nishimura M, Ihara F, Yamagishi J, Suzuki Y, Nishikawa Y.** 2013. Transcriptome Analysis of Mouse Brain Infected with Toxoplasma gondii. Infect Immun **81:**3609-3619.
143. **Deckert-Schluter M, Buck C, Weiner D, Kaefer N, Rang A, Hof H, Wiestler OD, Schluter D.** 1997. Interleukin-10 downregulates the intracerebral immune response in chronic Toxoplasma encephalitis. J Neuroimmunol **76:**167-176.
144. **Ferguson DJ, Hutchison WM.** 1987. An ultrastructural study of the early development and tissue cyst formation of Toxoplasma gondii in the brains of mice. Parasitol Res **73:**483-491.
145. **Boothroyd JC, Black M, Bonnefoy S, Hehl A, Knoll LJ, Manger ID, Ortega-Barria E, Tomavo S.** 1997. Genetic and biochemical analysis of development in Toxoplasma gondii. Philosophical transactions of the Royal Society of London. Series B, Biological sciences **352:**1347-1354.

146. **Tomita T, Bzik DJ, Ma YF, Fox BA, Markillie LM, Taylor RC, Kim K, Weiss LM.** 2013. The Toxoplasma gondii cyst wall protein CST1 is critical for cyst wall integrity and promotes bradyzoite persistence. PLoS Pathog **9:**e1003823.
147. **Caffaro CE, Koshy AA, Liu L, Zeiner GM, Hirschberg CB, Boothroyd JC.** 2013. A nucleotide sugar transporter involved in glycosylation of the Toxoplasma tissue cyst wall is required for efficient persistence of bradyzoites. PLoS Pathog **9:**e1003331.
148. **Buchholz KR, Fritz HM, Chen X, Durbin-Johnson B, Rocke DM, Ferguson DJ, Conrad PA, Boothroyd JC.** 2011. Identification of tissue cyst wall components by transcriptome analysis of in vivo and in vitro Toxoplasma gondii bradyzoites. Eukaryot Cell **10:**1637-1647.
149. **Bahl A, Davis PH, Behnke M, Dzierszinski F, Jagalur M, Chen F, Shanmugam D, White MW, Kulp D, Roos DS.** 2010. A novel multifunctional oligonucleotide microarray for Toxoplasma gondii. BMC Genomics **11:**603.
150. **Cleary MD, Singh U, Blader IJ, Brewer JL, Boothroyd JC.** 2002. Toxoplasma gondii asexual development: identification of developmentally regulated genes and distinct patterns of gene expression. Eukaryot Cell **1:**329-340.
151. **Fritz HM, Buchholz KR, Chen X, Durbin-Johnson B, Rocke DM, Conrad PA, Boothroyd JC.** 2012. Transcriptomic analysis of toxoplasma development reveals many novel functions and structures specific to sporozoites and oocysts. PLoS One **7:**e29998.
152. **Skariah S, Mordue DG.** 2012. Identification of Toxoplasma gondii genes responsive to the host immune response during in vivo infection. PLoS One **7:**e46621.
153. **Hill RD, Gouffon JS, Saxton AM, Su C.** 2012. Differential gene expression in mice infected with distinct Toxoplasma strains. Infect Immun **80:**968-974.
154. **Jia B, Lu H, Liu Q, Yin J, Jiang N, Chen Q.** 2013. Genome-wide comparative analysis revealed significant transcriptome changes in mice after Toxoplasma gondii infection. Parasit Vectors **6:**161.
155. **Hutchinson WM, Bradley M, Cheyne WM, Wells BW, Hay J.** 1980. Behavioural abnormalities in Toxoplasma-infected mice. Annals of tropical medicine and parasitology **74:**337-345.
156. **Hay J, Hutchison WM, Aitken PP, Graham DI.** 1983. The effect of congenital and adult-acquired Toxoplasma infections on activity and responsiveness to novel stimulation in mice. Annals of tropical medicine and parasitology **77:**483-495.
157. **Webster JP, Brunton CF, MacDonald DW.** 1994. Effect of Toxoplasma gondii upon neophobic behaviour in wild brown rats, Rattus norvegicus. Parasitology **109 (Pt 1):**37-43.
158. **Flegr J, Havlicek J, Kodym P, Maly M, Smahel Z.** 2002. Increased risk of traffic accidents in subjects with latent toxoplasmosis: a retrospective case-control study. BMC infectious diseases **2:**11.
159. **Vyas A, Kim SK, Giacomini N, Boothroyd JC, Sapolsky RM.** 2007. Behavioral changes induced by Toxoplasma infection of rodents are highly specific to aversion of cat odors. Proc Natl Acad Sci U S A **104:**6442-6447.
160. **Prandovszky E, Gaskell E, Martin H, Dubey JP, Webster JP, McConkey GA.** 2011. The neurotropic parasite Toxoplasma gondii increases dopamine metabolism. PLoS One **6:**e23866.

161. **Stibbs HH.** 1985. Changes in brain concentrations of catecholamines and indoleamines in Toxoplasma gondii infected mice. Annals of tropical medicine and parasitology **79:**153-157.
162. **Webster JP, Lamberton PH, Donnelly CA, Torrey EF.** 2006. Parasites as causative agents of human affective disorders? The impact of anti-psychotic, mood-stabilizer and anti-parasite medication on Toxoplasma gondii's ability to alter host behaviour. Proceedings. Biological sciences / The Royal Society **273:**1023-1030.
163. **Wang ZT, Harmon S, O'Malley KL, Sibley LD.** 2015. Reassessment of the Role of Aromatic Amino Acid Hydroxylases and the Effect of Infection by Toxoplasma gondii on Host Dopamine. Infect Immun **83:**1039-1047.
164. **Ruskin J, Remington JS.** 1968. Immunity and intracellular infection: resistance to bacteria in mice infected with a protozoan. Science **160:**72-74.
165. **Remington JS, Merigan TC.** 1969. Resistance to virus challenge in mice infected with protozoa or bacteria. Proc Soc Exp Biol Med **131:**1184-1188.
166. **Gentry LO, Remington JS.** 1971. Resistance against Cryptococcus conferred by intracellular bacteria and protozoa. J Infect Dis **123:**22-31.
167. **Mahmoud AA, Warren KS, Strickland GT.** 1976. Acquired resistance to infection with Schistosoma mansoni induced by Toxoplasma gondii. Nature **263:**56.
168. **Charest H, Sedegah M, Yap GS, Gazzinelli RT, Caspar P, Hoffman SL, Sher A.** 2000. Recombinant attenuated Toxoplasma gondii expressing the Plasmodium yoelii circumsporozoite protein provides highly effective priming for CD8+ T cell-dependent protective immunity against malaria. J Immunol **165:**2084-2092.
169. **O'Brien KB, Schultz-Cherry S, Knoll LJ.** 2011. Parasite-mediated upregulation of NK cell-derived gamma interferon protects against severe highly pathogenic H5N1 influenza virus infection. J Virol **85:**8680-8688.
170. **Hauser WE, Jr., Sharma SD, Remington JS.** 1982. Natural killer cells induced by acute and chronic toxoplasma infection. Cell Immunol **69:**330-346.
171. **Settles EW, Moser LA, Harris TH, Knoll LJ.** 2014. Toxoplasma gondii upregulates interleukin-12 to prevent Plasmodium berghei-induced experimental cerebral malaria. Infect Immun **82:**1343-1353.
172. **Neal LM, Knoll LJ.** 2014. Toxoplasma gondii profilin promotes recruitment of Ly6Chi CCR2+ inflammatory monocytes that can confer resistance to bacterial infection. PLoS Pathog **10:**e1004203.
173. **Hoffmann S, Batz MB, Morris JG, Jr.** 2012. Annual cost of illness and quality-adjusted life year losses in the United States due to 14 foodborne pathogens. Journal of food protection **75:**1292-1302.
174. **Buxton D, Thomson KM, Maley S, Wright S, Bos HJ.** 1993. Experimental challenge of sheep 18 months after vaccination with a live (S48) Toxoplasma gondii vaccine. Vet Rec **133:**310-312.
175. **Araujo F, Slifer T, Kim S.** 1997. Chronic infection with Toxoplasma gondii does not prevent acute disease or colonization of the brain with tissue cysts following reinfection with different strains of the parasite. J Parasitol **83:**521-522.
176. **Jensen KD, Camejo A, Melo MB, Cordeiro C, Julien L, Grotenbreg GM, Frickel EM, Ploegh HL, Young L, Saeij JP.** 2015. Toxoplasma gondii superinfection and virulence during secondary infection correlate with the exact ROP5/ROP18 allelic combination. mBio **6:**e02280.

177. **Fujii W, Kawasaki K, Sugiura K, Naito K.** 2013. Efficient generation of large-scale genome-modified mice using gRNA and CAS9 endonuclease. Nucleic Acids Res **41:**e187.
178. **Shen B, Brown KM, Lee TD, Sibley LD.** 2014. Efficient gene disruption in diverse strains of Toxoplasma gondii using CRISPR/CAS9. mBio **5:**e01114-01114.
179. **Koshy AA, Fouts AE, Lodoen MB, Alkan O, Blau HM, Boothroyd JC.** 2010. Toxoplasma secreting Cre recombinase for analysis of host-parasite interactions. Nature methods **7:**307-309.

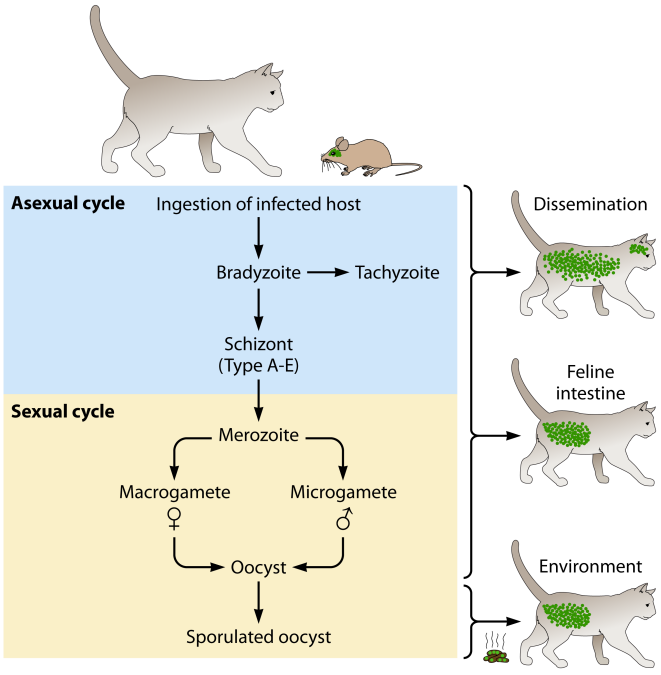

Figure 1. Sexual reproduction of *T. gondii*

Felines, the definitive host, are most often infected with *T. gondii* (depicted above in green) through ingestion of an infected host. Once ingested, *T. gondii* penetrates the epithelial cells of the small intestine and differentiates into tachyzoites and schizont stages. The asexual tachyzoites divide and disseminate throughout the feline. The schizont will remain within the intestinal epithelium and has 5 distinct stages identified as types A-E. They are classified based on their mode of division, the time post infection they are observed and their structural components. Type E schizonts give rise to merozoites, which differentiate into gametes. Gametes can be found throughout the small intestine as soon as three days and can last for a few weeks post-inoculation with tissue cysts. Males (microgametes) fertilize females (macrogametes) to produce oocysts. After fertilization occurs the oocyst wall forms around the parasite. Sporulation of oocysts occurs 1-5 days after being excreted in cat feces. Once sporulation occurs oocysts are infectious for an extended period of time depending on environmental conditions.

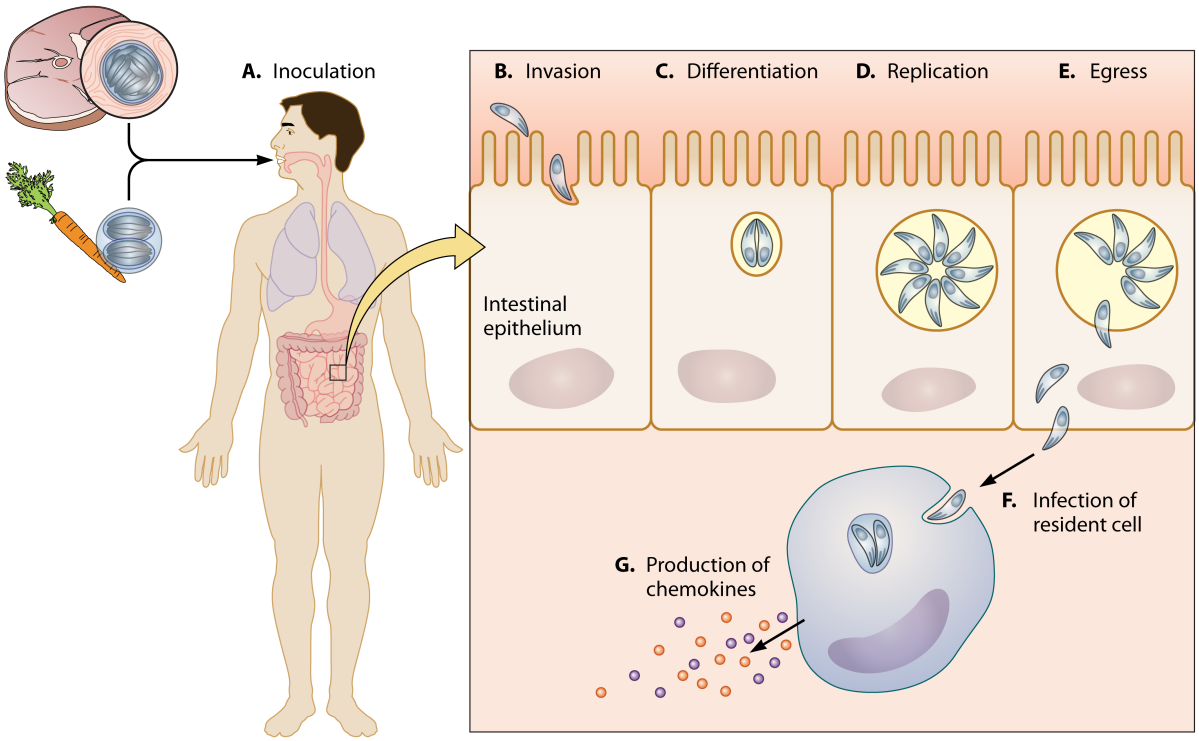

Figure 2. Ingestion of *T. gondii*

(A) Inoculation with *T. gondii* occurs from ingestion of undercooked meat containing encysted bradyzoites or food contaminated with sporozoites within oocysts. (B) Bradyzoites or sporozoites are released into the lumen of the small intestine where they invade intestinal enterocytes. (C) Parasites differentiate into the tachyzoite form where they (D) rapidly replicate and (E) egress from the cell. (F) Parasites begin invading cells of the lamina propria and encounter resident immune cells. (G) Infected resident immune cells produce chemokines to trigger migration and effector functions of circulating immune cells.

A. Recruitment of circulating immune cells

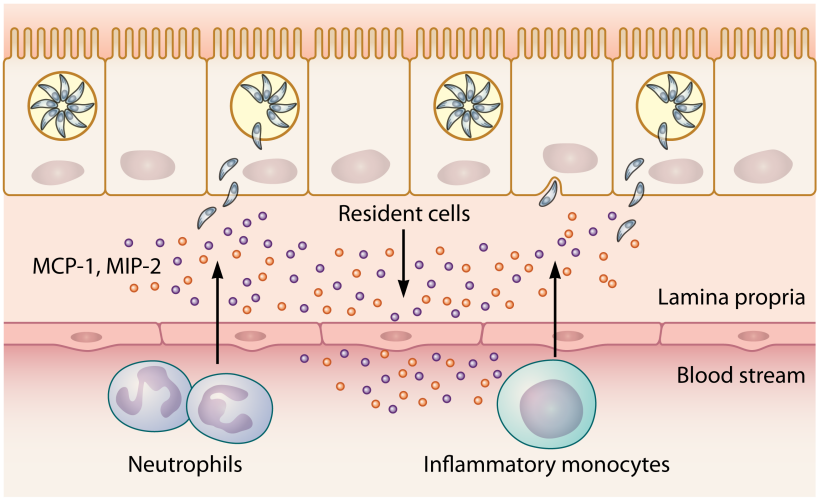

B. IL-12 production

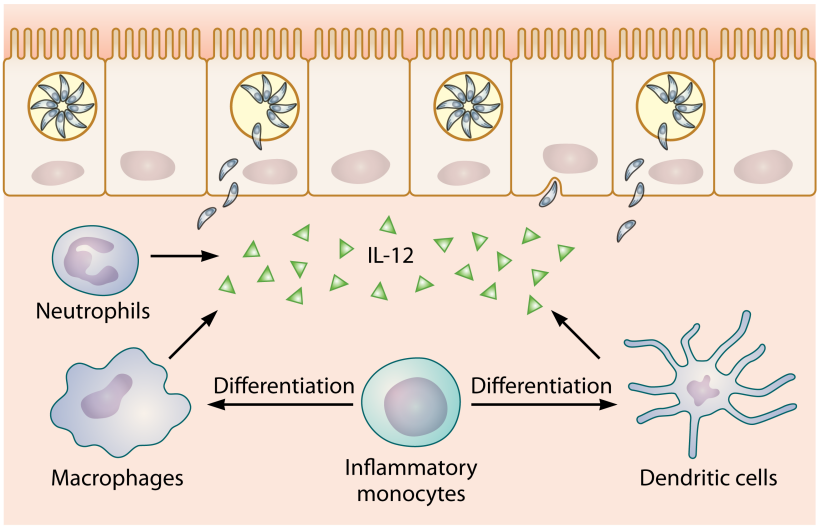

C. IL-12 response

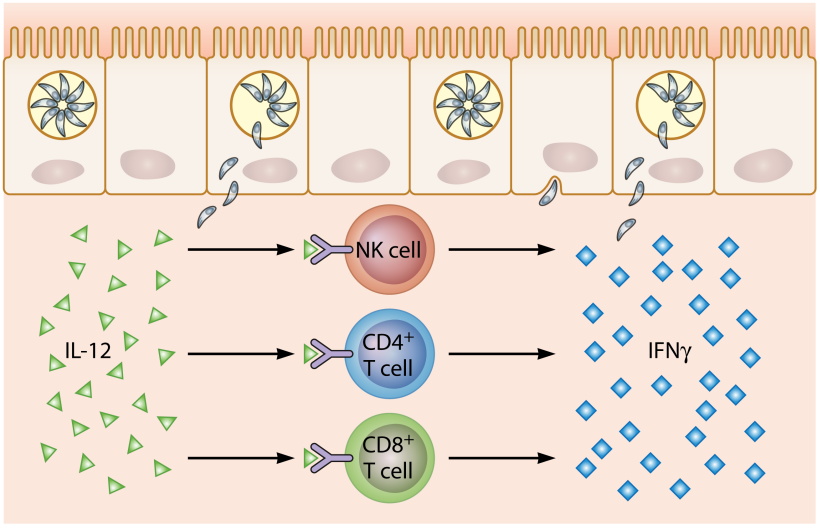

Figure 3. Innate Immune Response

(A) Chemokines secreted from cells at the site of infection, such as MCP-1 and MIP-2, trigger migration of circulating neutrophils and inflammatory monocytes to the site of infection. (B) Inflammatory monocytes differentiate into dendritic cells and macrophages where they, along with neutrophils, generate IL-12 in response to infection. (C) IL-12 stimulates NK cells, CD4+ and CD8+ T-cells to produce IFN-γ.

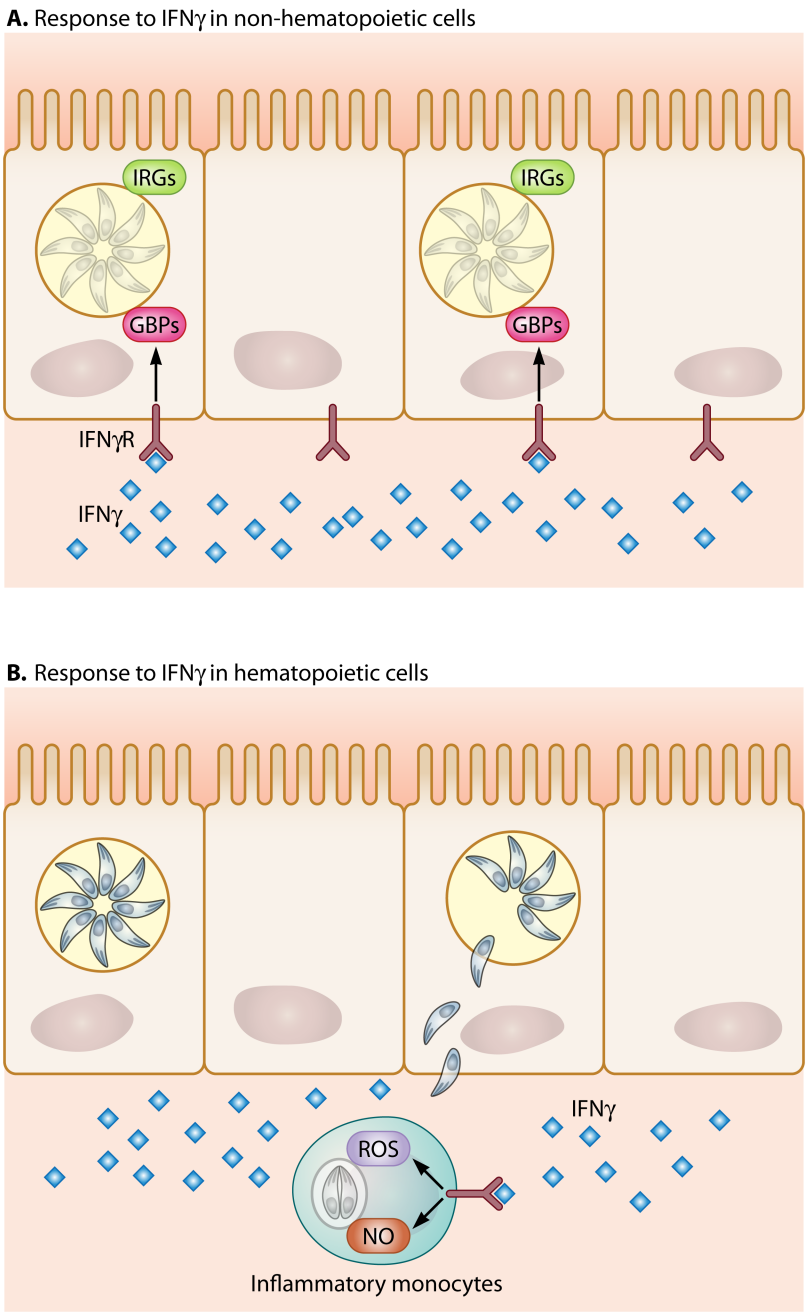

Figure 4. Cellular response to IFN-γ.

(A) A variety of host cells respond to *T. gondii* when stimulated with IFN-γ by up-regulating genes with antimicrobial functions. Two large protein families that are IFN-γ inducible are guanylate-binding proteins (GBPs) and immunity related GTPases (IRGs). GBPs and IRGs accumulate at the parasitophorous vacuole, formed upon entry of the parasite, and aid in

restriction of growth and destruction of *T. gondii* (depicted as light gray). (B) Different IFN-γ inducible mechanisms are used in immune cells, such as production of reactive oxygen species (ROS) and reactive nitrogen species (RNS). Reactive oxygen and nitrogen species are toxic and function to create unfavorable and unstable environments for intracellular parasites.

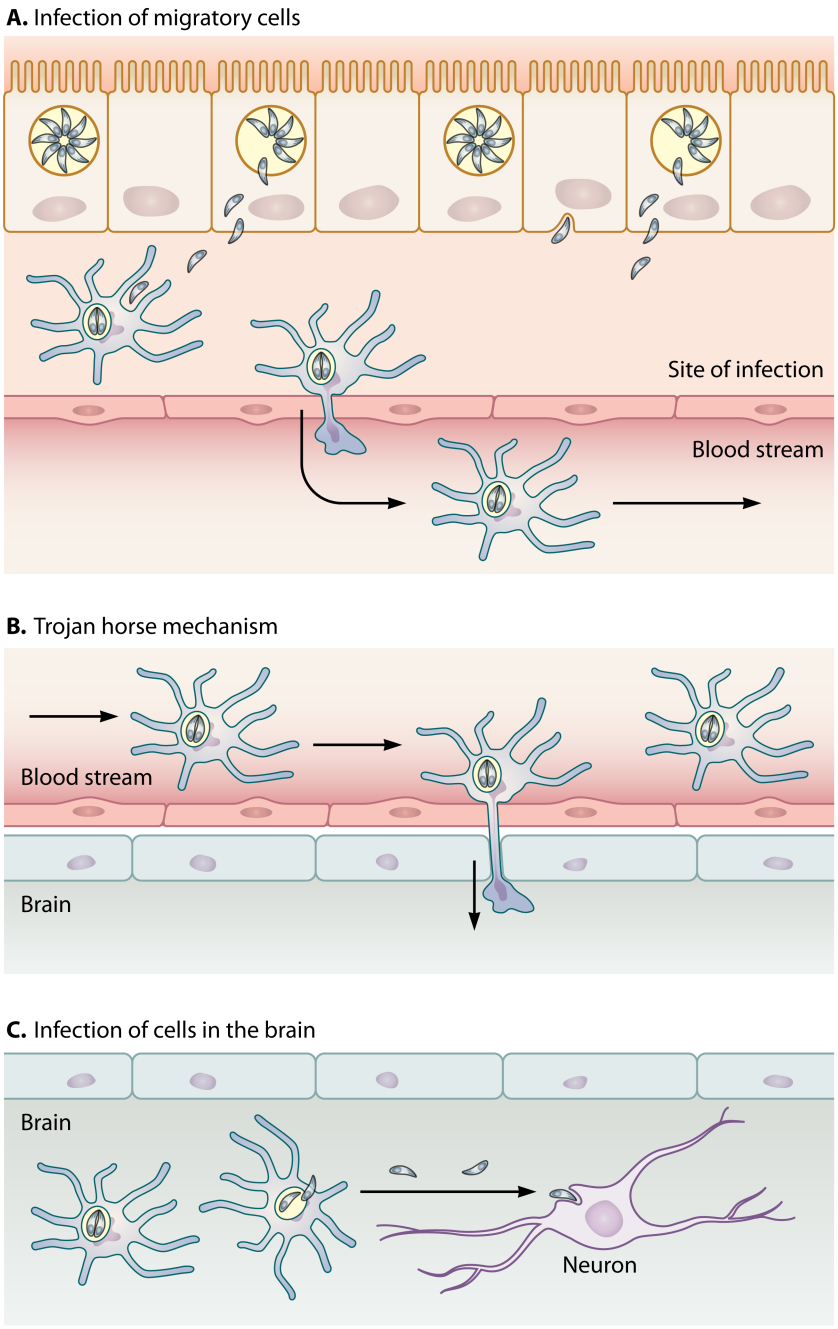

Figure 5. Infection of immunoprivileged sites.

(A) Migratory immune cells arrive at the site of infection to aid in the clearance of *T. gondii*. Some immune cells become infected, leave the site of infection and travel to other tissue carrying live parasites. This is the main mode of dissemination throughout the host. (B) *T. gondii* is able

to cross barriers, such as the blood brain barrier, into immune privileged sites by invading migratory immune cells referred to as the Trojan horse mechanism. (C) Once in brain, or other immunoprivileged site, *T. gondii* egresses from the cell and invades resident cells. In the central nervous system, *T. gondii* tachyzoites will differentiate to the bradyzoite stage, form a cyst wall, and establish a chronic infection.

Chapter 2

Dual transcriptional profiling of mice and *Toxoplasma gondii* during acute and chronic infection

Kelly J. Pittman, Matthew T. Aliota*, and Laura J. Knoll[a]

Department of Medical Microbiology and Immunology, University of Wisconsin - Madison, 1550 Linden Drive, Madison, WI 53706

This chapter was accepted for publication in BMC Genomics on September 20th 2014.

MTA and LJK designed and performed the mouse studies and collected the RNA. KJP performed all of the data analysis and prepared all of the figures. KJP and LJK wrote the manuscript. All authors have read and edited the manuscript.

Summary

Background: The obligate intracellular parasite *Toxoplasma gondii* establishes a life-long chronic infection within any warm-blooded host. After ingestion of an encysted parasite, *T. gondii* disseminates throughout the body as a rapidly replicating form during acute infection. Over time and after stimulation of the host immune response, *T. gondii* differentiates into a slow growing, cyst form that is the hallmark of chronic infection. Due to experimental limitations, a global transcriptome analysis of both host and parasite during the establishment of chronic *T. gondii* infection has not yet been performed. Here, we conducted a dual RNA-seq analysis of *T. gondii* and its rodent host to better understand host and parasite responses during acute and chronic infection.

Results: We obtained nearly one billion paired-end RNA sequences from the forebrains of uninfected, acutely and chronically infected mice, then aligned them to the genomic reference files of both *T. gondii* and *Mus musculus*. Gene ontology (GO) analysis of the 100 most highly expressed *T. gondii* genes showed less than half were shared between acute and chronic infection. The majority of the highly expressed genes common in both acute and chronic infection were involved in transcription and translation, underscoring that parasites in both stages are actively synthesizing proteins. Similarly, most of the *T. gondii* genes highly expressed during chronic infection were involved in metabolic processes, again highlighting the activity of the cyst stage at 28 days post-infection. Comparative analyses of host genes using uninfected forebrain revealed over twice as many immune regulatory genes were more abundant during chronic infection compared to acute. This demonstrates the influence of parasite development on host gene transcription as well as the influence of the host environment on parasite gene transcription.

Conclusions: RNA-seq is a valuable tool to simultaneously analyze host and microbe transcriptomes. Our data shows that *T. gondii* is metabolically active and synthesizing proteins at 28 days post-infection and that a distinct subset of host genes associated with the immune response are more abundant specifically during chronic infection. These data suggest host and pathogen interplay is still present during chronic infection and provides novel *T. gondii* targets for future drug and vaccine development.

Introduction

Toxoplasma gondii is an obligate intracellular parasite that can infect any nucleated cell of warm-blooded animals. The parasite has both sexual and asexual cycles where the sexual cycle takes place in the intestinal cells of the definitive feline host and the asexual cycle occurs in all warm-blooded animals [1]. The asexual stages of *T. gondii* consist of the rapidly replicating tachyzoite and the slow growing encysted bradyzoite. In the host, the tachyzoite is the prominent stage during initial acute infection [2]. Once the tachyzoite is subjected to stress from the host immune response, it differentiates to the bradyzoite form and eventually establishes a chronic infection [3]. The bradyzoite persists for the lifetime of the host as intracellular cysts present in striated muscle and the central nervous system [4].

T. gondii is one of the most prominent parasites in humans with prevalence rates between 10 and 80 percent worldwide, depending on the country [5]. Complications such as hydrocephaly, retinochoroiditis, mental retardation and even death can occur in developing fetuses [6, 7]. In immunocompetent humans, infection with *T. gondii* is generally asymptomatic presenting flu-like symptoms in approximately 10 percent of individuals [8]. Patients with compromised immune systems, such as those infected with HIV, are at great risk of developing severe symptoms such as Toxoplasmic Encephalitis (TE) and ocular infection that may result in

blindness [9, 10]. Disease is largely associated with sporadic reactivation of the latent bradyzoite back to the rapidly replicating tachyzoite [11]. Currently there are no drugs that can combat the bradyzoite form of the parasite or effective vaccines to protect against infection. These issues highlight the critical need to understand the cellular triggers that control development between the tachyzoite and bradyzoite stages.

Previous work to characterize the transcriptome of tachyzoite and bradyzoites from *T. gondii* has primarily used microarray technology from samples prepared in tissue culture [12-14]. Transcriptomic studies have also used a combination of in vitro and in vivo samples with in vitro tachyzoites, in vivo bradyzoites, and oocysts collected from infected felines as well as tissue culture tachyzoites and bradyzoites, developing oocysts, and bradyzoites purified from mouse brains 21 days post-infection [12, 15] While these studies have provided valuable insight into this developmental process, the information that can be extracted is limited because tissue culture conditions for tachyzoite and bradyzoite development do not precisely model animal infections. Other in vivo microarray studies have compared peritoneal-derived tachyzoites from different strain types of *T. gondii* from wild type and interferon-γ (IFN-γ) deleted mice, and transcriptional changes in the brain of mice eight days after *T. gondii* infection [16-18]. These studies have highlighted important aspects of the developmental process, but the dynamic range of microarrays is restricted and sample preparations are unable to be simultaneously processed and analyzed for both host and pathogen. One way to overcome these limitations is RNA sequencing (RNA-seq), a breakthrough molecular tool that can provide the transcript profile (transcriptome) of total cellular RNA with a large dynamic range and improved sensitivity [19]. RNA-seq has detected novel *T. gondii* tachyzoite transcripts and alternative splicing between strains [20]. RNA-seq of tissue culture-derived bradyzoites has shown dysregulation of

bradyzoite genes in the deletion mutant of a mucin domain containing cyst wall protein CST1 [21]. Using RNA-seq, transcriptome analysis has been performed to compare mouse brains that were uninfected or infected with *T. gondii* for 32 days [22]. These data highlight the sensitivity and depth of knowledge that can be obtained from RNA-seq studies; however, a time course of *T. gondii* infection and simultaneous analysis of the parasite transcriptome has not been performed.

To provide a more comprehensive analysis of *T. gondii* and the host during both acute and chronic infection, we collected RNA-seq data from three experimental groups of mice: uninfected, 10 and 28 days post-infection. Because *T. gondii* preferentially establishes cysts in the brains of mice and reactivation of cysts is the main cause of TE, we chose to analyze the brains of mice. A novel aspect of this dataset is that parasites were not purified from the brain tissue but instead, samples were rapidly processed so that RNA-seq reads represent the "interactome" between host and pathogen during the peak of acute and chronic infection. We report that many genes involved in *T. gondii* transcription, translation and metabolism are highly expressed during chronic infection. For the host, we find that more genes are increased in abundance during chronic versus (vs) acute infection, attesting to a continuously active host response even at 28 days post-infection.

Results

Sequencing and mapping the *T. gondii*/host interactome

To study parasite-host gene expression dynamics we used RNA-seq on samples collected from forebrains of mice infected with type II strains of *T. gondii* (schematized in Figure 1). Type II strains of *T. gondii* have been detected in the mouse brain as early as 4 days post-infection and

numbers continue to increase until 10 days post-infection [23, 24], the peak of acute infection [25]. Cyst structures are present in the brains of mice at 21 days post-infection [26], which is generally considered to be the beginning of chronic infection. By 28 days post-infection, cysts have stably formed in the brain while parasite numbers have decreased elsewhere in the body [23, 27]. When brains were sectioned and analyzed for parasite distribution, high numbers of *T. gondii* were observed in the frontal lobe at 32 days post-infection [22]. We examined mouse brains at 10 and 28 days post-infection using an In Vivo Imaging System (IVIS), which confirmed that parasites were primarily localized in the forebrains of mice (Figure 1). Therefore to maximize parasite transcripts as well as to compare the same host tissue during acute and chronic infection, we chose to collect mouse forebrain samples at 10 and 28 days post-infection as well as uninfected mice. Nine mouse forebrains were sequenced individually: three uninfected, three infected for ten days and three infected for 28 days. Nearly one billion 100 base-pair (bp) paired-end RNA sequences were generated. Between 81,000,000 and 114,000,000 reads were obtained from each forebrain sample (Table 1). Between 69-76% of the reads aligned to the *M. musculus* reference genome while approximately 0.1% aligned to the *T. gondii* TGME49 reference. Since *T. gondii* was not purified from the forebrains as a means to rapidly process the samples and preserve the interactome, uninfected mouse forebrain samples were mapped to the *T. gondii* TGME49 reference to determine the extent of false positive reads. A small number of uninfected mouse reads aligned to the *T. gondii* genomic reference file (Table 1). The reads aligned to *T. gondii* ribosomal associated RNA or small (~200-300 bp) hypothetical proteins, none of which were considered differentially expressed and were treated as background.

Transcript abundance of *T. gondii* during acute and chronic infection in mice

Abundance estimates for each *T. gondii* gene were calculated and the three biological replicates for each time point were averaged before differential expression analysis was performed using Cuffdiff, a Cufflinks program. Cuffdiff calculates the fold change to determine which genes are differentially regulated between time points. Cuffdiff also calculates a p-value and q-value to determine if the fold change and is significant. Each forebrain was treated as a biological replicate in Cuffdiff and therefore variation between replicates was considered when assigning a p-value. A p-value and q-value <0.05 were considered significant. It is important to note that parasites were not purified from mouse forebrains prior to RNA extraction. As a result, the concentration of *T. gondii* RNA could not be normalized between time points. To address the potential difference in parasite numbers between each sample and each experimental time point quantitative PCR was performed using genomic DNA extracted from the forebrains at the time of RNA extraction. Parasite numbers for each 10 day and 28 day post-infection sample was determined based on a standard curve generated from serial dilutions of genomic DNA extracted from a known number of parasites. Between 340 and 532 parasites per 350ng of genomic DNA were detected in 10 days post-infection samples (Table 2). Forebrains infected for 28 days were more variable with between 100 and 3160 parasites per 350ng of genomic DNA present (Table 2). The variability of parasite burden during later stages of *T. gondii* infection is common as cyst counts and number of bradyzoites in individual cysts differs over time[28, 29].

To determine how differences in parasite burden affects transcript levels, the FPKM fold change of housekeeping genes α-tubulin, actin, glyceraldehyde 3-phosphate dehydrogenase 1 and 2 (GAPDH 1 and 2), and hexokinase were examined between acute and chronic time points.(Table 3). The fold change of these housekeeping genes between chronic and acute time points were

0.59-1.8, suggesting that global parasite transcript levels in our acute and chronic infection samples do not dramatically change. When comparing the fold change of previously characterized tachyzoite-specific genes, surface antigen 1 (SAG1) and microneme protein (MIC) 1, and bradyzoite specific genes bradyzoite antigen 1 (BAG1) and enolase 1 (ENO1), we saw large differential expression between acute and chronic infected mice (Table 3). These results along with qPCR performed on genomic DNA suggest that the significant differential expression of genes between time points is due to a global shift in transcript abundance, rather than an overabundance of transcripts in chronically infected mice compared to acutely infected mice. To account for variability of parasite numbers at 28 days post-infection differentially expressed *T. gondii* genes with a fold-change of >5 were considered for further analysis. The low abundance of SAG-1 and high abundance of BAG-1 between 28 day post-infection and 10 day post infection time points also suggests that tachyzoites are the primary stage present at 10 days post-infection, while the majority of parasites at 28 days post-infection are in the bradyzoite stage.

To explore the similarities in expression of *T. gondii* genes during acute and chronic infection, the 100 most highly expressed genes from acute and chronic time points were compared. Forty-two of the most highly expressed *T. gondii* genes during the acute stage were also among the 100 most highly expressed transcripts during the chronic stage (Figure 2A). To help interpret the biological functions of these genes, statistically over-represented GO terms were compiled (Figure 2B) using the Blast2GO program, a GO term analysis program for non-model organisms [30]. The GO term categories for the genes with the greatest abundance in both acute and chronic samples were transcription, translation, macromolecule biosynthesis and cellular metabolism.

Differential expression of *T. gondii* between acute and chronic infection in mice

To further investigate the transcriptome of *T. gondii* during acute and chronic infection, differential expression analysis was performed. Fold change and significance values were calculated for each of the ~8900 annotated *T. gondii* genes (additional file 1). From this analysis, we found 547 significantly differentially expressed genes (DEGs, with p-value and q-value <0.05) between acute and chronic infection. Of these, the DEGs with a fold change of >5 are presented in Tables 4 and 5.

Sixty-three *T. gondii* genes were >5 fold more abundant in acute compared to chronic infection (Table 4). SAG-related sequence (SRS) are a family of GPI-anchored surface antigens related to the first characterized *T. gondii* surface antigen, SAG1 [31]. SRS2/SRS29C was the most differently expressed gene in acute compared to chronic infection, 305-fold. Five additional SRS genes were >5 fold more abundant: SRS20A, SAG1/SRS29B, SAG2/SRS34A, SRS54 and SRS52A. Four genes for rhoptry proteins (ROP) were >5 fold more abundant: during acute infection: ROP9, ROP16, ROP39, and ROP40. ROP16 is involved in decreased synthesis of cytokines in mouse bone marrow-derived macrophages [32]. ROP9 is a tachyzoite-specific protein with no known function [33]. ROP39 and ROP40 have homology to ROP2, but the functions have yet to be elucidated. Because of the extensive study of tachyzoites, most of the DEGs highly abundant in acute compared to chronic infection (Table 4) have been previously identified as tachyzoite-specific markers. Twenty-six of the 63 acute infection DEGs encode hypothetical proteins, with no homology to any annotated protein in the BLAST database. Characterizing these hypothetical proteins could be vital to understanding parasites during acute infection.

Fifty-one of the 107 *T. gondii* DEGs associated with chronic infection with a >5 fold change are annotated as hypothetical (Table 5). Among the chronic infection DEGs, four microneme proteins were identified MIC12, MIC13, MIC17A and MIC17C. MIC12 and MIC13 were previously shown to be bradyzoite specific [12], but our data revealed MIC17A and MIC17C abundant specifically during chronic infection. Another interesting group of chronic infection DEGs are those involved in glycolysis: glucose-6-phosphate isomerase, pyruvate kinase, lactate dehydrogenase 2, and glucosephosphate mutase. Previous data showed that tachyzoites and bradyzoites use the glycolytic pathway differently with lactate dehydrogenase 2 and pyruvate kinase being up-regulated during the bradyzoite stage [34] [35]. Our data shows that in addition to these two previously described bradyzoite-specific glycolytic enzymes, glucose-6-phosphate isomerase and glucosephosphate mutase are also more abundant in chronic vs acute infection. These results strengthen the idea that bradyzoites do not have an active TCA cycle because the transcripts of the key enzymes in the TCA cycle were less abundant in chronic infection compared to acute. Four SRS genes were also identified as more abundant in chronic compared to acute infection. SRS35A, also known as SAG4 and P18, is a long-known bradyzoite-specific marker [36]. SAG2C/SRS49D and SRS9/SRS16B are previously identified bradyzoite-specific genes that are important for persistence of infection [37-40]. SRS13 was identified as up-regulated in a microarray analysis comparing tissue culture tachyzoites to mouse-derived bradyzoites, but the function has yet to be determined [12]. Several novel chronic infection DEGs were found including DnAK-TPR, heat-shock protein 21, calcium dependent protein kinase CDPK5 (Table 5). The high number of novel and hypothetical DEGs highlights the fact that much is still unknown about *T. gondii* during animal infection. These hypothetical proteins have no known homology to proteins in the host and therefore could be essential and

specific to parasite function during infection. Identification of novel DEGs that could play critical roles in *T. gondii* infection is the first step in elucidating potential targets for both vaccine and drug development.

To highlight the accuracy and sensitivity of RNA-seq, qPCR was performed on a family of CCCH zinc fingers in *T. gondii* that are more abundant in our data set during chronic infection. TGME49_224630, TGME49_262970, and TGME49_311100 contain CCCH zinc finger domains and had a fold change of 86, 26, and 4.68, respectively (Table 5 excluding TGME49_311100 which did not meet the >5 fold cut-off). These genes were chosen based on the possible similarity in function and the range of transcript differential expression between chronic and acute infection. The increase in abundance of these transcripts between 10 day and 28 day post-infection was observed using qPCR when normalized to the house keeping gene tub1a. The fold change between chronic and acute infection for TGME49_224630, TGME49_262970, and TGME49_311100 were 53, 79, and 6.1 respectively. Not only does this data demonstrate the range and accuracy of RNA-seq, but also confirms the validity of the differential expression analysis.

Differential expression of host genes during *T. gondii* infection

To understand the transcriptional changes of the host during stages of *T. gondii* infection, differential expression analysis was conducted. Differential expression was determined between acute vs uninfected, chronic vs uninfected, and acute vs chronic time points. Genes were considered differentially expressed if the p-value and q-value was <0.05 and the fold change between time points was >2-fold. The host underwent extensive transcriptional changes during *T. gondii* infection (Figure 3A). When comparing acute *T. gondii* infected mice with uninfected, 1004 mouse genes were more abundant during acute infection and 143 were less abundant

(Figure 3A). Over twice as many mouse genes, 2510, were more abundant in mice with a chronic *T. gondii* infection compared to uninfected while only 132 genes were less abundant. Finally, 1872 mouse genes were more abundant and 190 were less abundant in chronically vs. acutely infected mice. This increase of differentially regulated host genes during chronic infection is illustrated by Venn diagram analysis of DEGs >2-fold (Figure 3B). To understand the similarities and differences between DEGs more abundant during acute vs uninfected and chronic vs uninfected time points, we identified genes that had increased abundance at both time points as well as those found only in acute or chronic (additional files 2, 3 and 4). Out of the 1004 DEGs more abundant in acute vs uninfected, 902 were also abundant in the chronic vs uninfected group. More mouse genes, 1608, were increased in abundance in the chronic vs uninfected time point that were not considered differentially expressed in acute. This data suggests genes activated during the peak of acute infection are maintained during chronic infection and that an entirely new subset of transcripts are expressed during chronic infection. The increase in differentially expressed genes during chronic infection could also be due to recruitment of cells to the site of infection.

GO term enrichment analysis of DEGs in mice during *T. gondii* infection

To understand the functions of DEGs in mice during acute and chronic *T. gondii* infection and to characterize the overlap between DEGs at these time points (Figure 3B) we performed GO term enrichment and DAVID analyses. Among the host genes more abundant during both acute and chronic infection stages, overrepresented GO terms were related to stress and immune responses (Figure 3C). This suggests infection with *T. gondii* stimulates the immune response and/or immune cell recruitment into the brain even when the majority of parasites are in the encysted

stage, as seen by the increased abundance of BAG1 and decreased abundance of SAG1 (Table 3). It also suggests a specific subset of host genes are responsible for immune stimulation during chronic infection that are distinct from acute, although many acute infection associated genes are still activated.

Only a small number of host DEGs were less abundant during both acute and chronic infection (Figure 4A). Go term analysis of DEGs with decreased abundance showed little functional overlap between the different stages of infection. The few commonalities in GO categories included secondary metabolism, membrane organization and phagocytosis (Figure 4B). The proposed functions of the DEGs that were less abundant specifically during acute infection were different from those less abundant during chronic infection. GO terms for genes with decreased abundance specifically during acute infection were proteolysis, protein metabolic process, and anatomical structure, while GO terms specific to chronic infection were cell-cell communication and primary metabolic function. The enrichment of metabolism-associated processes among less abundant DEGs suggests a link between *T. gondii* infection and host metabolism, possibly as a means of restricting parasite growth.

Analysis of the mouse genes with increased abundance during *T. gondii* infection

Given that more host transcripts had >2-fold increased abundance during chronic infection (Figure 3B), further examination of the most abundant mouse genes during acute and chronic time points was performed to enhance the understanding of the host response. DEGs with a FPKM fold change >20 were compared between acute vs uninfected and chronic vs uninfected mice (Figure 5A). 155 genes met this cut-off in the acute vs uninfected group while 540 genes had 20-fold or higher FPKM values in chronic vs uninfected time points. Of these more abundant

DEGs, 146 were shared between acute vs uninfected and chronic vs uninfected groups. Only 9 more abundant DEGs had a fold change >20 in acute vs uninfected that were not highly abundant in chronic vs uninfected time points. Several of these acute-infection specific host genes belong to the family of guanylate-binding proteins, which are GTPases that are induced by interferon-γ (Table 6). Conversely, 394 DEGs had a fold change of >20 in chronic vs uninfected that did not meet this cut-off in acute vs uninfected. The majority of genes increased in abundance during acute infection are maintained into chronic infection. These results show that few host genes are specifically increased during acute *T. gondii* infection. It also suggests a unique set of host genes are differentially expressed during chronic infection.

Elevation of immune response genes during chronic infection

To assess the function of the mouse genes increased in abundance specifically during chronic infection, GO term enrichment was performed on genes with a fold change >20 in chronic vs acute infection. GO terms for genes highly increased in abundance during chronic infection were related to stress and immune responses (Figure 5B). Table 7 shows the top 50 DEGs more abundant during chronic infection. Many of these genes are immunoglobulin heavy chain variable regions, which share sequence similarity and can be difficult to differentiate between. The variable regions of immunoglobulins are responsible for specificity of antibodies to antigens, suggesting a different subset of antibodies being produced in response to *T. gondii* antigens that may not be abundant during acute infection. Another highly differentially expressed set of genes are H2-EB2 and H2-M2, both of which are involved in antigen presentation. H2-EB2 is an MHC class I membrane-associated protein while H2-M2 is an MHC class II membrane-associated protein. These antigen-presenting proteins are key players in the continued

stimulation of the immune system at later time points. This increased in abundance of immune genes during chronic infection indicates a unique set of DEGs may be involved in the chronic infection immune response and/or a novel population of immune cells are recruited into the brain after acute infection.

Discussion

Infection with *T. gondii* is often asymptomatic in immune competent individuals, but presents serious health risks if acquired congenitally or if a person becomes immune-compromised. Rising evidence is showing complications, such as psychiatric disorders and increased rates of suicide, occur in people with healthy immune systems who have a chronic *T. gondii* infection [41, 42]. Currently, drug treatment is only effective against the acute stage of infection and there are no therapeutics interventions available to target the encysted form during chronic infection. There are also no vaccines against *T. gondii* approved for use in humans. This lack of therapeutic intervention highlights the need to better understand the biological differences between the acute rapidly replicating form of the parasite and the chronic associated cyst stage.

Our data provides a list of candidate genes that could be targeted for novel therapeutics or gene deletion to create a non-persistent vaccine strain (Tables 4 and 5). Many of these genes highly differentially regulated are hypothetical proteins with no known orthologs in other organisms. Hypothetical *T. gondii* genes not found in the mammalian host could be excellent pathogen specific drug targets. The fact that multiple *T. gondii* microneme proteins are more abundant in chronic infection stages raises the question of whether parasites during chronic infection are actively invading cells. If parasites are invading at this time, this could explain the continued stimulation of the host response so late in infection. Although microarray analysis of

human fibroblasts showed that tissue culture derived bradyzoites stimulated a weaker immune response than tachyzoites after two days [43]. An additional *T. gondii* gene that is more abundant in chronic infection is cAMP-dependent protein kinase. cAMP-dependent protein kinase is crucial for growth of tachyzoites and is proposed to be critical in tachyzoite to bradyzoite stage conversion[44] [45], but the mechanism is unknown. Another potentially interesting *T. gondii* gene that is more abundant in chronic infection is calcium dependent protein kinase 5, CDPK5. The *T. gondii* paralog, TgCDPK1, was shown to be necessary for tachyzoite motility, invasion and egress [46]. Studying the role of CDPK5 in bradyzoite development could be pivotal in understanding the biology of this stage.

Our study also provides crucial insight into host response to the parasite during both acute and chronic infection. It shows that, at least in the beginning stages of chronic infection, the host immune system is still actively combating infection. Chronic infection of *T. gondii* is typically thought of as a period in which the parasite transitions to the encysted, less immune stimulatory form resulting in a dampening of the immune response. Another study assessing the mouse transcriptome showed many immune associated genes are still expressed at 32 days post *T. gondii* infection [22]. To assess the overarching function of genes increased in abundance between acute and chronic infection Kyoto Encyclopedia of Genes and Genomes (KEGG) pathway analysis was performed. The KEGG database is a bioinformatics tool that assembles large-scale molecular datasets, such as gene lists, into biological pathway maps. Analysis of our dataset suggests active NK cells are recruited to the brain during chronic infection by the increased abundance of perforin, granzymes A and B, and IL-10 (additional file 4). NK cells have long been known to be essential for the control of acute *T. gondii* infection [47], but their role in chronic infection maintenance has yet to be elucidated. NK cells are a significant source

of IFN-γ during acute *T. gondii* infection [48, 49] and IFN-γ is also necessary to maintain chronic infection [50], but producers of IFN-γ during chronic infection have not been determined. In mice with an established chronic *T. gondii* infection, NK cells are a major source of IFN-γ essential to combat infection with H5N1 influenza virus [51]. Chronic *T. gondii* infection was equally effective to protect against lethal influenza virus whether the mice had been infected with *T. gondii* for 1 month or 4 months, suggesting that NK cells are active in late stages of chronic infection. Similarly, NK are elicited in peritoneal exudate 6 months after *T. gondii* infection [52]. Our data suggests that NK cells play a role in chronic *T. gondii* infection maintenance, which will be the focus of future studies in understanding infection persistence.

Production of nitric oxide (NO) is crucial for control of *T. gondii* growth [53, 54], and triggers differentiation of tachyzoites into bradyzoites in tissue culture [55]. Mice deficient in the inducible nitric oxide synthetase gene succumb to non-lethal doses of *T. gondii,* but only during chronic infection [53] [54]. One host gene differentially expressed during chronic infection is arginase-1 (ARG-1), which had a fold change of nearly 70 in chronic vs. acute samples (Table 7). Arginine is not only a substrate for NO production, but it is an essential amino acid for *T. gondii* [56]. ARG-1 depletes host cell arginine, possibly as means to starve the parasite, but in type I strains, *T. gondii* initiates expression of ARG-1 via ROP16, potentially to preserve infected tissue [32]. While NO is detrimental for parasite growth, it also results in inflammation and subsequent destruction of host tissue. In the brain, microglial cells are the main producers of NO and have the potential to cause neuronal degradation. *T. gondii*-infected astrocytes secrete factors that decrease NO production by microglial cells, thus preserving both host and pathogen during latent infection [57]. It is unclear whether the increase in ARG-1 transcripts are induced by *T. gondii* or the host as ROP16 is more abundant in *T. gondii* during acute infection (Table 4),

and ARG-1 is more abundant in the host during chronic infection. Furthermore, ROP16 is polymorphic and in type II strains, such as ME49 used in this study, does not maintain STAT3/6 activation and may not initiate ARG-1 expression [58]. An alternative mechanism may be responsible for the increased abundance of ARG-1 during chronic infection. Another highly differentiated host genes during chronic infection is kallikrein-6 peptidase. Kallikrein peptidases have been implicated in infection through involvement in vasodilation and permeability [59], but in the context of bacterial infections, kallikreins are also involved in the generation of NO [59, 60]. Specifically, kallikrein-6 has been shown to be up-regulated in the CNS during inflammation, possibly as a means to promote lymphocyte survival [61, 62]. Our data suggest kallikrein proteases could be involved in the parasite's transition from the rapidly replicating form to the encysted form in the host. Together these data suggest that regulation of NO production during chronic infection is of vital importance for both the host and the parasites, and will be a future avenue of research.

Conclusions

The depth of RNA-seq coverage allowed, for the first time, simultaneous sampling of both host and microbe during acute and chronic stages of animal infection. In this study, we show the majority of highly expressed *T. gondii* genes common to both acute and chronic infection are involved in transcription and translation, underscoring that parasites in both stages are actively synthesizing proteins. Similarly, most of the *T. gondii* genes highly expressed during chronic infection are involved in metabolism, highlighting the metabolic activity of the cyst at 28 days post-infection. For the host, analysis of transcripts at 10 and 28 days post-infection compared to uninfected mice showed that more immunity associated host genes are increased in abundance at

28 days post-infection vs 10 days post-infection. The increase in abundance of *T. gondii* genes during chronic infection is in conjunction with the heightened host response; indicative of the constant battle for survival between the host and the parasite. Discussed here are only a few examples of hypotheses that can be generated from this transcriptome data set. This dataset is novel because information from the host and pathogen is provided at multiple time points, allowing for the interplay between both to be studied. Many platforms, such as KEGG pathways and DAVID, are available for the research community to further investigate these data and cater to their scientific interests. This data provides the potential to elucidate mechanisms required for Apicomplexan parasites to maintain a relationship with their hosts, which will lead to better therapeutics, vaccines and diagnostic methods.

Materials and methods

IVIS detection of *T. gondii* in the mouse forebrain at 10 days and 28 days post-infection

The ME49 strain of *T. gondii* with a deletion of the gene *HPT* and an insertion of the coding region for firefly luciferase, as previously described [63], was used for these experiments. 6-8 week old BALB/C mice (National Cancer Institute, Charles River Laboratories, Frederick, MD) received an intraperitoneal (i.p.) inoculation of 10^4 freshly lysed tachyzoites. Mice were imaged using IVIS (PerkinElmer) at 10 days and 28 days post-infection. Mice were anesthetized with isoflurane and intravenous (i.v.) injected with 3mg of luciferin, the substrate for luciferase, and imaged ventrally, dorsally, and then sacrificed. The brains of the mice were removed and soaked in luciferin for 5 minutes prior to imaging.

Generation of mRNA and RNA-seq

A ME49 strain of *T. gondii* that was recently passaged through the sexual cycle was used to inoculate mice for RNA-seq analysis. ME49 was maintained as tachyzoites in monolayers of Human Foreskin Fibroblasts in Dulbecco's Modified Eagle's Medium supplemented with 10% FBS, 2 mM L-glutamine, and 1% penicillin-streptomycin. 6-8 week old CBA/J mice (National Cancer Institute, Charles River Laboratories, Frederick, MD) were either left uninfected or i.p. injected with 10^4 parasites and were sacrificed at 10 days and 28 days post-infection. Uninfected mice were sacrificed along with the 28 day post-infection group. We selected *T. gondii* infected mice that were healthy and not displaying any signs of disease, so samples would not contain host transcripts involved with inappetence, dehydration or general malaise to confound our analyses. To minimize changes to the transcriptome, the forebrains were rapidly and precisely sectioned at the intersection of the optic nerves using a mouse brain matrix (Zivic Instruments) with less than one minute between animal sacrifice to forebrain homogenization in 3 mL of TRIzol. Total RNA was isolated according to manufacturer's protocol. RNA was purified using Promega SV total RNA isolation system according to manufacturer's protocol. RNA was submitted to the University of Wisconsin Biotechnology Center for purity analysis using the Agilent 2100 Bioanalyzer and sequencing using the Illumina HiSeq2000. Sequencing was performed on each individual mouse and samples were not pooled. Infection was quantified in the un-used hindbrains collected at 28 days post-infection and stained with fluorescein labeled *Dolichos biflorus* agglutinin (Vector Laboratories) for cyst detection. All 28 day post-infection hindbrains contained a minimum of 10,000 cysts.

Determination of *T. gondii* parasite numbers in mouse forebrain samples

Genomic DNA was extracted from each mouse forebrain at the time of RNA extraction using TRIzol according to manufactures instructions. DNA was purified by phenol/chloroform

extraction followed by ethanol precipitation. Genomic DNA was used as the template for quantitative PCR using *T. gondii* primers for the housekeeping gene alpha-tubulin (TUB1A). Tub1A Forward primer 5'-GACGACGCCTTCAACACCTTCTTT-3', Tub1A Rev 5'-AGTTGTTCGCAGCATCCTCTTTCC-3'. Primer efficiency for TUB1A was 2.002 with an R^2 value of .99 using *T. gondii* genomic DNA. To determine parasite burden in the mouse forebrain samples, a standard curve was generated using a genomic DNA preparation of known parasite numbers. Quantitative PCR was performed on serial dilutions of parasite genomic DNA, using TUB1A primers, ranging from 1x10^6 to 10 parasites. A best-fit logarithmic line was generated with an R^2 of 0.999. The equation of the line along with Ct values obtained from qPCR of TUB1A on genomic DNA from each forebrain sample was used to extrapolate parasite numbers (Table 2). qPCR was performed on each sample in duplicate using BIO-RAD iTaq Universal SYBR Green Supermix product number 172-5121.

Quantitative PCR of *T. gondii* CCCH zinc fingers

Sequences for TGME49_224630, TGME49_269270, and TGME49_111100 were obtained from ToxoDB.org. Sequences were run through BLASTp to confirm presence of CCCH zinc finger motifs. cDNA was generated from the same RNA samples used for RNA sequencing with Invitrogen Superscript III Reverse Transcriptase cDNA synthesis kit. All CCCH zinc fingers were normalized to the *T. gondii* house keeping gene tub1A. Efficiencies were determined using in vitro bradyzoite cDNA. RNA was extracted from 5 day bradyzoites grown under low CO_2 and high pH conditions using TRIzol. cDNA was generated using the Invitrogen Superscript III Reverse Transcriptase cDNA synthesis kit. Efficiencies were calculated using the slopes of a 1:10 dilution series (neat through $10^{4)}$ and the formula $E = 10^{[-1/\text{slope}]}$. Efficiencies for tub1A, TGME49_224630, TGME49_269270, and TGME49_111100 were 1.96, 1.89, 2.14, and 2.04

(Between 90-107% efficient). Quantitative PCR was performed using Bio-Rad iTaq Universal SYBR Green Supermix on an Applied Biosystems StepOnePlus Real-Time PCR system. Primers were used at a 300nm concentration and an extension temperature of 60 °C for 60 seconds. Relative quantification was calculated using Pfaffl's method [64]. Three biological replicates were used and conducted in duplicate. Wells with only one melt curve and temperature were used, and duplicate Ct values were all at or below a 0.25 difference in cycle threshold value.

RNA-seq, mapping and differential expression analysis

Approximately 950,000,000 paired end 100 bp reads were generated from Illumina HiSeq2000 sequencing. Aligning RNA-seq data for eukaryotic organisms becomes difficult when mapping to a genomic reference because of the presence of introns in the reference and polyadenylated transcripts in the data. If an RNA-seq read spans an exon-exon junction or a polyadenylated region of a transcript it will be "unmappable" to the reference genome and is discarded. Bioinformatics software, such as TopHat, has been created to consider exon-exon boundaries during the mapping process [65]. Raw reads were uploaded onto the Galaxy platform [66-68]. Reads were filtered by Sanger quality score using FASTQ Groomer v. 1.0.4 and paired end reads were aligned against the genomes of *T. gondii* (TGME49 version 9.0; ToxoDB.org) and *M. musculus* (GRCm38 version 74.38; ensemble.org/Mus_musculus) references uploaded into Galaxy using TopHat2 [69]. Parameters for TopHat2: Max edit distance of 2, final read mismatch of 2, anchor length of 8, minimum intron length of 70, maximum intron length of 500000, max insertion and deletion length of 3, number of mismatches allowed of 2, and a minimum length of read segments of 25. Reads were not treated as strand specific as they were paired end reads. The total numbers of reads were as followed: Uninfected mouse 1 was 112075860, Uninfected mouse 2 was 112948998, Uninfected mouse 3 was 103209252, 10 day

post-infection mouse 1 was 102581171, 10 day post-infection mouse 2 was 125546828, 10 day post-infection mouse 3 was 81630704, 28 day post-infection mouse 1 was 103765423, 28 day post-infection mouse 2 was 113094439, and 28 day post-infection mouse 3 was 114177191. The number of reads that mapped to the *Toxoplasma gondii* genomic reference file and *mus musculus* genomic reference files are listed in Table 1.

The program Cufflinks [65] was used to convert aligned reads of BAM files, generated from Tophat2, into relative expression values for each gene represented as FPKM (fragments per kilobase of exon per million mapped reads). Cuffdiff was used to detect significant changes in differential expression between the experimental groups. When running Cuffdiff, a GTF file obtained from ToxoDB.org and ensemble.org/Mus_musculus was used as a guide and the TopHat2 aligned BAM files from each biological replicate were used as the source of comparison between experimental groups. A geometric library normalization and a pooled cross-replicate dispersion estimation method was used when comparing differential expression between each experimental group. Genes with a p-value, for statistical significance, and q-value, to detect the false discovery rate, of <0.05 were considered differentially expressed. The "gene differential testing" output file from Cuffdiff was used to identify differentially expressed genes.

GO term analysis

FASTA sequences of the most abundant *T. gondii* genes from different time points during infection were loaded into the program Blast2Go [30]. *T. gondii* is not an available organism on many GO term analysis programs, making Blast2Go ideal for uncommon models. Sequences were run with the blastx program against the nr database. Aligned sequences were mapped and assigned GO term annotations. Combined graphs were generated representing the most enriched GO terms in the provided gene list. A score was assigned to determine significance of

enrichment. For analysis of *M. musculus,* a gene list was generated from each experimental time point based on gene names in column C of Additional files 2,3, and 4. Ensembl gene IDs were obtained from the gene names, exported from BioMart, and uploaded to the functional annotation tool. A functional annotation chart of the enriched GO terms was generated using GO terms associated with biological process. GO terms were assigned a p-value to indicate significance of enrichment [70]. Only GO terms with a p-value <0.05 were used to represent functional enrichment. For further analysis of *M. musculus,* the online Database for Annotation, Visualization, and Integrated Discovery (DAVID) was used (david.abcc.ncifcrf.gov).

References

1. Dubey JP: **Advances in the life cycle of Toxoplasma gondii**. *Int J Parasitol* 1998, **28**(7):1019-1024.
2. Black MW, Boothroyd JC: **Lytic cycle of Toxoplasma gondii**. *Microbiol Mol Biol Rev* 2000, **64**(3):607-623.
3. Skariah S, McIntyre MK, Mordue DG: **Toxoplasma gondii: determinants of tachyzoite to bradyzoite conversion**. *Parasitol Res* 2010, **107**(2):253-260.
4. Weiss LM, Kim K: **The development and biology of bradyzoites of Toxoplasma gondii**. *Front Biosci* 2000, **5**:D391-405.
5. Robert-Gangneux F, Darde ML: **Epidemiology of and diagnostic strategies for toxoplasmosis**. *Clin Microbiol Rev* 2012, **25**(2):264-296.
6. Roizen N, Swisher CN, Stein MA, Hopkins J, Boyer KM, Holfels E, Mets MB, Stein L, Patel D, Meier P *et al*: **Neurologic and developmental outcome in treated congenital toxoplasmosis**. *Pediatrics* 1995, **95**(1):11-20.
7. McAuley J, Boyer KM, Patel D, Mets M, Swisher C, Roizen N, Wolters C, Stein L, Stein M, Schey W *et al*: **Early and longitudinal evaluations of treated infants and children and untreated historical patients with congenital toxoplasmosis: the Chicago Collaborative Treatment Trial**. *Clin Infect Dis* 1994, **18**(1):38-72.
8. Montoya JG, Liesenfeld O: **Toxoplasmosis**. *Lancet* 2004, **363**(9425):1965-1976.
9. Ong EL: **Common AIDS-associated opportunistic infections**. *Clin Med* 2008, **8**(5):539-543.
10. Luft BJ, Remington JS: **Toxoplasmic encephalitis in AIDS**. *Clin Infect Dis* 1992, **15**(2):211-222.
11. Feustel SM, Meissner M, Liesenfeld O: **Toxoplasma gondii and the blood-brain barrier**. *Virulence* 2012, **3**(2):182-192.
12. Buchholz KR, Fritz HM, Chen X, Durbin-Johnson B, Rocke DM, Ferguson DJ, Conrad PA, Boothroyd JC: **Identification of tissue cyst wall components by transcriptome analysis of in vivo and in vitro Toxoplasma gondii bradyzoites**. *Eukaryot Cell* 2011, **10**(12):1637-1647.
13. Bahl A, Davis PH, Behnke M, Dzierszinski F, Jagalur M, Chen F, Shanmugam D, White MW, Kulp D, Roos DS: **A novel multifunctional oligonucleotide microarray for Toxoplasma gondii**. *BMC Genomics* 2010, **11**:603.
14. Cleary MD, Singh U, Blader IJ, Brewer JL, Boothroyd JC: **Toxoplasma gondii asexual development: identification of developmentally regulated genes and distinct patterns of gene expression**. *Eukaryot Cell* 2002, **1**(3):329-340.
15. Fritz HM, Buchholz KR, Chen X, Durbin-Johnson B, Rocke DM, Conrad PA, Boothroyd JC: **Transcriptomic analysis of toxoplasma development reveals many novel functions and structures specific to sporozoites and oocysts**. *PLoS One* 2012, **7**(2):e29998.
16. Skariah S, Mordue DG: **Identification of Toxoplasma gondii genes responsive to the host immune response during in vivo infection**. *PLoS One* 2012, **7**(10):e46621.
17. Hill RD, Gouffon JS, Saxton AM, Su C: **Differential gene expression in mice infected with distinct Toxoplasma strains**. *Infect Immun* 2012, **80**(3):968-974.

18. Jia B, Lu H, Liu Q, Yin J, Jiang N, Chen Q: **Genome-wide comparative analysis revealed significant transcriptome changes in mice after Toxoplasma gondii infection**. *Parasit Vectors* 2013, **6**:161.
19. McGettigan PA: **Transcriptomics in the RNA-seq era**. *Curr Opin Chem Biol* 2013, **17**(1):4-11.
20. Hassan MA, Melo MB, Haas B, Jensen KD, Saeij JP: **De novo reconstruction of the Toxoplasma gondii transcriptome improves on the current genome annotation and reveals alternatively spliced transcripts and putative long non-coding RNAs**. *BMC Genomics* 2012, **13**:696.
21. Tomita T, Bzik DJ, Ma YF, Fox BA, Markillie LM, Taylor RC, Kim K, Weiss LM: **The Toxoplasma gondii cyst wall protein CST1 is critical for cyst wall integrity and promotes bradyzoite persistence**. *PLoS Pathog* 2013, **9**(12):e1003823.
22. Tanaka S, Nishimura M, Ihara F, Yamagishi J, Suzuki Y, Nishikawa Y: **Transcriptome Analysis of Mouse Brain Infected with Toxoplasma gondii**. *Infect Immun* 2013, **81**(10):3609-3619.
23. Derouin F, Garin YJ: **Toxoplasma gondii: blood and tissue kinetics during acute and chronic infections in mice**. *Exp Parasitol* 1991, **73**(4):460-468.
24. Mordue DG, Monroy F, La Regina M, Dinarello CA, Sibley LD: **Acute toxoplasmosis leads to lethal overproduction of Th1 cytokines**. *J Immunol* 2001, **167**(8):4574-4584.
25. Saeij JP, Boyle JP, Grigg ME, Arrizabalaga G, Boothroyd JC: **Bioluminescence imaging of Toxoplasma gondii infection in living mice reveals dramatic differences between strains**. *Infect Immun* 2005, **73**(2):695-702.
26. Ferguson DJ, Hutchison WM: **An ultrastructural study of the early development and tissue cyst formation of Toxoplasma gondii in the brains of mice**. *Parasitol Res* 1987, **73**(6):483-491.
27. Di Cristina M, Marocco D, Galizi R, Proietti C, Spaccapelo R, Crisanti A: **Temporal and spatial distribution of Toxoplasma gondii differentiation into Bradyzoites and tissue cyst formation in vivo**. *Infect Immun* 2008, **76**(8):3491-3501.
28. Berenreiterova M, Flegr J, Kubena AA, Nemec P: **The distribution of Toxoplasma gondii cysts in the brain of a mouse with latent toxoplasmosis: implications for the behavioral manipulation hypothesis**. *PLoS One* 2011, **6**(12):e28925.
29. Dubey JP, Lindsay DS, Speer CA: **Structures of Toxoplasma gondii tachyzoites, bradyzoites, and sporozoites and biology and development of tissue cysts**. *Clin Microbiol Rev* 1998, **11**(2):267-299.
30. Gotz S, Garcia-Gomez JM, Terol J, Williams TD, Nagaraj SH, Nueda MJ, Robles M, Talon M, Dopazo J, Conesa A: **High-throughput functional annotation and data mining with the Blast2GO suite**. *Nucleic Acids Res* 2008, **36**(10):3420-3435.
31. Jung C, Lee CY, Grigg ME: **The SRS superfamily of Toxoplasma surface proteins**. *Int J Parasitol* 2004, **34**(3):285-296.
32. Butcher BA, Fox BA, Rommereim LM, Kim SG, Maurer KJ, Yarovinsky F, Herbert DR, Bzik DJ, Denkers EY: **Toxoplasma gondii rhoptry kinase ROP16 activates STAT3 and STAT6 resulting in cytokine inhibition and arginase-1-dependent growth control**. *PLoS Pathog* 2011, **7**(9):e1002236.
33. Reichmann G, Dlugonska H, Fischer HG: **Characterization of TgROP9 (p36), a novel rhoptry protein of Toxoplasma gondii tachyzoites identified by T cell clone**. *Mol Biochem Parasitol* 2002, **119**(1):43-54.

34. Denton H, Roberts CW, Alexander J, Thong KW, Coombs GH: **Enzymes of energy metabolism in the bradyzoites and tachyzoites of Toxoplasma gondii**. *FEMS Microbiol Lett* 1996, **137**(1):103-108.
35. Al-Anouti F, Tomavo S, Parmley S, Ananvoranich S: **The expression of lactate dehydrogenase is important for the cell cycle of Toxoplasma gondii**. *J Biol Chem* 2004, **279**(50):52300-52311.
36. Odberg-Ferragut C, Soete M, Engels A, Samyn B, Loyens A, Van Beeumen J, Camus D, Dubremetz JF: **Molecular cloning of the Toxoplasma gondii sag4 gene encoding an 18 kDa bradyzoite specific surface protein**. *Mol Biochem Parasitol* 1996, **82**(2):237-244.
37. Lekutis C, Ferguson DJ, Boothroyd JC: **Toxoplasma gondii: identification of a developmentally regulated family of genes related to SAG2**. *Exp Parasitol* 2000, **96**(2):89-96.
38. Saeij JP, Arrizabalaga G, Boothroyd JC: **A cluster of four surface antigen genes specifically expressed in bradyzoites, SAG2CDXY, plays an important role in Toxoplasma gondii persistence**. *Infect Immun* 2008, **76**(6):2402-2410.
39. Van TT, Kim SK, Camps M, Boothroyd JC, Knoll LJ: **The BSR4 protein is up-regulated in Toxoplasma gondii bradyzoites, however the dominant surface antigen recognised by the P36 monoclonal antibody is SRS9**. *Int J Parasitol* 2007, **37**(8-9):877-885.
40. Kim SK, Karasov A, Boothroyd JC: **Bradyzoite-specific surface antigen SRS9 plays a role in maintaining Toxoplasma gondii persistence in the brain and in host control of parasite replication in the intestine**. *Infect Immun* 2007, **75**(4):1626-1634.
41. Wong WK, Upton A, Thomas MG: **Neuropsychiatric symptoms are common in immunocompetent adult patients with Toxoplasma gondii acute lymphadenitis**. *Scand J Infect Dis* 2013, **45**(5):357-361.
42. Godwin R: **Toxoplasma gondii and elevated suicide risk**. *Vet Rec* 2012, **171**(9):225.
43. Fouts AE, Boothroyd JC: **Infection with Toxoplasma gondii bradyzoites has a diminished impact on host transcript levels relative to tachyzoite infection**. *Infect Immun* 2007, **75**(2):634-642.
44. Kirkman LA, Weiss LM, Kim K: **Cyclic nucleotide signaling in Toxoplasma gondii bradyzoite differentiation**. *Infect Immun* 2001, **69**(1):148-153.
45. Kurokawa H, Kato K, Iwanaga T, Sugi T, Sudo A, Kobayashi K, Gong H, Takemae H, Recuenco FC, Horimoto T *et al*: **Identification of Toxoplasma gondii cAMP dependent protein kinase and its role in the tachyzoite growth**. *PLoS One* 2011, **6**(7):e22492.
46. Lourido S, Shuman J, Zhang C, Shokat KM, Hui R, Sibley LD: **Calcium-dependent protein kinase 1 is an essential regulator of exocytosis in Toxoplasma**. *Nature* 2010, **465**(7296):359-362.
47. Gazzinelli RT, Hieny S, Wynn TA, Wolf S, Sher A: **Interleukin 12 is required for the T-lymphocyte-independent induction of interferon gamma by an intracellular parasite and induces resistance in T-cell-deficient hosts**. *Proc Natl Acad Sci U S A* 1993, **90**(13):6115-6119.
48. Denkers EY, Gazzinelli RT, Martin D, Sher A: **Emergence of NK1.1+ cells as effectors of IFN-gamma dependent immunity to Toxoplasma gondii in MHC class I-deficient mice**. *J Exp Med* 1993, **178**(5):1465-1472.

49. Hunter CA, Subauste CS, Van Cleave VH, Remington JS: **Production of gamma interferon by natural killer cells from Toxoplasma gondii-infected SCID mice: regulation by interleukin-10, interleukin-12, and tumor necrosis factor alpha**. *Infect Immun* 1994, **62**(7):2818-2824.
50. Suzuki Y: **Host resistance in the brain against Toxoplasma gondii**. *J Infect Dis* 2002, **185 Suppl 1**:S58-65.
51. O'Brien KB, Schultz-Cherry S, Knoll LJ: **Parasite-mediated upregulation of NK cell-derived gamma interferon protects against severe highly pathogenic H5N1 influenza virus infection**. *J Virol* 2011, **85**(17):8680-8688.
52. Hauser WE, Jr., Sharma SD, Remington JS: **Natural killer cells induced by acute and chronic toxoplasma infection**. *Cell Immunol* 1982, **69**(2):330-346.
53. Khan IA, Schwartzman JD, Matsuura T, Kasper LH: **A dichotomous role for nitric oxide during acute Toxoplasma gondii infection in mice**. *Proc Natl Acad Sci U S A* 1997, **94**(25):13955-13960.
54. Scharton-Kersten TM, Yap G, Magram J, Sher A: **Inducible nitric oxide is essential for host control of persistent but not acute infection with the intracellular pathogen Toxoplasma gondii**. *J Exp Med* 1997, **185**(7):1261-1273.
55. Bohne W, Heesemann J, Gross U: **Reduced replication of Toxoplasma gondii is necessary for induction of bradyzoite-specific antigens: a possible role for nitric oxide in triggering stage conversion**. *Infect Immun* 1994, **62**(5):1761-1767.
56. Fox BA, Gigley JP, Bzik DJ: **Toxoplasma gondii lacks the enzymes required for de novo arginine biosynthesis and arginine starvation triggers cyst formation**. *Int J Parasitol* 2004, **34**(3):323-331.
57. Rozenfeld C, Martinez R, Figueiredo RT, Bozza MT, Lima FR, Pires AL, Silva PM, Bonomo A, Lannes-Vieira J, De Souza W *et al*: **Soluble factors released by Toxoplasma gondii-infected astrocytes down-modulate nitric oxide production by gamma interferon-activated microglia and prevent neuronal degeneration**. *Infect Immun* 2003, **71**(4):2047-2057.
58. Saeij JP, Coller S, Boyle JP, Jerome ME, White MW, Boothroyd JC: **Toxoplasma co-opts host gene expression by injection of a polymorphic kinase homologue**. *Nature* 2007, **445**(7125):324-327.
59. Maeda H, Wu J, Okamoto T, Maruo K, Akaike T: **Kallikrein-kinin in infection and cancer**. *Immunopharmacology* 1999, **43**(2-3):115-128.
60. Zhang X, Scicli GA, Xu X, Nasjletti A, Hintze TH: **Role of endothelial kinins in control of coronary nitric oxide production**. *Hypertension* 1997, **30**(5):1105-1111.
61. Scarisbrick IA, Blaber SI, Lucchinetti CF, Genain CP, Blaber M, Rodriguez M: **Activity of a newly identified serine protease in CNS demyelination**. *Brain* 2002, **125**(Pt 6):1283-1296.
62. Scarisbrick IA, Epstein B, Cloud BA, Yoon H, Wu J, Renner DN, Blaber SI, Blaber M, Vandell AG, Bryson AL: **Functional role of kallikrein 6 in regulating immune cell survival**. *PLoS One* 2011, **6**(3):e18376.
63. Tobin CM, Knoll LJ: **A patatin-like protein protects Toxoplasma gondii from degradation in a nitric oxide-dependent manner**. *Infect Immun* 2012, **80**(1):55-61.
64. Pfaffl MW: **A new mathematical model for relative quantification in real-time RT-PCR**. *Nucleic Acids Res* 2001, **29**(9):e45.

65. Trapnell C, Williams BA, Pertea G, Mortazavi A, Kwan G, van Baren MJ, Salzberg SL, Wold BJ, Pachter L: **Transcript assembly and quantification by RNA-Seq reveals unannotated transcripts and isoform switching during cell differentiation**. *Nat Biotechnol* 2010, **28**(5):511-515.
66. Goecks J, Nekrutenko A, Taylor J: **Galaxy: a comprehensive approach for supporting accessible, reproducible, and transparent computational research in the life sciences**. *Genome Biol* 2010, **11**(8):R86.
67. Blankenberg D, Von Kuster G, Coraor N, Ananda G, Lazarus R, Mangan M, Nekrutenko A, Taylor J: **Galaxy: a web-based genome analysis tool for experimentalists**. *Curr Protoc Mol Biol* 2010, **Chapter 19**:Unit 19 10 11-21.
68. Giardine B, Riemer C, Hardison RC, Burhans R, Elnitski L, Shah P, Zhang Y, Blankenberg D, Albert I, Taylor J *et al*: **Galaxy: a platform for interactive large-scale genome analysis**. *Genome Res* 2005, **15**(10):1451-1455.
69. Kim D, Pertea G, Trapnell C, Pimentel H, Kelley R, Salzberg SL: **TopHat2: accurate alignment of transcriptomes in the presence of insertions, deletions and gene fusions**. *Genome Biol* 2013, **14**(4):R36.
70. Huang da W, Sherman BT, Lempicki RA: **Systematic and integrative analysis of large gene lists using DAVID bioinformatics resources**. *Nat Protoc* 2009, **4**(1):44-57.

A

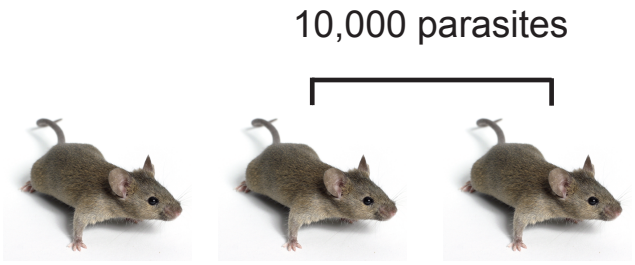
10,000 parasites
Uninfected
Acute infection
Chronic infection
10 day
28 day
Forebrains collected, TRIzol RNA extraction
Illumina HiSeq200 sequencing:
950,000,000 Reads
Alignment to *Toxoplasma gondii* and *Mus musculus*
Normalized reads (FPKM)
Differential Expression Analysis

B

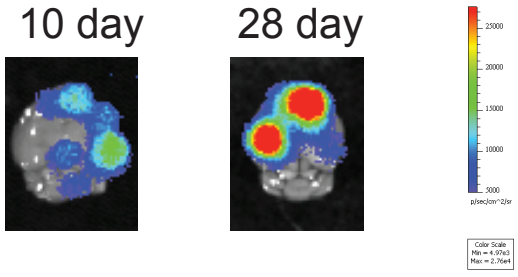
10 day
28 day

Figure 1. Schematic of *T. gondii*/host dataset generation.

(**A**) Nine mice were divided into three experimental groups: uninfected, 10 days post-infection, and 28 days post-infection. Infected mice were given 10,000 type II ME49 parasites and sacrificed on the corresponding days. The forebrains were removed and homogenized in TRIzol, and RNA was extracted and purified. A cDNA library was generated from the RNA prior to IlluminaHiSeq2000 sequencing. Raw reads were aligned to either the *T. gondii* or *M. musculus* genomes, normalized and analyzed for differential gene expression. (**B**) To examine *T. gondii* in the brains of mice at the designated time points, mice were infected with 10,000 parasites of a bioluminescent *T. gondii* [63]. Shown are representative brains for 10 and 28 day post-infection mice, after the brains were soaked for 5 minutes in luciferin prior to imaging.

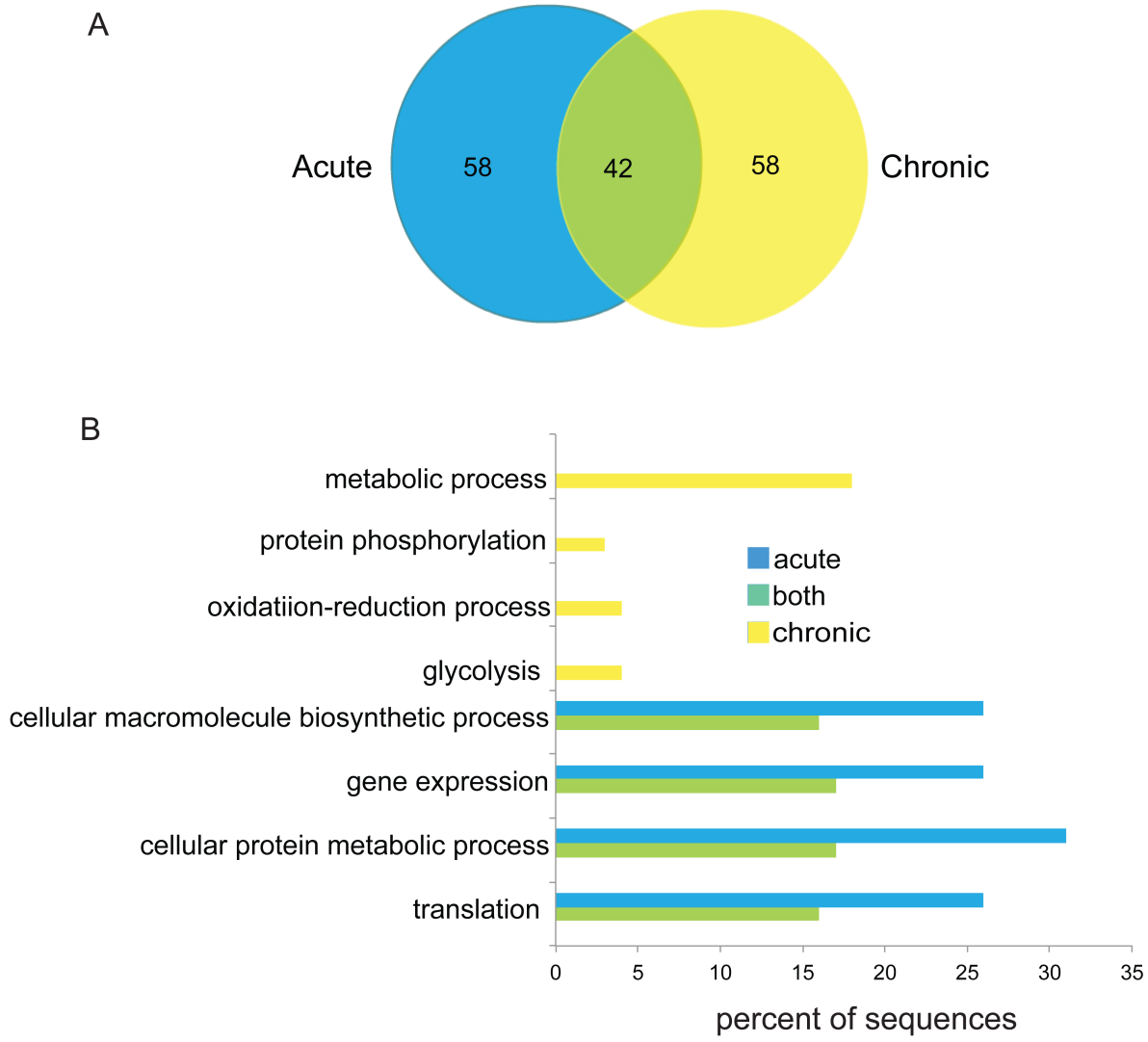

Figure 2. Top 100 *T. gondii* genes from acute and chronic infection

(**A**) Venn diagram compares the 100 *T. gondii* genes with the greatest FPKM value from acute and chronic time points. Of the top 100 genes for each stage, 42 genes were similarly abundant (green), and 58 were only abundant in acute (blue) or chronic (yellow) infection. (**B**) GO terms were assigned to the top 100 *T. gondii* genes from acute and chronic infection. Genes were grouped based on whether they are similar or different between time points prior to GO term analysis.

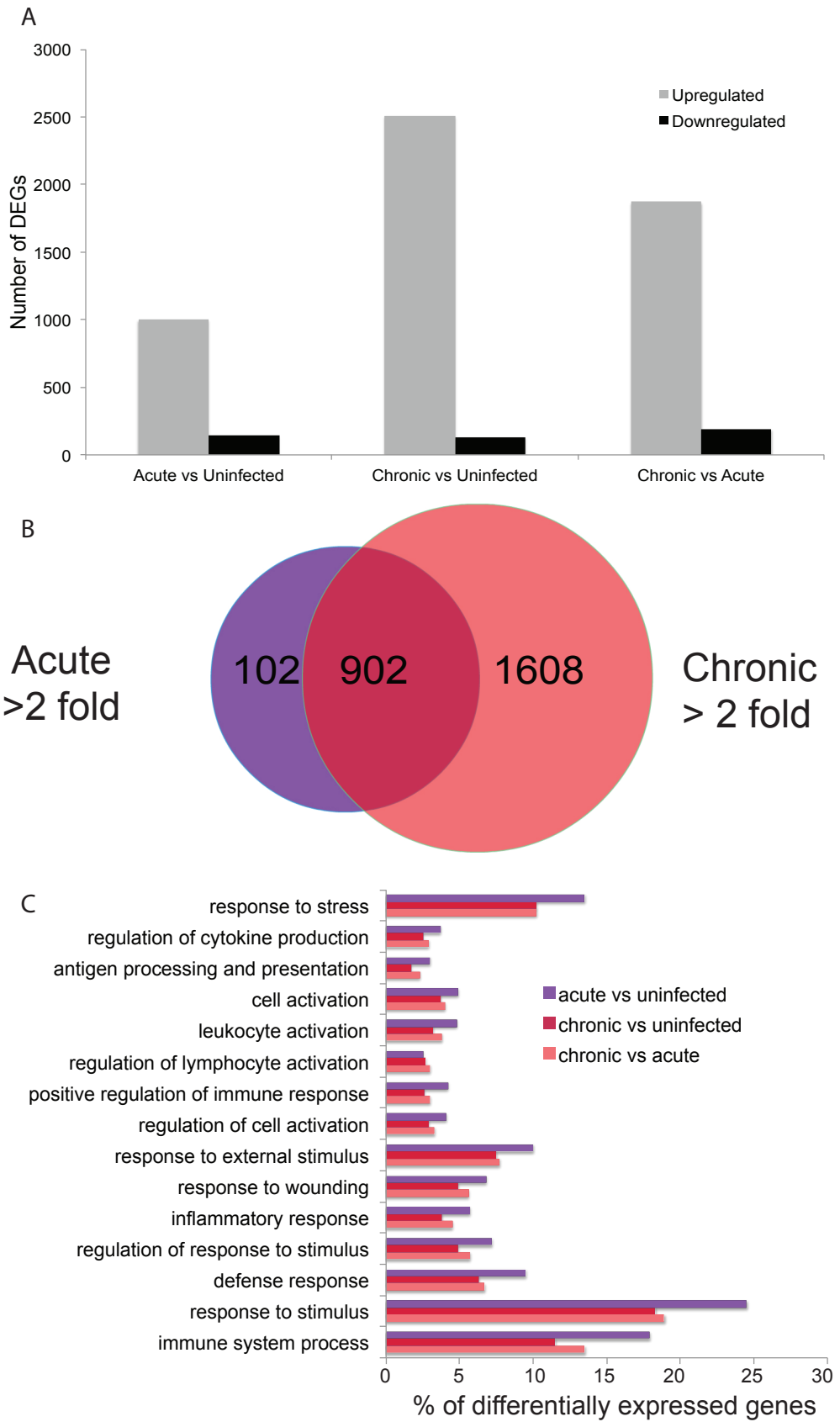
A
3000
2500
2000
1500
1000
500
0
Number of DEGs
Upregulated
Downregulated
Acute vs Uninfected
Chronic vs Uninfected
Chronic vs Acute
B
Acute
>2 fold
102
902
1608
Chronic
> 2 fold
C
response to stress
regulation of cytokine production
antigen processing and presentation
cell activation
leukocyte activation
regulation of lymphocyte activation
positive regulation of immune response
regulation of cell activation
response to external stimulus
response to wounding
inflammatory response
regulation of response to stimulus
defense response
response to stimulus
immune system process
acute vs uninfected
chronic vs uninfected
chronic vs acute
0
5
10
15
20
25
30
% of differentially expressed genes

Figure 3. More host genes have increased abundance during chronic infection.

(**A**) DEGs in the mouse with a fold change >2 were grouped based on increased abundance (grey) and decreased abundance (black) between acute vs uninfected, chronic vs uninfected, and chronic vs acute time points. (**B**) A Venn diagram was created to compare DEGs with increased abundance in acute vs uninfected (purple) and chronic vs uninfected time points (red). Of the 1004 more abundant DEGs in acute vs uninfected, 902 were also more abundant in the chronic vs uninfected group (magenta). (**C**) To explore the function of DEGs analyzed in the Venn diagram, a GO term enrichment analysis was performed.

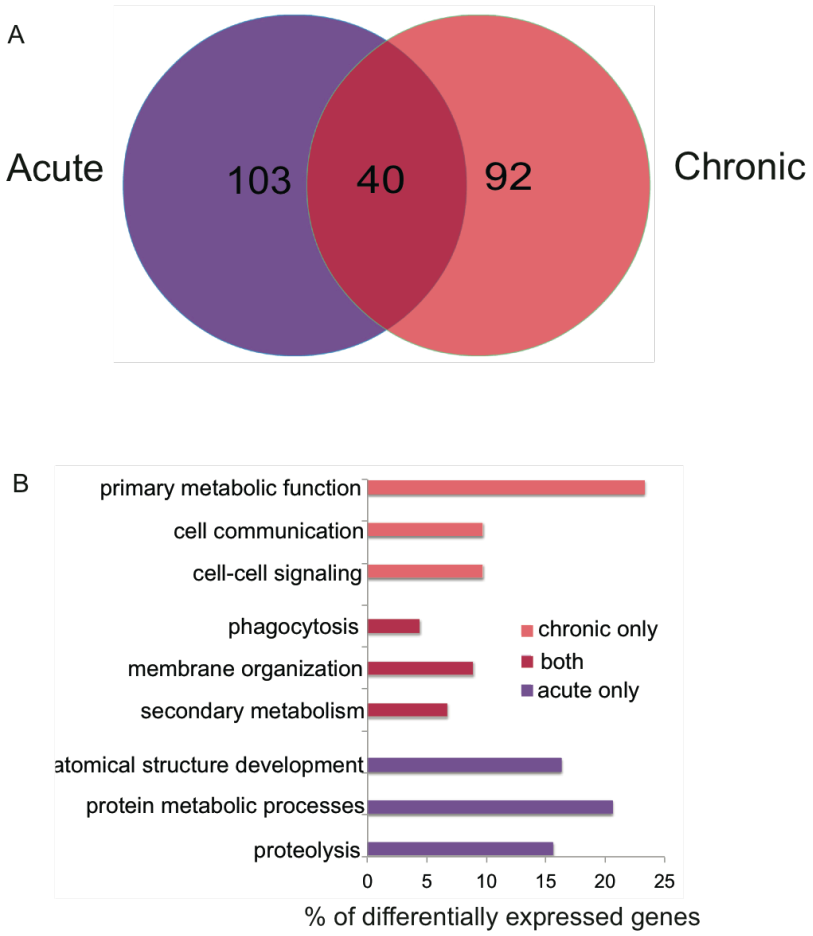

Figure 4. Analysis of host genes with decreased abundance during *T. gondii* infection. (**A**) A Venn diagram was created to compare DEGs >2-fold decreased abundance in acute vs uninfected (purple) and chronic vs uninfected (red) mice. Forty host genes were less abundant during both acute and chronic infection (magenta). (**B**) To explore the function of DEGs analyzed in the Venn diagram, a GO term enrichment analysis was performed. Functionally enriched GO terms display little similarity between time points.

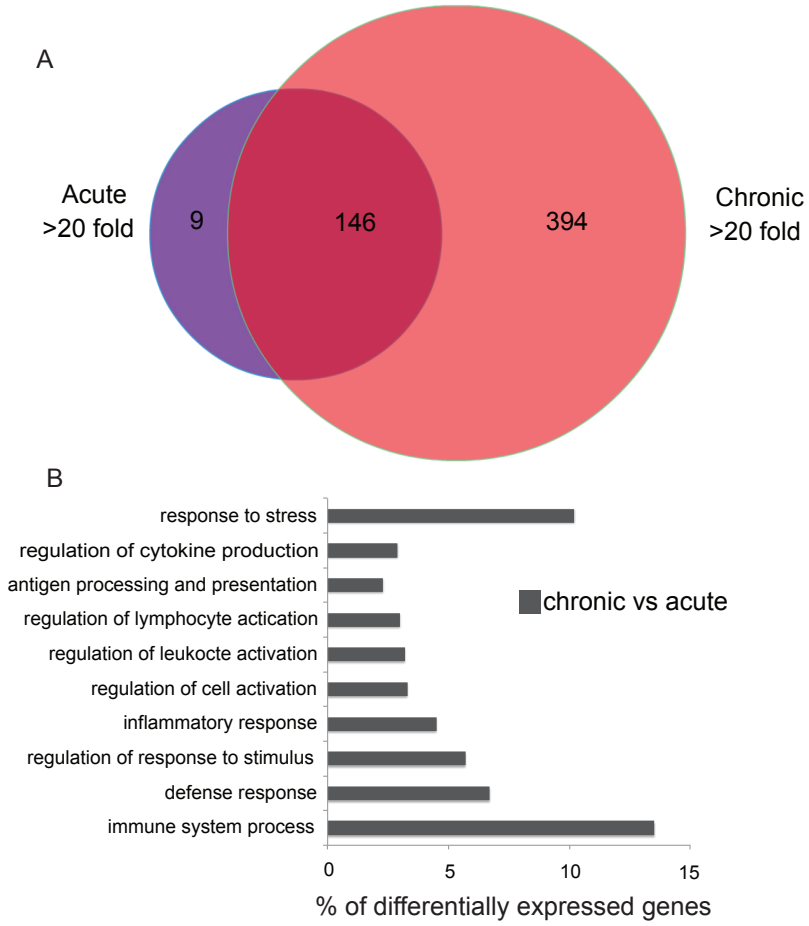

Figure 5. Few highly expressed DEGs are specific to acute infection.

(**A**) To better characterize abundant DEGs, a Venn diagram of the more abundant DEGs in the mouse with a fold change >20 between acute vs uninfected (purple) and chronic vs uninfected (red) time points. Of these more abundant DEGs, 146 were shared between acute and chronic infection (magenta). Only 9 DEGs had a fold change >20 in acute vs uninfected that were also not highly abundant in chronic vs uninfected time points. (**B**) To analyze the function of the host more abundant DEGs in chronic vs acute time points, GO term enrichment analysis was performed. Many genes differentially expressed in chronic infection are associated with immune regulation and stress response.

Table 1. Mapped paired-end reads of individual mouse forebrain samples.

Forebrain Sample	Total number of reads	mapped *Toxoplasma* paired reads	mapped mouse paired reads
Uninfected 1	112075860	10752	71901643
Uninfected 2	112948998	7272	72770895
Uninfected 3	103209252	12175	69295619
10 day 1	102581171	51734	68040784
10 day 2	125546828	51788	81691030
10 day 3	81630704	21234	47283570
28 day 1	103765423	90414	65891584
28 day 2	113094439	61481	69756643
28 day 3	114177191	89520	71828085

The first column is the time-point of *T. gondii* infection of the mouse forebrain samples used for RNA extraction. The second column is the total number of reads obtained from Illumina HiSeq sequencing. The third column is the total number of paired-end reads from each mouse forebrain sample that mapped to the *T. gondii* genomic reference file. The fourth column is the total number of paired-end reads from each experimental group that mapped to the *mus musculus* genomic reference file.

Table 2. Detection of parasite numbers in the mouse forebrain using quantitative PCR

Forebrain sample	Number of parasites/350 ng gDNA	Average per time point
10 day 1	632	
10 day 2	340	
10 day 3	517	496
28 day 1	3160	
28 day 2	100	
28 day 3	1111	1457

The first column is the time-point of *T. gondii* infection of the mouse forebrain samples used for RNA extraction. The second column is the number of parasites determined by qPCR for each sample. The third column is the average number of parasites in the 3 acute samples and 3 chronic samples.

Table 3. Fold change between chronic and acute infection for previously characterized *T. gondii* genes.

Gene ID	Description	Fold change: chronic/acute
TGME49_316400	α tubulin	0.59
TGME49_209030	actin	1.2
TGME49_289690	GAPDH 1	1.8
TGME49_269190	GAPDH 2	1
TGME49_265450	hexokinase	0.68
TGME49_291890	MIC1	0.024
TGME49_233460	SAG1	0.0055
TGME49_259020	BAG1	48
TGME49_268860	ENO1	38

First column is the gene number from ToxoDB.org. The middle column is gene description where α-tubulin, actin, hexokinase, GAPDH-1 and 2 are housekeeping genes, tachyzoite specific genes are SAG1 and MIC1, and bradyzoite specific genes are BAG1 and ENO1. The third column is the average FPKM value for chronic genes divided by the average FPKM value for acute genes.

Table 4. *T. gondii* DEGs that were more abundant >5-fold in acute vs chronic infection.

Gene ID	Description	Fold change: acute/chronic
TGME49_233480	SAG-related sequence SRS29C (SRS29C)	305
TGME49_233460	SAG-related sequence SRS29B (SAG1)	181
TGME49_291890	microneme protein MIC1 (MIC1)	41
TGME49_241240	hypothetical protein	40
TGME49_224460	aminopeptidase	26
TGME49_262050	rhoptry kinase family protein ROP39	23
TGME49_297880	dense granule protein DG32	19
TGME49_271050	SAG 34A/SAG/2	18
TGME49_294200	glucose-6-phosphate 1-dehydrogenase	13
TGME49_230160	hypothetical protein	12
TGME49_261740	hypothetical protein	12
TGME49_291960	rhoptry kinase family protein ROP40	10
TGME49_268850	enolase 2	9
TGME49_277490	hypothetical protein	9
TGME49_215960	hypothetical protein	9
TGME49_222170	dense-granule antigen DG32	8
TGME49_293430	hypothetical protein	8
TGME49_262730	rhoptry protein ROP16 (ROP16)	8
TGME49_314400	pyruvate dehydrogenase E1 component	8
TGME49_315320	SAG-related sequence SRS52A (SRS52A)	7
TGME49_200360	hypothetical protein	7
TGME49_285870	SAG-related sequence SRS20A (SRS20A)	7
TGME49_269950	hypothetical protein	7
TGME49_247280	hypothetical protein	7
TGME49_294800	elongation factor 1-alpha (EF-1-ALPHA)	7
TGME49_213050	hypothetical protein	6
TGME49_249180	bifunctional dihydrofolate reductase-thymidylate synthase	6
TGME49_226710	hypothetical protein	6
TGME49_237880	hypothetical protein	6
TGME49_250115	hypothetical protein	6
TGME49_254720	dense granule protein GRA8 (GRA8)	6
TGME49_253930	GCC2 and GCC3 domain-containing protein	6
TGME49_299780	hypothetical protein	6
TGME49_275860	hypothetical protein	6
TGME49_310780	dense granule protein GRA4 (GRA4)	6
TGME49_277080	microneme protein MIC5 (MIC5)	6
TGME49_226960	phosphofructokinase PFKII (PFKII)	6
TGME49_243730	rhoptry protein ROP9 (ROP9)	6
TGME49_207400	hypothetical protein	6

TGME49_259240	ribosomal protein RPS21 (RPS21)	6
TGME49_205340	ribosomal protein RPS12 (RPS12)	6
TGME49_209150	non-proton pumping type-II NADH dehydrogenase I (NDH2-I)	6
TGME49_253690	hypothetical protein	5
TGME49_229670	ribosomal protein RPS23 (RPS23)	5
TGME49_244690	hypothetical protein	5
TGME49_212290	ribosomal protein RPS19 (RPS19)	5
TGME49_288360	tryptophanyl-tRNA synthetase (TrpRS2)	5
TGME49_251810	translation initiation factor eIF-5A	5
TGME49_200350	subtilisin SUB3 (SUB3)	18*
TGME49_250955	KRUF family protein	21*
TGME49_279350	hypothetical protein	23*
TGME49_313250	hypothetical protein	26*
TGME49_307760	Tubulin-tyrosine ligase family protein	27*
TGME49_315740	SAG-related sequence SRS54	27*
TGME49_243700	hypothetical protein	29*
TGME49_293210	hypothetical protein	30*
TGME49_276110	cytochrome b5 family heme/steroid binding	34*
TGME49_218740	membrane protein	65*
TGME49_294805	hypothetical protein	77*
TGME49_294990	hypothetical protein	106*
TGME49_216770	hypothetical protein	125*
TGME49_230180	hypothetical protein	129*
TGME49_305050	calmodulin	295*

First column is the gene number from ToxoDB.org. The second column is the gene description. The far right column is the average FPKM value from acute infection divided by the average FPKM value from chronic infection, called the fold change. * in the fold change column indicates the average FPKM value during chronic infection was 0, and could not be divided by the average FPKM value in acute samples. A p-value and q-value of <0.05 was considered to be statistically significant and only genes that met these standards were included on this table.

Table 5 *T. gondii* DEGs that were more abundant >5 fold in chronic vs acute infection.

Gene ID	Description	Fold change: chronic/acute
TGME49_224630	zinc finger (CCCH type) protein	86
TGME49_259020	bradyzoite antigen BAG1 (BAG1)	48
TGME49_202020	DnAK-TPR	44
TGME49_278080	Toxoplasma gondii family A protein (SUSA-1)	32
TGME49_291040	lactate dehydrogenase LDH2 (LDH2)	31
TGME49_200250	microneme protein MIC17A (MIC17A)	29
TGME49_260190	microneme protein MIC13 (MIC13)	29
TGME49_267680	microneme protein MIC12 (MIC12)	28
TGME49_262970	hypothetical protein	26
TGME49_245530	hypothetical protein	26
TGME49_204420	oocyst wall protein OWP1 (OWP1)	23
TGME49_318880	hypothetical protein	18
TGME49_289370	hypothetical protein	18
TGME49_207210	hypothetical protein	18
TGME49_209985	cAMP-dependent protein kinase	18
TGME49_309930	melibiase subfamily protein	17
TGME49_320260	hypothetical protein	15
TGME49_293780	hypothetical protein	14
TGME49_216140	tetratricopeptide repeat-containing protein	14
TGME49_280570	SAG-related sequence SRS35A (SRS35A)	13
TGME49_320190	SAG-related sequence SRS16B (SRS16B)	11
TGME49_250940	hypothetical protein	11
TGME49_306620	AP2 domain transcription factor AP2IX-9 (AP2IX9)	11
TGME49_209755	hypothetical protein	11
TGME49_207160	SAG-related sequence SRS49D (SRS49D)	10
TGME49_202030	hypothetical protein	10
TGME49_312600	heat shock protein HSP21 (HSP21)	9
TGME49_290000	hypothetical protein	9
TGME49_256760	pyruvate kinase PyK1 (PYKI)	8
TGME49_225290	GDA1/CD39 (nucleoside phosphatase)	7
TGME49_269670	hypothetical protein	7
TGME49_253330	Rhoptry kinase family protein	7
TGME49_225540	hypothetical protein	7
TGME49_282130	hypothetical protein	6
TGME49_207710	phosphatidylinositol synthase	6
TGME49_205680	hypothetical protein	6
TGME49_276200	hypothetical protein	6
TGME49_283780	glucose-6-phosphate isomerase GPI (GPI)	6
TGME49_285980	glucosephosphate-mutase GPM1 (GPM1)	6
TGME49_264420	lipoprotein	6

TGME49_226420	peptidase family M3 protein	6
TGME49_290980	glycine C-acetyltransferase	6
TGME49_275320	penicillin amidase	5
TGME49_201840	aspartyl protease ASP1 (ASP1)	5
TGME49_246080	NAD dependent epimerase/dehydratase	5
TGME49_222370	SAG-related sequence SRS13 (SRS13)	5
TGME49_315760	AP2 domain transcription factor AP2XI-4 (AP2XI4)	5
TGME49_294400	hypothetical protein	5
TGME49_215910	hypothetical protein	5
TGME49_224950	calcium-dependent protein kinase CDPK5 (CDPK5)	5
TGME49_256060	nucleosome assembly protein (nap) protein	5
TGME49_205750	histone deacetylase complex subunit Sin3 (SIN3)	5
TGME49_253320	hypothetical protein	15*
TGME49_254330	lipase	16*
TGME49_309790	hypothetical protein	16*
TGME49_269300	lipase	17*
TGME49_223258	hypothetical protein	17*
TGME49_207875	GCC2 and GCC3 domain-containing protein	17*
TGME49_269020	hypothetical protein	18*
TGME49_261200	TBC domain-containing protein	18*
TGME49_254150	hypothetical protein	18*
TGME49_306500	hypothetical protein	18*
TGME49_245440	hypothetical protein	19*
TGME49_207980	PIG-P protein	19*
TGME49_220150	50S ribosomal protein L16	19*
TGME49_320720	hypothetical protein	19*
TGME49_268765	hypothetical protein	19*
TGME49_260530	Sel1 repeat-containing protein	22*
TGME49_269320	hypothetical protein	23*
TGME49_215300	hypothetical protein	24*
TGME49_308096	rhoptry kinase family protein	25*
TGME49_240470	hypothetical protein	25*
TGME49_460810	ribosomal RNA	25*
TGME49_310045	hypothetical protein	26*
TGME49_224180	hypothetical protein	26*
TGME49_205210	hypothetical protein	26*
TGME49_204040	hypothetical protein	27*
TGME49_297850	Branched-chain-amino-acid aminotransferase	27*
TGME49_215130	adaptor-related protein complex 3	27*
TGME49_207600	tubulin/FtsZ family, GTPase	27*
TGME49_200230	microneme protein MIC17C (MIC17C)	28*
TGME49_231125	hypothetical protein	30*

TGME49_219610	hypothetical protein	31*
TGME49_240480	cpw-wpc domain-containing protein	31*
TGME49_315520	calcium binding egf domain-containing protein	32*
TGME49_232430	hypothetical protein	33*
TGME49_244412	hypothetical protein	33*
TGME49_223855	RNA recognition motif-containing protein	35*
TGME49_260325	hypothetical protein	37*
TGME49_234625	EGF family domain-containing protein	37*
TGME49_255460	hypothetical protein	40*
TGME49_321710	IgA-specific serine endopeptidase	43*
TGME49_319090	proteasome maturation factor ump1 protein	50*
TGME49_209090	hypothetical protein	52*
TGME49_210682	hypothetical protein	53*
TGME49_213480	hypothetical protein	53*
TGME49_210095	hypothetical protein	57*
TGME49_313890	hypothetical protein	58*
TGME49_271450	hypothetical protein	59*
TGME49_321700	hypothetical protein	80*
TGME49_219742	hypothetical protein	87*
TGME49_266600	Kazal-type serine protease inhibitor	89*
TGME49_257970	hypothetical protein	89*
TGME49_258370	rhoptry kinase family protein ROP28 (ROP28)	103*
TGME49_295662	hypothetical protein	110*
TGME49_278882	GDA1/CD39 (nucleoside phosphatase)	113*
TGME49_264150	hypothetical protein	141*

First column is the gene number from ToxoDB.org. The far right column is the fold change calculated from the average FPKM value from chronic infection divided by the average FPKM value from acute infection. * in the fold change column indicates the average FPKM value during acute infection was 0, and could not be divided by the average FPKM value in chronic infection. A p-value and q-value of <0.05 was considered to be statistically significant and only genes that met these standards were included on this table.

Table 6. Mouse DEGs more abundant in acute, but not chronic infection.

Gene ID	Gene Name	Description	Fold Change Acute/Uninfected	Fold Change Chronic/Uninfected
ENSMUSG00000088071	Gm22818	predicted gene, 22818	276	1
ENSMUSG00000002831	Gbp10	guanylate-binding protein 10	183	No transcripts in Chronic
ENSMUSG00000002833	Gbp6	guanylate binding protein 6	130	No transcripts in Chronic
ENSMUSG00000024334	Gbp4*	guanylate binding protein 4	61	No transcripts in Chronic
ENSMUSG00000075010	Gbp8*	guanylate-binding protein 9	61	No transcripts in Chronic
ENSMUSG00000085377	Gbp9*	guanylate-binding protein 8	61	No transcripts in Chronic
ENSMUSG00000098049	BC042782#	cDNA sequence BC042782	52	1.8
ENSMUSG00000079362	n-R5s189#	nuclear encoded rRNA 5S 189	52	1.8
ENSMUSG00000005800	Plin4	perilipin 4	27	1

The first column is the ensemble gene ID and the second is the gene name. The third column is the official gene symbol from ensemble.org, and the fourth column is the fold change as average acute FPKM value was divided by uninfected. The fifth column is the fold change as average chronic FPKM value was divided by uninfected. Only genes with a p-value and q-value <0.05 were considered differentially expressed. * and # mark genes located in the same contiguous loci and thus reads mapping to this area were combined.

Table 7 The top 50 mouse DEGs more abundant in chronic vs. acute infection.

Gene ID	Description	Gene symbol	Fold change (chronic vs acute)
ENSMUSG00000076652	immunoglobulin heavy variable 7-3	Ighv7-3	672*
ENSMUSG00000076653	immunoglobulin heavy variable 7-2	Ighv7-2	672*
ENSMUSG00000095571	immunoglobulin heavy variable 5-17	Ighv5-17	672*
ENSMUSG00000076564	immunoglobulin kappa chain variable 12-46	Igkv12-46	656*
ENSMUSG00000096422	immunoglobulin kappa variable 12-44	Igkv12-44	656*
ENSMUSG00000076604	immunoglobulin kappa joining 1	Igkj1	353*
ENSMUSG00000076605	immunoglobulin kappa joining 2	Igkj2	353*
ENSMUSG00000076607	immunoglobulin kappa joining 4	Igkj4	353*
ENSMUSG00000076608	immunoglobulin kappa joining 5	Igkj5	353*
ENSMUSG00000076612	immunoglobulin heavy constant gamma 2C	Ighg2c	23*
ENSMUSG00000076617	immunoglobulin heavy constant	Ighm	23*
ENSMUSG00000076618	immunoglobulin heavy joining 4	Ighj4	23*
ENSMUSG00000076619	immunoglobulin heavy joining 3	Ighj3	23*
ENSMUSG00000076621	immunoglobulin heavy joining 1	Ighj1	23*
ENSMUSG00000094028	immunoglobulin heavy diversity 4-1	Ighd4-1	23*
ENSMUSG00000095079	immunoglobulin heavy constant alpha	Igha	23*
ENSMUSG00000095007	immunoglobulin kappa chain variable 12-41	Igkv12-41	356
ENSMUSG00000076609	immunoglobulin kappa chain, constant region	Igkc	353
ENSMUSG00000016283	histocompatibility 2, M region locus 2	H2-M2	111
ENSMUSG00000002992	apolipoprotein C-II	Apoc2	70
ENSMUSG00000074336	apolipoprotein C-IV	Apoc4	70
ENSMUSG00000019987	arginase, liver	Arg1	69
ENSMUSG00000071716	apolipoprotein L 7e	Apol7e	60
ENSMUSG00000058216	cDNA sequence BC021614	BC021614	45
ENSMUSG00000042262	chemokine (C-C motif) receptor 8	Ccr8	44
ENSMUSG00000014453	B lymphoid kinase	Blk	38
ENSMUSG00000050063	kallikrein related-peptidase 6	Klk6	38
ENSMUSG00000082976	predicted gene 15056; similar to beta-defensin 52	Gm15056	38
ENSMUSG00000053977	CD8 antigen, alpha chain	Cd8a	37
ENSMUSG00000030577	CD22 antigen; hypothetical protein LOC100047973	Cd22	36
ENSMUSG00000020017	histidine ammonia lyase	Hal	35
ENSMUSG00000027863	CD2 antigen	Cd2	35
ENSMUSG00000067149	immunoglobulin joining chain	Igj	35
ENSMUSG00000030724	CD19 antigen	Cd19	34
ENSMUSG00000067341	histocompatibility 2, class II antigen E beta2	H2-Eb2	34
ENSMUSG00000068129	cystatin F (leukocystatin)	Cst7	33
ENSMUSG00000079293	C-type lectin domain family 7, member a	Clec7a	32

ENSMUSG00000096594	immunoglobulin kappa variable 8-19	Igkv8-19	32
ENSMUSG00000002033	CD3 antigen, gamma polypeptide	Cd3g	31
ENSMUSG00000050232	chemokine (C-X-C motif) receptor 3	Cxcr3	28
ENSMUSG00000053044	CD8 antigen, beta chain 1	Cd8b1	28
ENSMUSG00000054672	RIKEN cDNA 5830411N06 gene	5830411N06 Rik	28
ENSMUSG00000094738	predicted gene, 26177	Gm26177	28
ENSMUSG00000005947	integrin alpha E, epithelial-associated	Itgae	27
ENSMUSG00000022657	CD96 antigen	Cd96	27
ENSMUSG00000024669	CD5 antigen	Cd5	27
ENSMUSG00000024910	cathepsin W	Ctsw	27
ENSMUSG00000031933	folate receptor 4 (delta)	Folr4	27
ENSMUSG00000026070	interleukin 18 receptor 1	Il18r1	26
ENSMUSG00000035042	chemokine (C-C motif) ligand 5	Ccl5	25

The first column is the ensemble gene ID and the second is the gene name. The third column is the official gene symbol from ensemble.org, and the fourth column is the fold change as average chronic FPKM value was divided by acute. Only genes with a p-value and q-value <0.05 were considered differentially expressed.

Chapter 3

Characterizing the role of ZBP1 during *Toxoplasma gondii* infection

Kelly J. Pittman and Laura J. Knoll

Department of Medical Microbiology and Immunology, University of Wisconsin - Madison,

1550 Linden Drive, Madison, WI 53706

This chapter will be submitted to PNAS after completion of experiments

Summary

T. gondii is an intracellular parasite with the ability to infected nucleated cells in any warm-blooded animal. Intrinsic to *T. gondii* infection is the parasite-induced modulation of the host immune response, which ensures establishment of a chronic life long infection. This is especially specific to type II strains of *T. gondii* as they establish cysts in the central nervous system and brain tissue of the host. *T. gondii* cysts persist indefinitely and currently there are no drugs that can eliminate them. The manipulation of the host immune response is a way for the parasite to not only dampen the ability of the host to kill the parasite, but also to force differentiation to the slow growing, encysted form of the parasite. In this paper we have identified a new host target that affects growth of *T. gondii*, Z-DNA binding protein 1 (ZBP1). ZBP1 was highly up-regulated in a previous RNAseq analysis performed by our laboratory in the brains of mice during both acute and chronic *T. gondii* infection. ZBP1 has been identified as an IFN-γ regulated product in activated macrophages, but the function has yet to be elucidated. Here, we describe a novel role for ZBP1 in the degradation of *T. gondii* through nitric oxide production in activated macrophages.

Introduction

Toxoplasma gondii is an obligate intracellular parasite capable of infecting any nucleated cell in warm-blooded animals. With such a large host range, *T. gondii* has become one of the most prevalent eukaryotic parasites in the world, with approximately 30 percent of the human population infected (1). *T. gondii* has both a sexual and asexual cycle, with the sexual cycle occurring only in the feline intestine, and asexual cycle existing in all other warm-blooded hosts. Two asexual forms of the parasite exist in infected animals; the rapidly replicating tachyzoite and

the slower growing encysted bradyzoite. During acute infection, the tachyzoite disseminates throughout the host until pressure from the immune system trigger differentiation to the slower growing encysted bradyzoite, which signifies the establishment of a chronic life-long infection. Cysts containing bradyzoites only occur in cells of the central nervous system and striated muscle (2). Cysts persist for the lifetime of the host and remain infectious if contaminated tissue is consumed. The most common route of exposure to *T. gondii* is ingestion of undercooked meat containing bradyzoite cysts or consumption of unwashed food contaminated with environmentally stable oocysts (3). In the United States, prevalence rates are approximately 20% resulting in *T. gondii* as the second leading cause of food borne disease resulting in hospitalization or death (4).

Infection with *T. gondii* is typically asymptomatic, but does present issues in the immune compromised and unborn fetuses when acquired congenitally. If passed congenitally from mother to fetus outcomes range in severity from blindness to hydrocephaly and even death (5-8). Infection with *T. gondii* is more detrimental in immune compromised individuals, such as those with HIV, patients receiving organ transplants or undergoing cancer treatment, and the elderly (9-13). In these individuals, either primary infection with *T. gondii* or reactivation of latent bradyzoite cysts cannot be controlled, resulting in encephalitis and eventual death.

In those with healthy immune systems a multitude of defenses to combat *T. gondii* infection are present with the majority of them involved in production of interferon-gamma (IFN-γ). The significance of IFN-γ during infection is attributed to its ability to stimulate hundreds of genes (14). These genes initiate an array of responses necessary for control of parasite growth and dissemination including host immune cell proliferation, differentiation, and destruction of infected cells. *T. gondii* has developed strategies to evade these host immune

responses. An interesting example of *T. gondii* modulation of host cell responses lies in the ability of *T. gondii* to block its degradation by activated macrophages (15, 16). At least part of this block is due to the ability of *T. gondii* to suppress NO production by limiting the availability of intracellular arginine (15, 17, 18). Type I strain parasites initiate arginine starvation by secreting ROP16, a kinase that activates STAT6 resulting in expression of host arginase-1(15). Arginase-1 degrades available host cell arginine thus limiting the availability for NO (19). A decrease in NO synthesis would appear to be beneficial to the parasite, but *T. gondii* is an arginine auxotroph and exhibits decreased growth in media lacking arginine (15). Another example of *T. gondii* manipulation is the MyD88 dependent production of IL-12 and subsequent expression of IFN-γ. The downstream effector of the MyD88 pathway that triggers IL-12 transcription is NF-ϰB. Type II strains of *T. gondii* actually promote expression and translocation of NF-ϰB to the nucleus via secretion of GRA15 (20). The promotion of pro-inflammatory signal would seem detrimental to the parasite, but stimulation of this mechanism may be adapted by the parasite to ensure survival of the host, establishment of a stable chronic infection and subsequent persistence of the parasite.

Previously, our laboratory sought out to determine other instances of host and parasite interactions through dual analysis of mice infected with *T. gondii* during acute and chronic infection. From this dataset, an interesting host gene, Z DNA-binding protein 1 (*ZBP1*) was shown to be highly abundant in acute and chronic time points when compared to uninfected samples. *ZBP1* also had a fold change difference of over 20 in a similar study where *T. gondii* infected mice were compared at 30 days post-infection to uninfected mice (21). Currently, the contribution of ZBP1 during *T. gondii* infection has not been examined.

Since its initial identification, ZBP1 has been implicated in the cytosolic sensing of foreign bacterial and viral DNA and subsequent activation of type I interferon pathways (22-24). Known binding partners are RIPK3 and RIPK1 through the RHIM binding domain of ZBP1 and can activate NF-κB through IRF3 and TBK1 recruitment (22-25). In more recent years ZBP1 has been studied in the context of viral induced necroptosis through RIPK3, in the absence of RIPK1 (26). It has been demonstrated that ZBP1 and RIPK3 form a complex that triggers necroptosis of infected cells with viruses lacking the M45 gene responsible for blocking the interaction of RIPK3 and ZBP1 with the RHIM domain (26). ZBP1 also initiates type I interferon production in response to viral infection, which is a critical response for clearance. Although it has been implicated in multiple host defense pathways, ZBP1 was deemed indispensable for the innate and adaptive immune response to B-DNA and DNA vaccine (27), possibly due to redundancy in DNA sensing proteins. The role of ZBP1 during parasitic infection has yet to be elucidated. In this paper, we address the significance of ZBP1 expression during *T. gondii* infection.

Results

RNAseq analysis reveals ZBP1 is highly abundant during acute and chronic *T. gondii* infection in mouse forebrains.

Previously, our laboratory generated an in vivo RNAseq time course of the forebrains of mice during acute and chronic *T. gondii* infection (28). Briefly, 9 mice were used in this experiment: three uninfected, three infected for 10 days and three infected for 28 days. Mice were sacrificed and their forebrains harvested, RNA was extracted, and Illumina Hiseq2000 was performed individually on each sample. Nearly one billion 100 base-pair (bp) paired-end RNA sequences were generated. Sequences were normalized, averaged within time points, and differential expression analysis was conducted. Comparisons were made between uninfected, 10 days post-

infection and 28 days post infection. One of the highest differentially expressed transcripts between acute vs. uninfected and chronic vs uninfected time points was *ZBP1*. The average FPKM fold change between acute vs uninfected and chronic vs uninfected time points was 300 and 1000, respectively (Table 1). Another group who conducted studies on the brains of mice infected with *T. gondii* also found ZBP1 to have a large fold change (approximately 240 fold increase) in mice during chronic infection (21). qPCR was conducted on these samples to verify the increase in abundance of ZBP1 transcripts between each experimental time point (Table 1). Fold changes of ZBP1 levels were similar between qPCR and RNAseq analysis with ZBP1 transcript fold changes of 300 (RNAseq) and 480 (qPCR) between acute vs uninfected and 1000 (RNAseq) and 1500 (qPCR) between chronic vs uninfected samples. Next, we set out to explore the contribution of ZBP1 during *T. gondii* infection.

Necroptosis is not a significant pathway during *T. gondii* infection

The role of ZBP1 during infection has been studied in the context of viral induced necroptosis. In this pathway, ZBP1 senses viral DNA and binds to RIPK3 to form a protein complex, called a necrosome, that initiates necroptosis. The necrosome can be formed with a variety of protein-protein interactions, with RIPK3 as an essential component to the structure. We first examined the role of necroptosis during *T. gondii* infection prior to determining the involvement of ZBP1 in this pathway. Since RIPK3 is an essential factor in necroptosis, *RIPK3*$^{-/-}$ cells and mice were used to elucidate whether necroptosis is a significant form of cell death during *T. gondii* infection.

T. gondii can inhibit apoptosis in a dose dependent manner, therefore we first investigated whether *T. gondii* had the same affect on the necroptosis pathway (29-31). It is possible that

apoptosis and necroptosis are interconnected pathways as chemical induction of necroptosis, using z-VAD-FMK, functions through inhibition of caspase-mediated apoptosis (32-34). To compare the ability of *T. gondii* to inhibit cell death under apoptosis and necroptosis conditions, wild type mouse embryonic fibroblasts (MEFs) were infected and treated with tumor necrosis factor alpha (TNF-α) in combination with either 5ng/mL of cycloheximide (CHX), to induce apoptosis, or z-VAD-FMK to stimulate necroptosis. The viability of infected and treated cells was determined using a CellTiter glo assay and compared to uninfected treated and uninfected untreated cells (Figure 1A-B). Uninfected wild type MEFs treated with CHX displayed low cell viability (Figure 1A). As previously studied, the viability of MEFs treated with CHX was enhanced as the multiplicity of infection (MOI) with *T. gondii* increased. The trend in the rise of cell viability was not seen in MEFs treated with z-VAD-FMK and infected over a range of MOIs, suggesting *T. gondii* affects apoptosis and not necroptosis (Figure 1B).

To elucidate the significance of the necroptosis pathway in vivo, *RIPK3*$^{-/-}$ and wild type C57/BL6 mice were infected with 500 parasites and the outcome of infection was compared (Figure 1C-D). *RIPK3*$^{-/-}$ mice succumb to *T. gondii* infection at a faster, but not statistically significant rate (Figure 1C). To analyze the clinical symptoms of infection, mice were weighed daily (Figure 1D). *RIPK3*$^{-/-}$ mice lost a higher percentage of their overall weight over time and appeared more symptomatic during infection compared to wild type mice (Figure 1D). Overall, there was no statistical significance in the in vivo experiments, therefore it was concluded that necroptosis was not a biologically relevant pathway during *T. gondii* infection. These data also suggest that the high abundance of ZBP1 expression during *T. gondii* infection is not due to its previously characterized role in initiating necroptosis in infected cells.

ZBP1 expression is altered by *T. gondii* in activated macrophages

ZBP1 was originally described as a highly up-regulated product of IFN- γ stimulation in macrophages (35). Since macrophages are a more biologically relevant cell type during *T. gondii* infection, and MEFs are intrinsically heterogeneous populations of cells, we transitioned into studying the function of ZBP-1 in macrophages. Bone marrow derived macrophages (BMDMs) were harvested from wild type and *ZBP1*$^{-/-}$ mice as described in the materials and methods. To characterize the expression of ZBP1 in macrophages, qPCR was performed on wild type and *ZBP1*$^{-/-}$ macrophages under infected stimulated, uninfected stimulated, infected naïve and uninfected naïve conditions. In wild type uninfected macrophages stimulated with LPS and IFN-γ, a 11.5-fold increase in ZBP1 expression was detected when compared to uninfected naive macrophages (Figure 2). When wild type uninfected naïve macrophages were compared to *T. gondii* infected stimulated macrophages, only a 5-fold increase in expression of ZBP1 was observed. In wild type infected naïve macrophages, a 1.5 fold increase in ZBP1 transcript levels was detected. There was no substantial expression of ZBP1 in *ZBP1*$^{-/-}$ macrophages. These results confirm that ZBP1 is up-regulated by IFN-γ in macrophages and that macrophages do not initiate expression of ZBP1 in response to *T. gondii* infection alone. Interestingly, there was a significant decrease in ZBP1 transcript levels between wild type stimulated infected and uninfected macrophages, suggesting *T. gondii* down regulates expression of ZBP1.

ZBP1 affects parasite replication in activated macrophages in a dose dependent manner in.

To determine if ZBP1 contributes to *T. gondii* development in macrophages, a growth assay was conducted. BMDMs were plated on glass cover slips and infected with *T. gondii* at an MOI of 5. Two hours post-infection macrophages were primed and stimulated with LPS and IFN-γ at a

concentration of 100ng/mL and 25U/mL, respectively. 24 hours after infection, cells were fixed and an immunofluorescence assay was performed to determine the number of parasites per vacuole (Figure 3A). In wild type BMDMs there was a statistically higher percentage of single parasite vacuoles, 44%, compared to 28% *ZBP1*$^{-/-}$ cells (Figure 3A). The percentage of vacuoles containing two parasites per vacuole was consistent between wild type and *ZBP1*$^{-/-}$ cells, 40% and 43%, respectively. Only 13% of wild type cells contained vacuoles with 4 parasites and 24% in *ZBP1*$^{-/-}$ cells. These data suggests that ZBP1 has an influence on parasite replication in activated macrophages. The number of total parasites within the 150 random vacuoles evaluated was then quantified and averaged between the slides. In *ZBP1*$^{-/-}$ stimulated BMDMs, 334 parasites were present while only 282 total parasites were observed in wild type stimulated BMDMs (Figure 3B). To analyze whether the difference in parasite numbers was intrinsic to stimulated BMDMs, we compared the number of parasites per vacuole in naïve wild type and *ZBP1*$^{-/-}$ BMDMs. There was no statistical difference between the number of parasites per vacuole between wild type and *ZBP1*$^{-/-}$ naïve macrophages (Figure 3C). These data suggests ZBP1 has an influence on parasite replication in activated and not naive BMDMs.

NO production is decreased in *ZBP1*$^{-/-}$ activated BMDMs

The macrophage response to *T. gondii* infection is of great biological significance due to the cells role in producing nitric oxide (NO), which is critical for survival during chronic infection (36, 37). Macrophage production NO induces degradation of intracellular *T. gondii*, with detectable levels of NO at 48 hours post-stimulation (38). Because of the significance of NO production to macrophage function during infection, and the decrease in parasite growth in wild type BMDMs, compared to *ZBP1*$^{-/-}$ BMDMs, we assessed NO production 48 hours post-stimulation. *T. gondii*

can inhibit macrophage production of NO in response to stimulation, so we also examined NO production in a dose dependent manner to also characterize the affect of dose (39). To address this, wild type and *ZBP1*$^{-/-}$ BMDMs were grown in 96 well plates and infected with *T. gondii* at an MOI of 0, 2, 5, and 20. Two hours post-infection, BMDMs were primed and stimulated with LPS and IFN-γ, as described previously. 48 hours post-infection, a Griess reaction was performed to quantify production of NO. Wild type cells produced significantly higher levels of NO in response to stimulation, compared to *ZBP1*$^{-/-}$ cells, at MOIs of 0, 2, and 5 (Figure 4A). At an MOI of 20, there were no detectable levels of NO due to many of the cells being overwhelmed by parasite replication. There was a *T. gondii* dose-dependent decrease in NO production in both wild type and *ZBP1*$^{-/-}$ BMDMs, indicating ZBP1 is not involved in the interference of NO levels by *T. gondii*.

To evaluate whether the decrease in NO production in *ZBP1*$^{-/-}$ BMDMs is due to a difference in transcriptional expression of iNOS, the enzyme that catalyzes the conversion of L-arginine into NO, qPCR was performed. Uninfected and infected wild type and *ZBP1*$^{-/-}$ BMDMs were stimulated and RNA was collected 48 hours later. No difference in iNOS transcript expression was observed between wild type and *ZBP1*$^{-/-}$ infected or uninfected stimulated macrophages (Figure 4B). A decrease in iNOS transcript levels was seen between infected and uninfected wild type and *ZBP1*$^{-/-}$ BMDMs, indicating that *T. gondii* infection can inhibit transcription of iNOS independently of ZBP1.

A decrease in nitric oxide production can also be attributed to reduction in the availability of the substrate of iNOS, L-arginine. *T. gondii* up-regulates expression of Arginase-1 (ARG1), an enzyme that competes with iNOS for L-arginine in the cell, in order to decrease the ability of cells to produce nitric oxide (54). qPCR was also performed to determine if the decrease in nitric

oxide production in *ZBP1*$^{-/-}$ BMDMs was due to an increase of ARG1 expression and therefore a decrease in cellular L-arginine levels (Figure 4C). Infected *ZBP1*$^{-/-}$ BMDMs increased ARG1 expression at similar levels to wild type BMDMs, indicating the reduced nitric oxide levels in *ZBP1*$^{-/-}$ BMDMs is not due to ZBP1 influence on ARG1 expression.

Absence of ZBP-1 leads decreased parasite degradation in activated BMDMs

Generation of reactive nitrogen species, such as nitric oxide, by macrophages is critical for control of *T. gondii* infection (40, 41). To address the biological significance of the decrease in NO levels between stimulated wild type and *ZBP1*$^{-/-}$ BMDMs, we assessed the ability of these cells to degrade intracellular *T. gondii*. Using serum from chronically infected mice to stain the outer surface of *T. gondii*, parasites were visualized via immunofluorescence within stimulated macrophages. Parasites were classified as degraded based on the lack of consistent staining around the membrane of the parasites (Figure 5A). The parasites on the left (green) have bright, even staining around the entire membrane whereas parasites on the right have irregular, patchy staining. Parasites were verified as being intracellular via differential interference contrast (DIC) microscopy to ensure the degraded appearance was due to actions of the macrophage as opposed to parasites being extracellular and therefore dying (Figure 5B). A total of 100 vacuoles were counted and the percentage of degradation was quantified. Over 60 percent of parasites within wild type activated BMDMs appeared degraded (Figure 5C). Only 30 percent of parasites were degraded in activated *ZBP1*$^{-/-}$ BMDMs (figure 5C). Although activated *ZBP1*$^{-/-}$ BMDMs are capable of producing NO at detectable levels (Figure 4A), this data suggests slight but significant decreases in NO has a profound affects on biological function.

Increased levels of pro-inflammatory cytokines in *ZBP1*$^{-/-}$ BMDMs

To assess whether lack of ZBP1 leads to other defects in the response to LPS and IFN-γ stimulation in BMDMs, a cytometric bead array was used to determine levels of IL-12, IFN-γ, TNF-α, IL-10, MCP-1, and IL-6. There was no difference in IL-12, IFN-γ, or IL-10 between stimulated wild type and *ZBP1*$^{-/-}$ BMDMs. An increase in levels of TNF-α, MCP-1, and IL-6 were observed in *ZBP1*$^{-/-}$ BMDMs compared to wild type cells (Figure 7). TNF-α, MCP-1, and IL-6 are known pro-inflammatory attributes, but whether the observed increase is directly due to absence of ZBP1, lower levels of nitric oxide production, or a secondary affect of uncontrolled *T. gondii* infection will be determined in the future.

ZBP-1*$^{-/-}$ mice have a decreased resistance to lethal challenge of *T. gondii

Since ZBP1 was highly abundant in both acute and chronic mouse forebrain samples, compared to uninfected controls (Table 1), we sought out to determine whether ZBP1 influences outcome of acute toxoplasmosis. *ZBP1* $^{+/-}$ mice were bred to each other to produce *ZBP1* $^{+/+}$, *ZBP1* $^{+/-}$, and *ZBP1*$^{-/-}$ mice. All mice were fed brains of mice chronically infected with *T. gondii*, receiving approximately 4300 cysts each, and time to death was determined. Both *ZBP1* $^{+/-}$ and *ZBP1* $^{-/-}$ showed an increase in susceptibility to lethal doses of *T. gondii* compared to *ZBP1* $^{+/+}$ mice. In conjunction with our previous data, which suggest *ZBP1* $^{-/-}$ BMDMs have an increase in specific pro-inflammatory cytokines (Figure 6), the decrease in survival could be attributed to an over-abundant cytokine response. Over production of the Th1 cytokine response has been attributed previously to early death during lethal challenge with *T. gondii* (42).

Discussion

Nitric oxide is produced through the oxidation of the terminal guanidine nitrogen of L-arginine by the enzyme inducible nitric oxide synthase iNOS. iNOS is absolutely critical to this reaction as blocking iNOS function through addition of aminoguanidine 3 hours prior to stimulation leads to complete abolishment on NO levels (43). iNOS expression is induced by cytokines IFN-γ and TNF-α (44). Our data shows that a statistically significant increase in TNF-α and IL-6, as well as slight increase in MCP-1, are detected in *ZBP1* $^{-/-}$ BMDMs. As TNF-α is considered a master regulator of cytokine responses in various diseases, we hypothesize that this increase observed in *ZBP1* $^{-/-}$ BMDMs is in response to the lack of parasite degradation in the absence of ZBP1. *ZBP1* $^{-/-}$ cells produce higher levels of TNF-α and MCP-1 as a means to initiate antimicrobial actions against *T. gondii* infection. The higher levels of IL-6, which can act in either pro or anti-inflammatory mechanisms, in stimulated *ZBP1* $^{-/-}$ BMDMs will need to be studied further to elucidate whether it is acting to increase or decrease the cytokine response. Future studies will determine whether the same trends in cytokine production are observed in wild type and *ZBP1* $^{-/-}$ mice during the course of acute and chronic infection. Both the degradation phenotype and increase in cytokine production observed in vitro has potential significance for future in vivo studies. If *T. gondii* has increased survival in *ZBP1* $^{-/-}$ BMDMs, through lack of degradation, and the proper immune response is not mounted, then more parasites can survive within activated macrophages and travel throughout the host. This could lead to higher parasitemia in many organs including those in immunoprivileged areas (45).

Nitric oxide production during *T. gondii* infection has dichotomous roles. Absence of nitric oxide has been deemed dispensable for survival of *T. gondii* during acute infection although tight regulation of nitric oxide production is critical as too much can lead to substantial tissue damage

(46, 47). These studies focus on comparison of iNOS knockout mice to IL-12 and IFN-γ knockout mice, which rapidly succumb to *T. gondii* infection at low doses. The role of iNOS has not been studied in the context of lethal doses of *T. gondii* as the wild type controls from this study did not begin to die of infection until 12 weeks post-inoculation. The iNOS knockout mice showed an intermediate phenotype between the severely compromised IFN-γ and IL-12 knockout mice and the wild type controls, dying at the beginning of chronic infection (20 days p.i.). This study proves that nitric oxide production during early infection is not as critical as IL-12 or IFN-γ. These data do not address the potential role of nitric oxide during lethal challenge of *T. gondii* infection, which involves the comparison of wild type and *iNOS*$^{-/-}$ mice inoculated with a lethal dose of *T. gondii*. Lethal challenge with type II strains of *T. gondii* is representative of infection with the highly virulent type I strains. Therefore, we conducted experiments in wild type and *ZBP1* $^{-/-}$ mice that were orally fed 4300 cysts from the brains of mice infected with *T. gondii* for 4 weeks, simulating ingestion of a lethal challenge of *T. gondii*. Our data suggests a reassessment of NO production in response to acute toxoplasmosis should be examined.

In terms of the previously characterized functions of ZBP1, we have carefully ruled them out as being significant during *T. gondii* infection. In terms of the role of ZBP1 in initiation of type I interferon transcription, type-1 interferons have been deemed not essential for survival of *T. gondii* infection. Mice lacking the IFN-α/IFN-β receptor do not succumb to *T. gondii* infection in the same way as *IFN-γ*$^{-/-}$ mice do (48-50). Because of this acceptance that type-I interferons are essential to viral infection, and not protozoan infection, and the fact that no IFN-α transcripts were detected in stimulated wild type or *ZBP1* $^{-/-}$ BMDMs, we ruled this pathway indispensible for our observations (data not shown). We also extensively studied the role of ZBP1 during necroptosis in mouse embryonic fibroblasts, which is the cell line used to elucidate the role of

ZBP1 in viral induced necroptosis. Our data suggests necroptosis is not a significant form of cell death during *T. gondii* infection (Figure 1).

ZBP1 was described over a decade ago as a gene up-regulated in macrophages in response to LPS and IFN-γ (35). Since its discovery, the function in activated macrophages has not been elucidated. In this paper we have identified ZBP1 as another IFN-γ product that is manipulated by *T. gondii* upon infection. We have also identified a novel function for ZBP1 as a regulator of nitric oxide production in activated macrophages. We have also determined that absence of ZBP1 in activated macrophages leads to a defect in parasite degradation. The affect on nitric oxide production is not due to a difference in transcriptional control of iNOS or ARG1, two vital proteins in the process of producing nitric oxide. In the future, we will determine whether ZBP1 is involved in regulation of iNOS on the protein level. We will also focus on elucidating the interaction between ZBP1 and production of nitric oxide in activated macrophages as well as determining the contributions of ZBP1 during chronic infection.

Materials and Methods

Cell viability assays. Wild type, *RIPK3* $^{-/-}$ and *ZBP-1* $^{-/-}$ mouse embryonic fibroblasts (MEFs) were graciously provided by Jason Upton and cultured in Dulbecco's Modified Eagle Medium (DMEM). Cell viability assays were performed with wild type MEFs in 96 well plates with cells grown at 37°C and 5% CO_2. Wild type MEFs were plated at $1x10^4$ cells per well the day prior to infection with *T. gondii*. *T. gondii* was maintained in HFFs cultured in DMEM, as previously described, prior to infection. Wild type MEFs were infected with *T. gondii* at an MOI of 0, 20, 40 and 60 for 24 hours. 24 hours post-infection, the media was changed and fresh media was added containing either 1% DMSO (vehicle treated), 25ng/mL of TNF-α (Peprotech 315-01A)

and 5μg/mL of Cyclohemamide (Cayman chemical), or 25ng/mL of TNF-α and Z-VAD-FMK (Enzo Life Sciences) to induce apoptosis or necroptosis, respectively. Cycloheximide is a potent stimulator of apoptosis through inhibition of protein synthesis and displays enhanced killing in combination with TNF-α (51, 52). Z-VAD is a caspase inhibitor that induces necroptosis, another cell death pathway that can be initiated when caspase mediated apoptosis is inhibited (32-34). Cells were treated for 24 hours and cell viability was assessed using a Cell TiterGlo kit according to manufacturer's instructions (Promega). Background wells were measured using media only as controls. Percent cell viability was calculated as a percentage of cell viability compared to control 1% DMSO treated cells.

Preparation of bone marrow derived macrophages. CSF was collected from L929 cells prior to harvesting bone marrow from mice. CSF aids in maturation of bone marrow derived macrophages (BMDM). To produce CSF, L929 cells were cultured in Dulbecco's Modified Eagle Medium (DMEM). Cells were grown to confluency and left for 7-9 days. Supernatant was then collected and added to RPMI media supplemented with 10% FBS, 1% penicillin-streptomycin, 1% L-glutamine, .1% BME, and 1% sodium pyruvate. Once media was prepared, a wild type and *ZBP1* $^{-/-}$ C57BL/6 mouse was sacrificed and sterilized with 70% ethanol. The tibia and the femur were removed and the muscle tissue was cleaned from the leg bones using scissors. The bones were sterilized by soaking in 70% ethanol for 30 seconds. The bones were then cut to expose the marrow. A 10cc syringe with a filled with BMDM media and a 25-gauge needle was used to dislodge the bone marrow into a sterile 50 ml conical tube. The cell mixture was pipetted up and down until it was mixed thoroughly. Cell mixture was divided up evenly into 10cm petri dishes, supplemented with extra media, and incubated for 7 days. 3 days post plating fresh BMDM media was added to each dish. By day 7, the cells were fully developed

and were frozen down and stored in liquid nitrogen until use. Fresh cells were thawed for every experiment.

Nitric Oxide Production Wild type and *ZBP1* $^{-/-}$ BMDMs were seeded at $1x10^4$ cells per well in a 96-well plate. Three hours after cells were plated, they were infected with *T. gondii* at an MOI of 0, 2, 5, and 20. Two hours post-infection, the media was changed and RPMI containing 5ng/mL of LPS and 25U/mL of IFN-γ or fresh untreated RPMI. Supernatants from the cells were removed 48 and 72 hours post-infection and transferred to a new 96 well plate. Nitric oxide levels were determined using the Promega Griess reagent system according to the manufacturer's protocol. Absorbance was measured at 530 nm using a Synergy HT plate reader. Concentrations were determined using a standard curve generated for each reaction. Experiments were conducted with three technical replicates and three biological replicates. Statistical significance was determined using GraphPad Prism's two-way ANOVA analysis.

Mouse experiments. 6–8 week old C57BL/6 mice (National Cancer Institute, Charles River Laboratories, Frederick, MD) were ordered and compared to *RIPK3* $^{-/-}$ mice, Genentech (53). *RIPK3* $^{-/-}$ mice were backcrossed to C57BL/6 mice 19 times, and therefore were used in direct comparison between wild type C57BL/6 mice from NCI. Jason Upton graciously provided *ZBP1* $^{-/-}$ mice. *ZBP1* $^{-/-}$ mice were backcrossed 6 times to C57BL/6 mice, therefore to generate *ZBP1*$^{+/+}$ and *ZBP1* $^{-/-}$ mice we established heterozygous *ZBP1*$^{+/-}$ breeding colonies. *ZBP1*$^{+/}$ mice were then bred together to produce wild type, heterozygous, and knockout mice. Tail snips were collected from mice, digested with Proteinase K, and purified with phenol: chloroform prior to genotyping via PCR. Primers used for genotyping were as follows, WT Forward: GCTCTGGGAATGACGACAGC. Knockout Forward: CTAAAGCGCATGCTCCAGACTG. Reverse: CACTTCGTCTGCCCCTCAATTAGA

qPCR. To verify the increase in abundance of ZBP1 in the forebrains of *T. gondii* infected mice qPCR was performed (Table 1). cDNA was generated from the same RNA samples used for previous RNAseq analysis with Invitrogen Superscript III Reverse Transcriptase cDNA synthesis kit. PrimeTime qPCR primers from IDT targeting GAPDH, a house keeping control, and ZBP1 were used in this experiment. Fold changes were determined using the ΔΔCT method and normalized to GAPDH, then compared to uninfected samples. All other qPCR experiments were conducted from RNA extracted from BMDMs. PrimeTime qPCR primers from IDT targeting GAPDH (control), iNOS, ZBP-1, and ARG1 were used in these experiments.

Determination of parasites per vacuole $1x10^5$ wild type or *ZBP1* $^{-/-}$ BMDMs were plated in 4 well plates on glass cover slips in RPMI media. Cells were infected with $5x10^5$ parasites per well. Two hours post-infection, the media was changed and RPMI containing 5ng/mL of LPS and 25U/mL of IFN-γ or fresh untreated RPMI was added to the cells. 24 hours post-infection the media was removed and the cells were washed with 1xPBS. After the wash, 3% formaldehyde was added and cells were fixed for 30 minutes. After 30 minutes, 0.1M glycine was added for 5 minutes to stop the fixation. A blocking solution was added containing 5% BSA and 0.2% TrintonX-100 in 1X PBS and stored overnight at 4°C. The following day, serum from chronically infected mice was added as the primary antibody at a 1:300 dilution. Slides were incubated at room temperature with light shaking for one hour. The slides were then washed three times for minutes with a solution of 0.2% TrintonX-100 in 1X PBS. Alexa Flour 488 anti-mouse was added as the secondary antibody and incubated in darkness for 1 hour. Three more rinses with 0.2% TrintonX-100 in 1X PBS was preformed prior to mounting the coverslips on slides. Parasites were visualized using a Zeiss inverted Axiovert 200 motorized microscope with a 100X objective (PlanApo 1.4 na oil PH3 objective). A total of 6 slides for wild type and 6

slides for *ZBP1* $^{-/-}$ cells were quantified with 150 vacuoles counted on each slide. Slides were blinded prior to the counting. The percent of vacuoles containing 1, 2, 4, and 8 parasites were calculated based on number of total vacuoles counted on each slide.

Immunofluorescence Assay $1x10^5$ cells were plated on coverslips as described above. Cells were infected with $5x10^5$ parasites per well and 2 hours later stimulated with LPS and IFN-γ or left as naïve, as detailed above. 48 hours post-infection, the media was removed and cells were washed with 1X PBS and fixed with 3% formaldehyde. Following fixation, cells were incubated with 0.1M glycine for 5 minutes, followed by overnight blocking with a solution of 5% BSA and 0.2% TrintonX-100 in 1X PBS at 4°C.

References

1. **Pappas G, Roussos N, Falagas ME.** 2009. Toxoplasmosis snapshots: global status of Toxoplasma gondii seroprevalence and implications for pregnancy and congenital toxoplasmosis. Int J Parasitol **39:**1385-1394.
2. **Dubey JP, Lindsay DS, Speer CA.** 1998. Structures of Toxoplasma gondii tachyzoites, bradyzoites, and sporozoites and biology and development of tissue cysts. Clin Microbiol Rev **11:**267-299.
3. **Jones JL, Dubey JP.** 2012. Foodborne toxoplasmosis. Clin Infect Dis **55:**845-851.
4. **Scallan E, Hoekstra RM, Angulo FJ, Tauxe RV, Widdowson MA, Roy SL, Jones JL, Griffin PM.** 2011. Foodborne illness acquired in the United States--major pathogens. Emerg Infect Dis **17:**7-15.
5. **McAuley J, Boyer KM, Patel D, Mets M, Swisher C, Roizen N, Wolters C, Stein L, Stein M, Schey W, et al.** 1994. Early and longitudinal evaluations of treated infants and children and untreated historical patients with congenital toxoplasmosis: the Chicago Collaborative Treatment Trial. Clin Infect Dis **18:**38-72.
6. **Luft BJ, Remington JS.** 1992. Toxoplasmic encephalitis in AIDS. Clin Infect Dis **15:**211-222.
7. **Grigg ME, Ganatra J, Boothroyd JC, Margolis TP.** 2001. Unusual abundance of atypical strains associated with human ocular toxoplasmosis. J Infect Dis **184:**633-639.
8. **Montoya JG, Liesenfeld O.** 2004. Toxoplasmosis. Lancet **363:**1965-1976.
9. **Ong EL.** 2008. Common AIDS-associated opportunistic infections. Clin Med **8:**539-543.
10. **Chaudhry SA, Gad N, Koren G.** 2014. Toxoplasmosis and pregnancy. Can Fam Physician **60:**334-336.
11. **Barsoum RS.** 2006. Parasitic infections in transplant recipients. Nat Clin Pract Nephrol **2:**490-503.
12. **Israelski DM, Remington JS.** 1993. Toxoplasmosis in patients with cancer. Clin Infect Dis **17 Suppl 2:**S423-435.
13. **Derouin F, Pelloux H.** 2008. Prevention of toxoplasmosis in transplant patients. Clin Microbiol Infect **14:**1089-1101.
14. **de Veer MJ, Holko M, Frevel M, Walker E, Der S, Paranjape JM, Silverman RH, Williams BR.** 2001. Functional classification of interferon-stimulated genes identified using microarrays. Journal of leukocyte biology **69:**912-920.
15. **Butcher BA, Fox BA, Rommereim LM, Kim SG, Maurer KJ, Yarovinsky F, Herbert DR, Bzik DJ, Denkers EY.** 2011. Toxoplasma gondii rhoptry kinase ROP16 activates STAT3 and STAT6 resulting in cytokine inhibition and arginase-1-dependent growth control. PLoS Pathog **7:**e1002236.
16. **Butcher BA, Kim L, Johnson PF, Denkers EY.** 2001. Toxoplasma gondii tachyzoites inhibit proinflammatory cytokine induction in infected macrophages by preventing nuclear translocation of the transcription factor NF-kappa B. J Immunol **167:**2193-2201.
17. **Chao CC, Anderson WR, Hu S, Gekker G, Martella A, Peterson PK.** 1993. Activated microglia inhibit multiplication of Toxoplasma gondii via a nitric oxide mechanism. Clinical immunology and immunopathology **67:**178-183.

18. **Peterson PK, Gekker G, Hu S, Chao CC.** 1995. Human astrocytes inhibit intracellular multiplication of Toxoplasma gondii by a nitric oxide-mediated mechanism. J Infect Dis **171:**516-518.
19. **Green SJ, Mellouk S, Hoffman SL, Meltzer MS, Nacy CA.** 1990. Cellular mechanisms of nonspecific immunity to intracellular infection: cytokine-induced synthesis of toxic nitrogen oxides from L-arginine by macrophages and hepatocytes. Immunology letters **25:**15-19.
20. **Rosowski EE, Lu D, Julien L, Rodda L, Gaiser RA, Jensen KD, Saeij JP.** 2011. Strain-specific activation of the NF-kappaB pathway by GRA15, a novel Toxoplasma gondii dense granule protein. J Exp Med **208:**195-212.
21. **Tanaka S, Nishimura M, Ihara F, Yamagishi J, Suzuki Y, Nishikawa Y.** 2013. Transcriptome Analysis of Mouse Brain Infected with Toxoplasma gondii. Infect Immun **81:**3609-3619.
22. **Takaoka A, Wang Z, Choi MK, Yanai H, Negishi H, Ban T, Lu Y, Miyagishi M, Kodama T, Honda K, Ohba Y, Taniguchi T.** 2007. DAI (DLM-1/ZBP1) is a cytosolic DNA sensor and an activator of innate immune response. Nature **448:**501-505.
23. **Wang Z, Choi MK, Ban T, Yanai H, Negishi H, Lu Y, Tamura T, Takaoka A, Nishikura K, Taniguchi T.** 2008. Regulation of innate immune responses by DAI (DLM-1/ZBP1) and other DNA-sensing molecules. Proc Natl Acad Sci U S A **105:**5477-5482.
24. **Kaiser WJ, Upton JW, Mocarski ES.** 2008. Receptor-interacting protein homotypic interaction motif-dependent control of NF-kappa B activation via the DNA-dependent activator of IFN regulatory factors. J Immunol **181:**6427-6434.
25. **Rebsamen M, Heinz LX, Meylan E, Michallet MC, Schroder K, Hofmann K, Vazquez J, Benedict CA, Tschopp J.** 2009. DAI/ZBP1 recruits RIP1 and RIP3 through RIP homotypic interaction motifs to activate NF-kappaB. EMBO reports **10:**916-922.
26. **Upton JW, Kaiser WJ, Mocarski ES.** 2012. DAI/ZBP1/DLM-1 complexes with RIP3 to mediate virus-induced programmed necrosis that is targeted by murine cytomegalovirus vIRA. Cell host & microbe **11:**290-297.
27. **Ishii KJ, Kawagoe T, Koyama S, Matsui K, Kumar H, Kawai T, Uematsu S, Takeuchi O, Takeshita F, Coban C, Akira S.** 2008. TANK-binding kinase-1 delineates innate and adaptive immune responses to DNA vaccines. Nature **451:**725-729.
28. **Pittman KJ, Aliota MT, Knoll LJ.** 2014. Dual transcriptional profiling of mice and Toxoplasma gondii during acute and chronic infection. BMC Genomics **15:**806.
29. **Nash PB, Purner MB, Leon RP, Clarke P, Duke RC, Curiel TJ.** 1998. Toxoplasma gondii-infected cells are resistant to multiple inducers of apoptosis. J Immunol **160:**1824-1830.
30. **Goebel S, Gross U, Luder CG.** 2001. Inhibition of host cell apoptosis by Toxoplasma gondii is accompanied by reduced activation of the caspase cascade and alterations of poly(ADP-ribose) polymerase expression. Journal of cell science **114:**3495-3505.
31. **Vutova P, Wirth M, Hippe D, Gross U, Schulze-Osthoff K, Schmitz I, Luder CG.** 2007. Toxoplasma gondii inhibits Fas/CD95-triggered cell death by inducing aberrant processing and degradation of caspase 8. Cell Microbiol **9:**1556-1570.
32. **Bohgaki T, Mozo J, Salmena L, Matysiak-Zablocki E, Bohgaki M, Sanchez O, Strasser A, Hakem A, Hakem R.** 2011. Caspase-8 inactivation in T cells increases

necroptosis and suppresses autoimmunity in Bim-/- mice. The Journal of cell biology **195:**277-291.

33. **Steinhart L, Belz K, Fulda S.** 2013. Smac mimetic and demethylating agents synergistically trigger cell death in acute myeloid leukemia cells and overcome apoptosis resistance by inducing necroptosis. Cell death & disease **4:**e802.
34. **Melo-Lima S, Celeste Lopes M, Mollinedo F.** 2014. Necroptosis is associated with low procaspase-8 and active RIPK1 and -3 in human glioma cells, vol. 1.
35. **Fu Y, Comella N, Tognazzi K, Brown LF, Dvorak HF, Kocher O.** 1999. Cloning of DLM-1, a novel gene that is up-regulated in activated macrophages, using RNA differential display. Gene **240:**157-163.
36. **Scharton-Kersten TM, Yap G, Magram J, Sher A.** 1997. Inducible nitric oxide is essential for host control of persistent but not acute infection with the intracellular pathogen Toxoplasma gondii. J Exp Med **185:**1261-1273.
37. **Hibbs JB, Jr., Taintor RR, Vavrin Z, Rachlin EM.** 1988. Nitric oxide: a cytotoxic activated macrophage effector molecule. Biochemical and biophysical research communications **157:**87-94.
38. **Lowry MA, Goldberg JI, Belosevic M.** 1998. Induction of nitric oxide (NO) synthesis in murine macrophages requires potassium channel activity. Clinical and experimental immunology **111:**597-603.
39. **Luder CG, Algner M, Lang C, Bleicher N, Gross U.** 2003. Reduced expression of the inducible nitric oxide synthase after infection with Toxoplasma gondii facilitates parasite replication in activated murine macrophages. Int J Parasitol **33:**833-844.
40. **Adams LB, Hibbs JB, Jr., Taintor RR, Krahenbuhl JL.** 1990. Microbiostatic effect of murine-activated macrophages for Toxoplasma gondii. Role for synthesis of inorganic nitrogen oxides from L-arginine. J Immunol **144:**2725-2729.
41. **Murray HW, Teitelbaum RF.** 1992. L-arginine-dependent reactive nitrogen intermediates and the antimicrobial effect of activated human mononuclear phagocytes. J Infect Dis **165:**513-517.
42. **Mordue DG, Monroy F, La Regina M, Dinarello CA, Sibley LD.** 2001. Acute toxoplasmosis leads to lethal overproduction of Th1 cytokines. J Immunol **167:**4574-4584.
43. **Imai Y, Kolb H, Burkart V.** 1993. Nitric oxide production from macrophages is regulated by arachidonic acid metabolites. Biochemical and biophysical research communications **197:**105-109.
44. **Yamada K, Otabe S, Inada C, Takane N, Nonaka K.** 1993. Nitric oxide and nitric oxide synthase mRNA induction in mouse islet cells by interferon-gamma plus tumor necrosis factor-alpha. Biochemical and biophysical research communications **197:**22-27.
45. **Courret N, Darche S, Sonigo P, Milon G, Buzoni-Gatel D, Tardieux I.** 2006. CD11c- and CD11b-expressing mouse leukocytes transport single Toxoplasma gondii tachyzoites to the brain. Blood **107:**309-316.
46. **Khan IA, Matsuura T, Fonseka S, Kasper LH.** 1996. Production of nitric oxide (NO) is not essential for protection against acute Toxoplasma gondii infection in IRF-1-/- mice. J Immunol **156:**636-643.
47. **Scharton-Kersten TM, Yap G, Magram J, Sher A.** 1997. Inducible nitric oxide is essential for host control of persistent but not acute infection with the intracellular pathogen Toxoplasma gondii. J Exp Med **185:**1261-1273.

48. **Beiting DP.** 2014. Protozoan parasites and type I interferons: a cold case reopened. Trends in parasitology **30:**491-498.
49. **Suzuki Y, Orellana MA, Schreiber RD, Remington JS.** 1988. Interferon-gamma: the major mediator of resistance against Toxoplasma gondii. Science **240:**516-518.
50. **Yap GS, Sher A.** 1999. Effector cells of both nonhemopoietic and hemopoietic origin are required for interferon (IFN)-gamma- and tumor necrosis factor (TNF)-alpha-dependent host resistance to the intracellular pathogen, Toxoplasma gondii. J Exp Med **189:**1083-1092.
51. **Ruff MR, Gifford GE.** 1981. Rabbit tumor necrosis factor: mechanism of action. Infect Immun **31:**380-385.
52. **Alessenko AV, Boikov P, Filippova GN, Khrenov AV, Loginov AS, Makarieva ED.** 1997. Mechanisms of cycloheximide-induced apoptosis in liver cells. FEBS letters **416:**113-116.
53. **Newton K, Sun X, Dixit VM.** 2004. Kinase RIP3 is dispensable for normal NF-kappa Bs, signaling by the B-cell and T-cell receptors, tumor necrosis factor receptor 1, and Toll-like receptors 2 and 4. Molecular and cellular biology **24:**1464-1469.
54. **Butcher BA, Fox BA, Rommereim LM, Kim SG, Maurer KJ, Yarovinsky F, Herbert DR, Bzik DJ, Denkers EY.** 2011. Toxoplasma gondii rhoptry kinase ROP16 activates STAT3 and STAT6 resulting in cytokine inhibition and arginase-1-dependent growth control. PLoS Pathog **7:**e1002236.

Table 1. Comparison of ZBP1 transcripts as determined by RNAseq and qPCR.

	Acute vs Uninfected	Chronic vs uninfected
RNAseq	300	1000
qPCR	480	1500

Fold change of ZBP1 transcript levels between acute vs uninfected and chronic vs uninfected mouse forebrains was analyzed through RNAseq analysis, as descripted previously (28). To verify the dramatic increase in ZBP1 transcripts between each sample, qPCR using the same cDNA samples was performed. Primers targeting ZBP1 and GAPDH were used. qPCR fold change was determined by normalization to GAPDH and then comparing to uninfected samples using the ΔΔCT method.

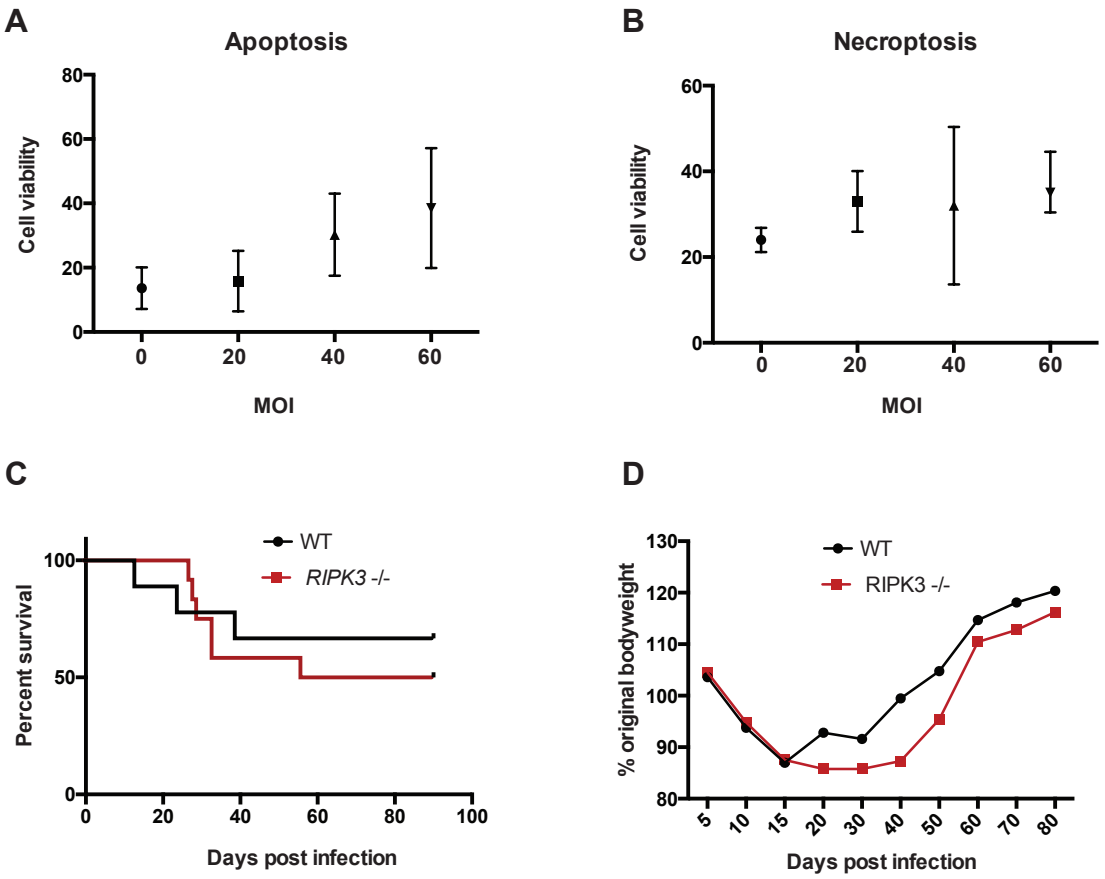

Figure 1. Necroptosis is not a significant pathway during *T. gondii* infection.

Wild type MEFs were infected with *T. gondii* at an MOI of 0, 20, 40, and 60 for 24 hours. (**A**) Cells were then treated with 25ng/mL of TNF-α and 5μg/mL of Cyclohemamide or (**B**) 25ng/mL of TNF-α and Z-VAD-FMK to induce apoptosis (**A**) or necroptosis (**B**). Cell viability was determined 24 hours after drug treatment using a CellTiter Glo assay. Percent viability was determined through comparison of treated cells to uninfected cells containing 1% DMSO (vehicle treated). (**C**) Wild type and *RIPK3*$^{-/-}$ mice were infected with 500 parasites and time to death was determined. (**D**). To assess the morbidity of infection, wild type and *RIPK3*$^{-/-}$ mice were weighed daily and the percentage of weight loss, as compared to initial weights prior to infection, were calculated.

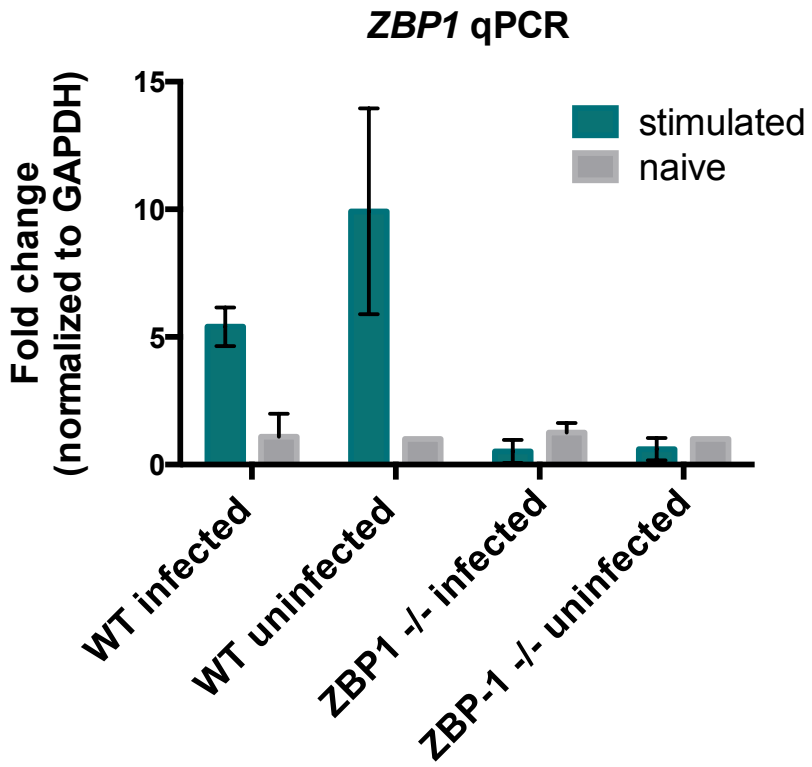

Figure 2. ZBP1 is up-regulated in activated bone marrow derived macrophages.

Wild type and *ZBP1*$^{-/-}$ bone marrow derived macrophages (BMDMs) were plated and infected at an MOI of 5. Two hours post-infection, BMDMs were stimulated with 5ng/mL of LPS and 25U/mL of IFN-γ. 48 hours post-infection RNA was extracted using TRIzol and cDNA was synthesized from the RNA. qPCR was performed using primers targeting ZBP1 and GAPDH. ZBP1 transcript levels were normalized to GAPDH transcripts and then compared to uninfected naive BMDM samples for both wild type and *ZBP1*$^{-/-}$ cells using the ΔΔCT method.

A

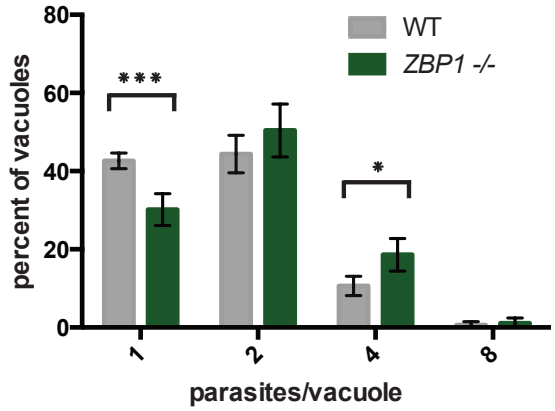
24 hours infected stimulated
WT
ZBP1 -/-
percent of vacuoles
80
60
40
20
0
***
*
1
2
4
8
parasites/vacuole

B

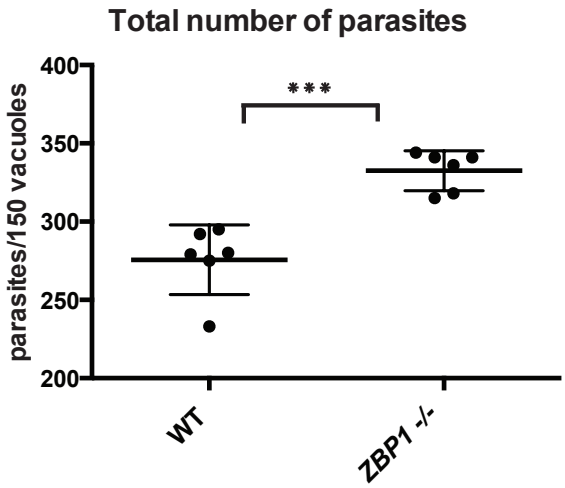
Total number of parasites
parasites/150 vacuoles
400
350
300
250
200
***
WT
ZBP1 -/-

C

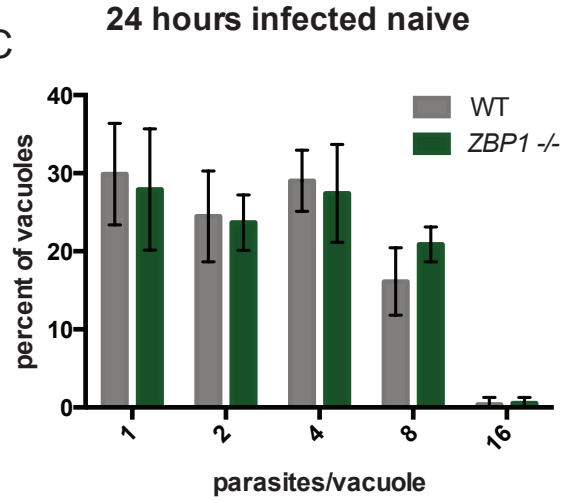
24 hours infected naive
WT
ZBP1 -/-
percent of vacuoles
40
30
20
10
0
1
2
4
8
16
parasites/vacuole

Figure 3. ZBP1 influences parasite replication in activated bone marrow derived macrophages.

(**A-C**) *T. gondii* was cultured in wild type and *ZBP1*$^{-/-}$ bone marrow derived macrophages and stimulated with 5ng/mL of LPS and 25U/mL of IFN-γ (**A-B**) or left untreated (naïve). 24 hours post-infection, parasites were fixed and the number of parasites per vacuole was determined by IFA using serum from chronically infected mice (**A-C**). (**B)** The number of total parasites was determined by adding together the number of 1, 2, and 4 parasites per vacuole in (**A**). For each experiment, 6 slides were examined and150 vacuoles were counted from each slide. Percentage of 1, 2, and 4 parasites per vacuole was determined from total number of vacuoles counted.

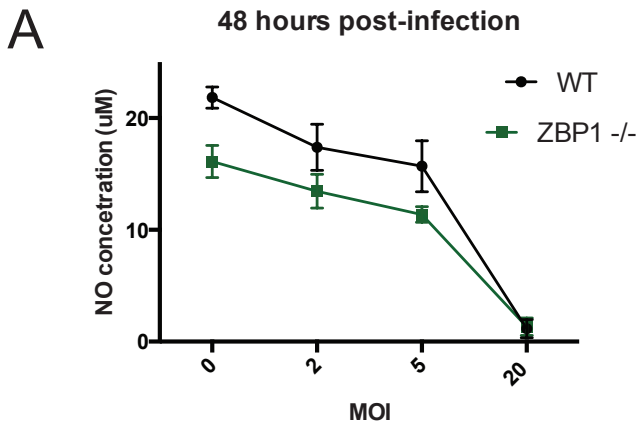
A
48 hours post-infection
WT
ZBP1 -/-
NO concetration (uM)
20
10
0
0
2
5
20
MOI

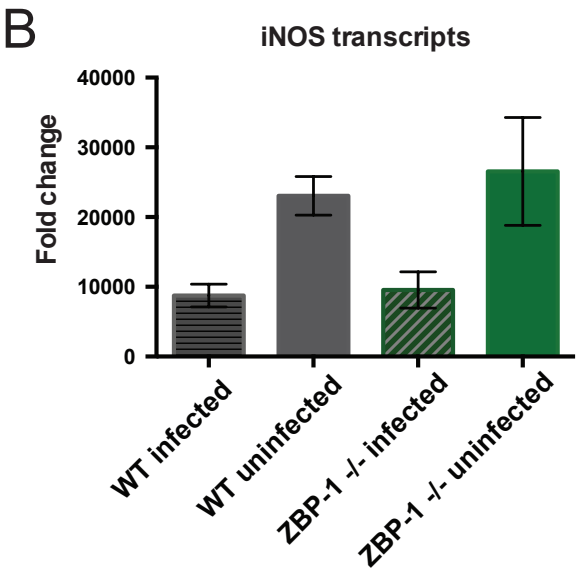
B
iNOS transcripts
Fold change
40000
30000
20000
10000
0
WT infected
WT uninfected
ZBP-1 -/- infected
ZBP-1 -/- uninfected

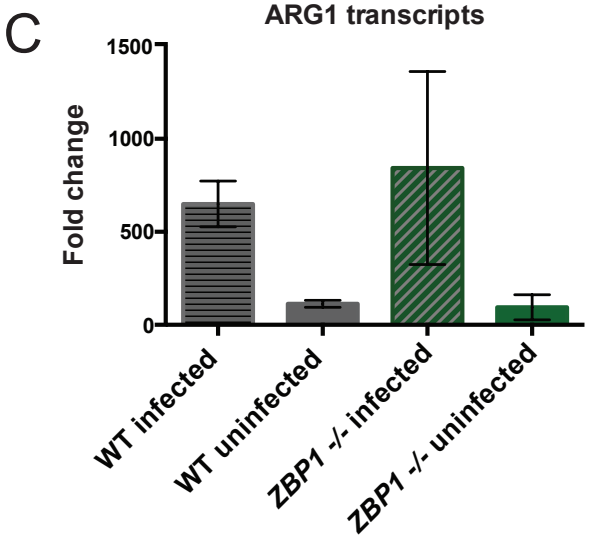
C
ARG1 transcripts
Fold change
1500
1000
500
0
WT infected
WT uninfected
ZBP1 -/- infected
ZBP1 -/- uninfected

Figure 4. Nitric oxide production is decreased in stimulated *ZBP1* $^{-/-}$ bone marrow derived macrophages.

(**A**) Wild type and *ZBP1* $^{-/-}$ bone marrow derived macrophages (BMDMs) were infected with *T. gondii* at an MOI of 0, 2, 5, 20. 2 hours post-infection, cells were stimulated with 5ng/mL of LPS and 25U/mL of IFN-γ. 48 hours post-infection, supernatants from the cells were used in a Griess reaction to determine nitric oxide. Concentration. (**B and C**) To determine the mechanism of nitric oxide reduction in *ZBP1* $^{-/-}$ cells qPCR was performed targeting iNOS and ARG1 transcripts. Expression between wild type and *ZBP1* $^{-/-}$ BMDMs was compared between stimulated infected and uninfected samples using GAPDH as a control using the ΔΔCT method. All samples were compared to uninfected naïve samples.

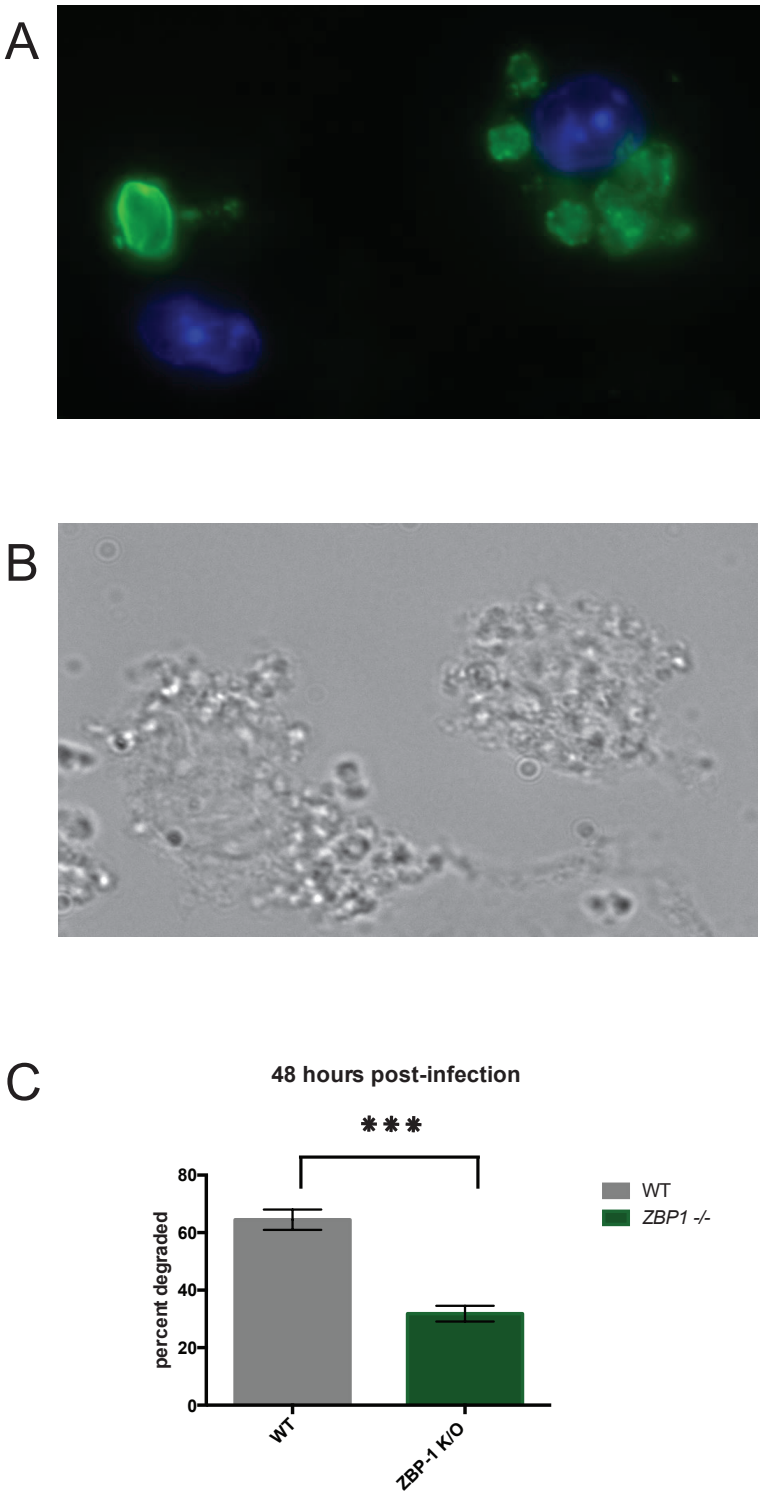

Figure 5. Degradation of *T. gondii* is decreased in in stimulated *ZBP1* $^{-/-}$ bone marrow derived macrophages.

(**A-C**) An immunofluorescence assay (IFA) was performed on wild type and *ZBP1* $^{-/-}$ bone marrow derived macrophages infected with *T. gondii* and stimulated with 5ng/mL of LPS and 25U/mL of IFN-γ for 48 hours. Serum from chronically infected mice was used to stain *T. gondii* (**A**-green). Parasites were assessed as being intact or degraded based on appearance of IFA staining. (**A)** Depiction of intact (left) and degraded (right) parasites stained with chronic serum. (**B**) Differential interference contrast (DIC) was used to determine whether degraded parasites were intracellular or extracellular. (**C**) 100 vacuoles were counted and the percentage of intact vs degraded parasites was verified.

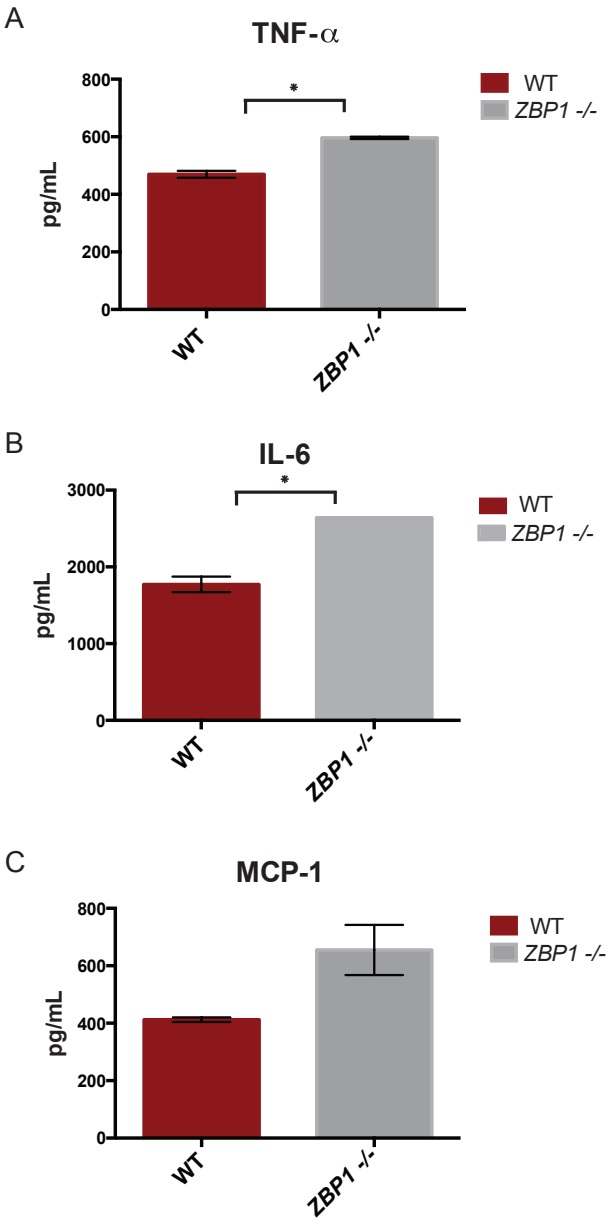

Figure 6. Expression of pro-inflammatory cytokines is increased in *ZBP1* $^{-/-}$ bone marrow derived macrophages.

(**A-C**) A cytometric bead array (CBA) kit from BD Biosciences was used to determine levels of IL-12, IFN-γ, TNF-α, IL-10, MCP-1, and IL-6. Supernatants from wild type and *ZBP1* $^{-/-}$ bone marrow derived macrophages (BMDMs) infected with *T. gondii* at an MOI of 5 were used for the assay. BMDMs were stimulated with 5ng/mL of LPS and 25U/mL of IFN-γ for 48 hours prior to analysis.

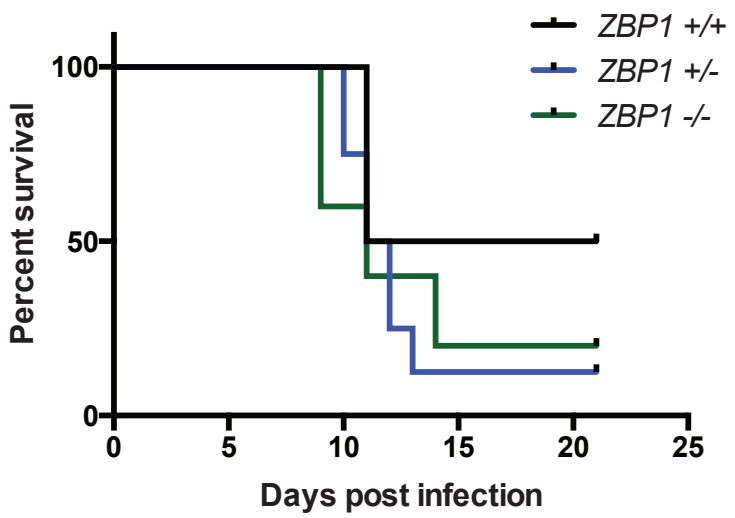

Figure 7. *ZBP1* $^{-/-}$ mice are more susceptible to lethal doses of *T. gondii*.

ZBP1 $^{+/-}$ mice were bred to each other to produce *ZBP1* $^{+/+}$, *ZBP1* $^{+/-}$, and *ZBP1* $^{-/-}$ mice. All mice were fed brains of mice chronically infected with *T. gondii*, receiving approximately 4300 cysts each, and time to death was determined.

Chapter 4

Conclusions and Future Directions

Conclusions

T. gondii is one of the most successful parasites in the world with approximately 30 percent of the human population infected. The success of the parasite is due to the ability of *T. gondii* to remain infectious in all life stages. During acute infection, the asexual tachyzoite rapidly disseminates throughout the host. *T. gondii* rapidly disseminates within the host by infecting migratory immune cells, such as macrophages and dendritic cells. *T. gondii* invades these cells and manipulates their function to gain access to immunoprivileged areas of the body, like the brain (1, 2). Pressure from the immune system, along with other unknown factors, triggers tachyzoite differentiation into the slower growing, encysted bradyzoite form (3). The bradyzoite persists for the lifetime of the host as intracellular cysts present in striated muscle and the central nervous system (4).

T. gondii has developed a multitude of strategies to evade the host immune response. One pathway of particular interest to our laboratory is the ability of *T. gondii* to block parasite degradation by nitric oxide (NO) production in activated macrophages (5, 6). *T. gondii* accomplishes this through multiple strategies including down-regulating transcription of the enzyme iNOS, which is required for nitric oxide production (2). The other part of this hindrance is due to the ability of *T. gondii* to suppress NO production by limiting the availability of the substrate required for NO production, L-arginine (5, 7, 8). This is accomplished through *T. gondii* mediated up-regulation of host arginine-1, an enzyme that degrades intracellular arginine. The mechanism of action has been studied in type I strains, where parasites initiate arginine starvation by secreting ROP16, a kinase that activates STAT6 resulting in expression of host arginase-1 (5). Arginase-1 up-regulation leads to limiting the availability of L-arginine and thus NO synthesis (9). The mechanism of arginase-1 up-regulation and iNOS down-regulation in cells

infected with type II parasites is currently unknown. A decrease in NO synthesis would appear to be beneficial to the parasite, but *T. gondii* is an arginine auxotroph and exhibits decreased growth in media lacking arginine (5). This is an example of *T. gondii* triggering a response that leads to reduction in parasite growth for the purpose of long-term survival of the parasite within the host. While NO plays an important role during acute infection, it is most important during chronic infection, as iNOS knockout mice succumb to *T. gondii* in the early stages of chronic infection (20-25 days) (10).

In this thesis an RNAseq approach was used to study both host and parasite interactions during acute and chronic *T. gondii* infection. The goal of this analysis was to elucidate *T. gondii* specific elements that contribute to establishment and maintenance of a life-long infection as well as identify host factors that aid in parasite survival. From this dataset, the host specific gene Z-DNA binding protein 1 (*ZBP1)* was highly expressed in the forebrains of mice during both acute and chronic infection (11).

Initially, ZBP1 was identified as an IFN-γ regulated product in activated macrophages, but the function has yet to be elucidated (12). In recent studies we have identified ZBP1 as a new host target that *T. gondii* down regulates upon infection. We have described a novel role for ZBP1 in the degradation of *T. gondii* through nitric oxide production in activated macrophages. In this paper we have identified ZBP1 as another IFN-γ product that is manipulated by *T. gondii* upon infection. We have also characterized a novel function for ZBP1 as a regulator of nitric oxide production in activated macrophages. We have also determined that absence of ZBP1 in activated macrophages leads to a defect in parasite degradation. The affect on nitric oxide production is not due to a difference in transcriptional control of iNOS or ARG1, two vital proteins in the process of producing nitric oxide. In the future, we will determine whether ZBP1

is involved in regulation of iNOS on the protein level. We will also focus on elucidating the interaction between ZBP1 and production of nitric oxide in activated macrophages as well as determining the contributions of ZBP1 during chronic infection.

The future of this data set is in providing a better understanding of host targets that are modulated by infection with *T. gondii*. This understanding is critical for development of future therapeutics. Identification of host cell targets alter by *T. gondii* is of specific interest for vaccine development as it is hypothesized that a live-attenuated parasite must be used for long-term protection. Currently, the only vaccine on the market is a live, attenuated strain that has been passaged for 30 years in the laboratory (13). This vaccine only provides protection for 3 years and has a short shelf life (14). Knowledge of host cell defense mechanisms that are disrupted by the parasite gives insight into potential adjuvants to incorporate into future vaccines as well as parasitic proteins involved in blocking these pathways for generation of *T. gondii* mutants, with target deletions in genes responsible for down regulating certain host responses, such as iNOS and ZBP1, or other IFN-γ regulated genes that would be safe for use in vaccines. Our approach of using dual RNA-seq analysis is ideal as in vivo host and pathogen targets are now available.

Future Directions

There are still many unknown aspects to the role of ZBP1 during *T. gondii* infection. We have ruled out two of the previously identified mechanisms on ZBP1 function involving expression of type I interferons and induction of necroptosis during infection (15, 16). Our data suggests ZBP1 is involved in degradation of intracellular *T. gondii* in activated macrophages, potentially through nitric oxide production. Future studies will be focused on addressing the exact mechanism of action for ZBP1 mediated degradation in activated macrophages.

What is ZBP1 interacting with during stimulation in bone marrow derived macrophages?

Identifying the binding partners of ZBP1 during bone marrow derived macrophage (BMDM) stimulation would help elucidate the exact mechanism of function. We have previously used two commercially available ZBP1 antibodies (BioLegend and BioRad) but have determined both antibodies have high amounts of nonspecific binding through both IFA and western blot analysis. To overcome this issue a C-terminal and N-terminal HA-tag ZBP1 construct will be made. This construct will initially be transfected into wild type BMDMs. After transfection, BMDMs will be infected with *T. gondii*, or left uninfected, stimulated with LPS and IFN-γ, or left naïve, and protein samples will be collected at 12, 24, and 48 hours post-stimulation. Protein samples will be run on an acrylamide gel and analyzed via western blot analysis with a primary antibody targeting the HA-tag. If a single target is detected at the appropriate size of ZBP1-HA, then an immunoprecipitation (IP) will be performed. For the IP analysis, wild type BMDM protein samples will be collected as described above. BMDM protein extracts will be incubated with HA-conjugated agarose beads. The bead and protein mixture will then be run on an acrylamide gel and stained with ProtoBlue Safe to visualize the proteins pulled-down from the total cellular samples. Bands will be excised from the gel and submitted for mass-spectrometry analysis to determine poteintial ZBP1 binding partners.

Where is ZBP1 localized during stimulation in bone marrow derived macrophages?

Using the HA-tagged ZBP1 construct described above, immunofluorescence assays (IFA) will be conducted to compare the localization of ZBP1 in uninfected stimulated, infected stimulated, infected naïve and uninfected naïve wild type BMDMs. We will co-stain the parasitophorous vacuole, formed upon *T. gondii* entry into the host cell, to determine if ZBP1 is interacting with

parasite material. This, in conjunction with the IP studies described above, will elucidate how ZBP1 is affecting degradation of *T. gondii*.

Are there differences in the cytokine responses to *T. gondii* infection between wild type and *ZBP1*$^{-/-}$ mice?

Our previous data suggests there is a difference in production of TNF-α, MCP-1, and IL-6 between wild type and *ZBP1*$^{-/-}$ BMDMs when stimulated with LPS and IFN-γ. In the future we will determine if there is a difference in these cytokine levels during in vivo *T. gondii* infection in mice. Wild type and *ZBP1*$^{-/-}$ C57BL/6 mice will be infected with 5,000 TgME49 parasites and blood will be collected at 2, 4, 6, and 10 days post-infection. Serum will be collected from the blood and analyzed with a cytometric bead array. The cytometric bead array assay will detect levels of IL-12, IFN-γ, TNF-α, MCP-1, IL-6 and IL-10. Serum levels of all cytokines will be compared between wild type and *ZBP1*$^{-/-}$ samples.

Do ZBP1$^{-/-}$ mice have higher cyst burdens in the brain during chronic *T. gondii* infection?

Our results suggest ZBP1 influences production of NO in stimulated BMDMs. The significance to this in an animal model could be that more parasites remain alive and infections within macrophages. Macrophages are migratory cells, so an increase intracellular intact parasites could lead to an increased ability of the parasite to disseminate throughout the host. Specifically, this may cause a higher level of parasites that reach the brain. These parasites will eventually differentiate into bradyzoites within the brain and lead to an overall higher cyst burden. To examine this hypothesis, wild type and *ZBP1*$^{-/-}$ C57BL/6 mice will be infected with 500 TgME49 parasites for four weeks. At four weeks post-infection, mice will be sacrificed and their brains will be removed. These brains will be homogenized and stained with *Dolichos bifluorous*

agglutinin (DBA). An immunofluorescence assay will be performed to determine overall cyst burdens in the brains of infected mice.

Do ZBP1$^{-/-}$ mice have a decrease in susceptibility to Toxoplasmic Encephalitis?

Work from a previous graduate student in the laboratory determined *T. gondii* possessing a gene deletion in ΔTgPLI, a patatin-like protein of previously unknown function, caused a delay in the develop of Toxoplasmic Encephalitis (TE). These same cytokines were up-regulated in stimulated ZBP1$^{-/-}$BMDMs. To test the hypothesis that ZBP1$^{-/-}$ mice are more resistant to development of TE over time, wild type and *ZBP1*$^{-/-}$ C57BL/6 mice will be infected with 500 TgME49 parasites and the time to death will be determined. Onset of TE in wild type mice occurs between 12-16 weeks post-infection. Mice will be closely monitored at these time points.

References

1. **Lambert H, Hitziger N, Dellacasa I, Svensson M, Barragan A.** 2006. Induction of dendritic cell migration upon Toxoplasma gondii infection potentiates parasite dissemination. Cell Microbiol **8:**1611-1623.
2. **Luder CG, Algner M, Lang C, Bleicher N, Gross U.** 2003. Reduced expression of the inducible nitric oxide synthase after infection with Toxoplasma gondii facilitates parasite replication in activated murine macrophages. Int J Parasitol **33:**833-844.
3. **Skariah S, McIntyre MK, Mordue DG.** 2010. Toxoplasma gondii: determinants of tachyzoite to bradyzoite conversion. Parasitol Res **107:**253-260.
4. **Weiss LM, Kim K.** 2000. The development and biology of bradyzoites of Toxoplasma gondii. Front Biosci **5:**D391-405.
5. **Butcher BA, Fox BA, Rommereim LM, Kim SG, Maurer KJ, Yarovinsky F, Herbert DR, Bzik DJ, Denkers EY.** 2011. Toxoplasma gondii rhoptry kinase ROP16 activates STAT3 and STAT6 resulting in cytokine inhibition and arginase-1-dependent growth control. PLoS Pathog **7:**e1002236.
6. **Butcher BA, Kim L, Johnson PF, Denkers EY.** 2001. Toxoplasma gondii tachyzoites inhibit proinflammatory cytokine induction in infected macrophages by preventing nuclear translocation of the transcription factor NF-kappa B. J Immunol **167:**2193-2201.
7. **Chao CC, Anderson WR, Hu S, Gekker G, Martella A, Peterson PK.** 1993. Activated microglia inhibit multiplication of Toxoplasma gondii via a nitric oxide mechanism. Clinical immunology and immunopathology **67:**178-183.
8. **Peterson PK, Gekker G, Hu S, Chao CC.** 1995. Human astrocytes inhibit intracellular multiplication of Toxoplasma gondii by a nitric oxide-mediated mechanism. J Infect Dis **171:**516-518.
9. **Green SJ, Mellouk S, Hoffman SL, Meltzer MS, Nacy CA.** 1990. Cellular mechanisms of nonspecific immunity to intracellular infection: cytokine-induced synthesis of toxic nitrogen oxides from L-arginine by macrophages and hepatocytes. Immunology letters **25:**15-19.
10. **Scharton-Kersten TM, Yap G, Magram J, Sher A.** 1997. Inducible nitric oxide is essential for host control of persistent but not acute infection with the intracellular pathogen Toxoplasma gondii. J Exp Med **185:**1261-1273.
11. **Pittman KJ, Aliota MT, Knoll LJ.** 2014. Dual transcriptional profiling of mice and Toxoplasma gondii during acute and chronic infection. BMC Genomics **15:**806.
12. **Fu Y, Comella N, Tognazzi K, Brown LF, Dvorak HF, Kocher O.** 1999. Cloning of DLM-1, a novel gene that is up-regulated in activated macrophages, using RNA differential display. Gene **240:**157-163.
13. **O'Connell E, Wilkins MF, Te Punga WA.** 1988. Toxoplasmosis in sheep. II. The ability of a live vaccine to prevent lamb losses after an intravenous challenge with Toxoplasma gondii. New Zealand veterinary journal **36:**1-4.
14. **Buxton D, Thomson KM, Maley S, Wright S, Bos HJ.** 1993. Experimental challenge of sheep 18 months after vaccination with a live (S48) Toxoplasma gondii vaccine. Vet Rec **133:**310-312.

15. **Takaoka A, Wang Z, Choi MK, Yanai H, Negishi H, Ban T, Lu Y, Miyagishi M, Kodama T, Honda K, Ohba Y, Taniguchi T.** 2007. DAI (DLM-1/ZBP1) is a cytosolic DNA sensor and an activator of innate immune response. Nature **448:**501-505.
16. **Upton JW, Kaiser WJ, Mocarski ES.** 2012. DAI/ZBP1/DLM-1 complexes with RIP3 to mediate virus-induced programmed necrosis that is targeted by murine cytomegalovirus vIRA. Cell host & microbe **11:**290-297.

Appendix A

A Toxoplasma patatin-like protein changes localization and alters the cytokine response during toxoplasmic encephalitis

Crystal Tobin Magle, **Kelly J. Pittman**, Lindsey A. Moser, Kyle M. Boldon and Laura J. Knoll[1]

Department of Medical Microbiology and Immunology University of Wisconsin-Madison

1550 Linden Drive, Madison, WI 53706

Summary

Toxoplasma gondii is an obligate intracellular parasite that forms a life-long infection within the central nervous system of its host. The *T. gondii* genome encodes six members of the patatin-like phospholipase family; related proteins are associated with host-microbe interactions in bacteria. *T. gondii* patatin-like protein 1 (*TgPL1*) was previously determined to be necessary for parasites to suppress nitric oxide and prevent degradation in activated macrophages. Here we show that in the rapidly replicating tachyzoite stage, TgPL1 is localized within vesicles inside the parasite that are distinct from the dense granules; however, in the encysted bradyzoite stage, TgPL1 localizes to the parasitophorous vacuole (PV) and cyst wall. While we had not previously seen a defect of the TgPL1 deletion mutant (ΔTgPL1) during acute and early chronic infection, the localization change of TgPL1 in bradyzoites caused us to reevaluate the ΔTgPL1 mutant during late chronic infection and in a toxoplasmic encephalitis (TE) mouse model. Mice infected with ΔTgPL1 are more resistant to TE and have fewer inflammatory lesions than wild type and ΔTgPL1 genetically complemented with *TgPL1* infected mice. This increased resistance to TE could result from several contributing factors. First, we found that ΔTgPL1 bradyzoites did not convert back to tachyzoites readily in tissue culture. Second, a subset of cytokine levels were higher in ΔTgPL1 infected mice, including interferon gamma (IFN-γ), tumor necrosis factor α (TNF-α), interleukin-6 (IL-6) and monocyte chemotactic protein-1 (MCP-1). These studies suggest that the TgPL1 plays a role in the maintenance of *T. gondii* chronic infection.

Introduction

Patatin-like phospholipases (PLPs) belong to a diverse family of proteins that are found in a variety of biological systems. The founding member of this family is patatin, a major component of the soluble glycosylated protein found in potatoes (1). Patatin localizes to the plant storage vacuole (2) but exhibits phospholipase A_2 (PLA_2) activity when it relocalizes to the cytoplasm during stress conditions (3, 4). Plants induce PLA_2 activity in response to stresses such as infection, using the fatty acid and lysophospholipid products as signaling molecules to mount antimicrobial responses (5). Other plant species have patatin homologs that also appear to respond to infection (6, 7). PLPs are also encoded in a number of bacterial genomes and have been associated with severe disease (8). The genomes of host-associated bacteria, including commensals as well as pathogens, have a higher frequency of PLPs than the genomes of free-living bacteria, indicating a role in host-microbe interactions (9). The genome of the obligate intracellular parasite *Toxoplasma gondii* encodes six predicted PLPs, the functions of which have not been thoroughly characterized.

Throughout the *T. gondii* life cycle, the parasite is exposed to many types of stresses within its host. When *T. gondii* parasites enter the host through the digestive tract, they are confronted with digestive enzymes in the stomach, which they use as a signal to egress from the cysts, escape this acidic environment, and replicate in the peritoneal cells outside of the stomach (10). As the parasite replicates in these tissues, the host mounts an immune response whereupon the parasite is assaulted by a variety of antimicrobial responses including nitric oxide (NO), reactive oxygen species, and engulfment by phagocytic cells (11, 12). The parasite is able to reduce these antimicrobial responses and to hijack immune cells, such as macrophages and dendritic cells, to disseminate to distal sites in the body (13, 14). Stress from the immune

response likely drives the rapidly dividing tachyzoite form to transition to the latent, slow growing bradyzoite form (15). Immunocompromised individuals often suffer disease symptoms due to the reactivation of a latent infection in the form of encephalitis (16). While pharmaceuticals are effective against the tachyzoite form of *T. gondii*, novel therapeutics that combat the chronic stage of infection before reactivation are sorely needed.

The *T. gondii* gene TgPL1 has homology to PLPs, is known to be important for parasite survival in activated macrophages. TgPL1 is localized to punctate vesicles within tachyzoites grown in fibroblasts (17), but changes localization to outside the parasite but within the parasitophorous vacuole (PV) in activated macrophages (18). In this study, we see that TgPL1 localizes to punctate spots in tachyzoites, but in bradyzoites, TgPL1 localizes to the PV and cyst wall. While we had not previously seen a defect of the TgPL1 deletion mutant (ΔTgPL1) during acute and early chronic infection, the localization change caused us to further access the ΔTgPL1 mutant in a toxoplasmic encephalitis (TE) mouse model. Within tissue cysts TgPL1 is involved in regulating the host immune response during chronic infection as ΔTgPL1 infected mice succumb less frequently to encephalitis with fewer inflammatory lesions and higher cytokine levels.

Results

TgPL1 is secreted from the parasite to localize with the PV and cyst wall in bradyzoites

Due to its homology to plant patatin, which changes localization during stress conditions, we were not surprised to see TgPL1 localize to the PV when parasites were grown in macrophages (18). We therefore wanted to examine if TgPL1 changed localization under the stress of bradyzoite inducing conditions. After 5 days in bradyzoite conditions, TgPL1 partially

colocalizes with the cyst wall marker *Dolichos bifluorous* agglutinin (DBA) and the dense granule proteins GRA4 and GRA7 (Fig. 1). Similar to the localization change seen for TgPL1 in activated macrophages (18), the localization of TgPL1 to the PV is not readily apparent until the parasites had been in bradyzoite development conditions for at least 5 days. TgPL1 does not colocalize with BAG1, a bradyzoite specific heat shock protein that is localized in the parasite cytoplasm (Fig. 1). We had previously seen that TgPL1 did not colocalize with any markers of secretory organelles including dense granules (17), so we re-examined localization of TgPL1 with GRA4 in tachyzoites. Intracellular tachyzoites were allowed to invade and divide in confluent fibroblast monolayers for 24 hours before fixation. As we had seen previously, TgPL1 does not colocalize with GRA4 (Fig. 1). These results show that in tachyzoites, TgPL1 is intracellular, but does not co-localize with the dense granules. In bradyzoites, TgPL1 is secreted from the parasite to the PV space.

To examine whether the TgPL1 localization change occurs during chronic infection, we stained bradyzoite cysts purified from mouse brains 22 days after infection for TgPL1. Within in vivo bradyzoite cysts, most TgPL1 is present on the cyst wall, partially colocalizing with DBA (Fig. 2).

TgPL1 begins translation at one of the first two in-frame methionines in tachyzoites and bradyzoites

The mechanism of the localization change of TgPL1 between the tachyzoite and bradyzoite stages is intriguing. The length of time for TgPL1 to change locations, 5 days in either activated macrophages or bradyzoite development conditions, suggests that new protein synthesis may occur. TgPL1 has three potential initiator methionines near the predicted

translation start site (Fig. 3A), the first two AUGs are adjacent and directly followed by a predicted endoplasmic reticulum (ER)-type signal sequence. The third AUG is found directly after the predicted cleavage site for the signal sequence. To examine the start codon usage for TgPL1, site directed mutagenesis was employed to remove the first two initiator methionines (M1-2) or the third (M3) of HA-tagged TgPL1 (Fig. 3A). While clones containing WT and M3 versions of TgPL1 showed robust expression, none of clones containing the M1-2 plasmid expressed TgPL1 (Fig. 3B and S1). Likewise, in bradyzoite conditions, the M1-2 mutant does not produce TgPL1 protein, in contrast to clones containing WT and the M3 mutant (Fig. 3B). TgPL1 expressed from the M3 mutant also appears to be a similar size to WT TgPL1. The WT and M3 proteins also appear to be of equal abundance between tachyzoites and bradyzoites, as confirmed by quantitative PCR (qPCR) analysis (Fig. 3C). PCR analysis of the *TgPL1* mRNA from tachyzoite and bradyzoites showed that the message is not alternatively spliced between the two stages (data not shown). These results indicate that TgPL1 is translated from one of the first two methionines in both tachyzoite and bradyzoites and that the open reading frame does not change between stages.

ΔTgPL1 parasites form bradyzoite cysts in vitro and in vivo

Because TgPL1 expression localizes to the cyst wall, we determined whether the *TgPL1* gene is necessary for cyst formation. In vitro cyst formation was assayed by culturing parasites in low CO_2 and high pH conditions for 2, 3 or 5 days. No differences were seen in the ability of ΔTgPL1 to form cysts at any of the time points when assayed for DBA expression and cyst wall formation (data not shown). In vivo cyst formation was assayed using C57BL/6 mice infected with 10^3 tachyzoites, a nonlethal dose that allows brain cyst formation, of either WT, ΔTgPL1 or

ΔTgPL1 genetically complemented with the *TgPL1* genomic locus (complement). At 4, 6 and 8 weeks post infection, brains were collected and the numbers of cysts per brain enumerated. Cyst numbers from WT-, ΔTgPL1- and complement-infected mice were similar (Fig. 4).

Mice infected with ΔTgPL1 parasites are less susceptible to TE than WT-infected mice

To discover whether the *TgPL1* gene has a role in the development of TE, C57BL/6 mice were infected with 10^3 WT, ΔTgPL1, or complement tachyzoites and allowed to progress into chronic infection. Survival rates for mice infected with all three strains were similar during late acute and early chronic infection prior to 7 weeks post infection. Between 7-11 weeks, all of the WT-infected mice were sacrificed due to encephalitic symptoms including paralysis, tremors, head tilt, and/or severe balance and coordination problems (Fig. 5A). In contrast, the majority of ΔTgPL1-infected mice were asymptomatic and survived past 12 weeks post infection. Mice infected with the complement strain were symptomatic and needed to be sacrificed at rates similar to WT-infected mice. The differences in mortality rates were statistically significant between those infected with WT and ΔTgPL1 ($p<0.0001$), ΔTgPL1 and complement ($p=0.0147$), but not significant between WT and complement. When we examined the histology of the WT-infected brains, we saw a large number of inflammatory lesions, another indication of encephalitis. These data indicate that *TgPL1* may contribute to the induction of TE by 12 weeks post infection.

ΔTgPL1-infected mice maintain viable cysts at 12 weeks post infection

One possibility for why the ΔTgPL1-infected mice did not succumb to TE was that the mice had cleared the tissue cysts from the brain. To examine this possibility, cyst burden was

assessed in the surviving mice at 12 weeks post infection. Cyst burdens in the surviving ΔTgPL1-infected mice ranged from 20,000 to 65,000 cysts per brain, which was comparable to cyst burdens in the ΔTgPL1-infected mice at 4, 6 and 8 weeks post infection (Fig. 4). Another explanation for the lack of TE in ΔTgPL1 infected mice was that the parasites within the cysts were no longer viable and therefore unable to cause disease. To assay the viability of the ΔTgPL1 cysts, we performed a mouse bioassay in IFNγ$^{-/-}$ mice, which are highly susceptible to *T. gondii*. All mice succumbed to infection at day 7 post infection, indicating that ΔTgPL1 cysts are infectious at 12 weeks post infection (data not shown).

ΔTgPL1 parasites do not convert from bradyzoite to tachyzoite efficiently

Another possible explanation for the reduced TE in ΔTgPL1-infected mice is that ΔTgPL1 parasites do not readily revert from bradyzoite cysts into tachyzoites. To examine this hypothesis we cultured WT, ΔTgPL1 or complement parasites in bradyzoite induction conditions for 5 days, syringe lysed the cysts and grew them under tachyzoite conditions. Western blot analysis of the tachyzoite-specific surface antigen SAG1 showed that while ΔTgPL1 parasites express SAG1 normally when grown continuously as tachyzoites, SAG1 is not readily induced in ΔTgPL1 bradyzoites grown in tachyzoite conditions, even after 72 hours (Fig. 5B). Conversely, BAG1 was highly induced in ΔTgPL1 bradyzoites and was still abundant when ΔTgPL1 bradyzoites were grown for 72 hours in tachyzoite conditions (Fig. 5B). In fact, BAG1 protein was apparent in ΔTgPL1 tachyzoites when the blot was overexposed, despite the fact that the parasites had been continuously grown as tachyzoites for many passages (data not shown). These

results indicate that certain stage specific genes are misregulated in ΔTgPL1 parasites and that ΔTgPL1 parasites may be defective in bradyzoite to tachyzoite reactivation.

ΔTgPL1-infected mice have fewer inflammatory lesions at 8 weeks post infection

We had seen inflammatory lesions in the brains of WT-infected mice, most likely resulting from reactivation of bradyzoite cysts. As ΔTgPL1 parasites may be defective in bradyzoite reactivation, we quantified the number of inflammatory lesions in WT, ΔTgPL1 or complement-infected mice. Eight weeks after infection, the brains were perfused, fixed, serial sectioned and stained with hematoxylin & eosin. Sections throughout the whole brain were analyzed by counting the number of foci of inflammatory cells per section (example Fig. 5C). Mice infected with WT or ΔTgPL1-complemented parasites had statistically higher numbers of inflammatory lesions per brain section than ΔTgPL1 infected brains (Fig. 5D). No inflammatory lesions were seen in uninfected, age-matched control mice.

ΔTgPL1-infected mice have higher cytokine levels at 8 weeks post infection

To understand why ΔTgPL1-infected mice had fewer inflammatory lesions in their brains, we measured the levels of cytokines associated with *T. gondii* chronic infection (IL-12p70, IFNγ, TNFα, MCP-1, IL-6 and IL-10). There were no significant difference in serum levels of any of these cytokines between WT-and ΔTgPL1-infected mice at 4 or 6 weeks post infection (Fig. S2 and S3). At 8 weeks post infection, the average level of IFNγ, TNFα, MCP-1, and IL-6 was significantly higher in ΔTgPL1-infected compared to WT-infected mice (Fig. 6). These cytokines were also higher in ΔTgPL1-infected compared to complement-infected mice,

but the differences did not reach the significance cut-off. These results indicate that high cytokine levels are maintained in the absence of TgPL1, which prevents the encephalitic state seen in C57BL/6 mice.

Discussion

The development of TE in mice has been well characterized, but the contribution of specific parasite factors involved in this disease has not been determined. In response to stress, TgPL1 protein changes its localization to the host-parasite interface and alters the parasites interactions with the host cell. To our knowledge, this is the first report to identify a specific *T. gondii* gene involved in the development of encephalitis. ΔTgPL1-infected animals are less susceptible to TE, have fewer brain inflammatory lesions and higher serum levels of IFNγ, TNFα, MCP-1, and IL-6 than WT-infected controls. ΔTgPL1 parasites also appear to be defective in bradyzoite to tachyzoite reactivation. These data suggest that in WT parasites, TgPL1 plays a role in reactivation and reducing cytokines levels during chronic infection, which contribute to the development of TE.

Mice with the H-2^b haplotype (which includes C57BL/6) develop inflammatory changes in their brains during chronic infection with *T. gondii,* whereas mice with H-2^a or H-2^d haplotypes do not (22). Examining cytokine levels in WT-and ΔTgPL1-infected C57BL/6 mice leading up to the onset of TE gives insights into which immunological process are likely to be subverted by TgPL1. IFNγ (23), TNFα (24) and IL-6 (25) have been shown to be directly involved with resistance to TE. Likewise, MCP-1 is transcribed to high levels in the brains of chronically infected mice (26) and *MCP-1*$^{-/-}$ mice have more severe neuropathology early in chronic infection compared to wild type mice (27). While the serum levels of IL-12 and IL-10

did not consistently drop in ΔTgPL1-infected animals as they do for WT-infected mice at 8 weeks post-infection, both of these cytokines have also been previously shown to be critical for limiting inflammation during TE (28, 29). The consistency of our findings with previous results suggests that ΔTgPL1 parasites will be a useful model for studies of TE in H-2^b haplotype mice.

We examined multiple possibilities for why ΔTgPL1-infected mice did not succumb to TE. First, we determined whether ΔTgPL1-infected mice clear the tissue cysts over time. Cysts counts performed at 12 weeks post infection showed cyst burdens comparable to 4, 6 and 8 weeks post infection. Another explanation was that ΔTgPL1-cysts were no longer viable, but a mouse bioassay concluded that ΔTgPL1-cysts were infectious. A third possibility is that ΔTgPL1 cysts are defective in reactivation. While reactivation was grossly examined in the bioassay in IFN$\gamma^{-/-}$ mice, these mice are so susceptible to *T. gondii* that a single viable parasite is lethal, therefore subtle defects in reactivation would be missed. Therefore we examined reactivation of tissue culture bradyzoites by western blot for the stage specific proteins SAG1 and BAG1. When stress induced bradyzoites were grown under tachyzoite conditions, SAG1 was readily induced in WT and ΔTgPL1-complemented parasites, but not in ΔTgPL1 parasites. Expression of BAG1 was higher in ΔTgPL1 bradyzoites than WT and ΔTgPL1-complemented bradyzoites and was still apparent after 72 hours of growth under tachyzoite conditions. These studies indicate that suppression and induction of certain genes may be defective during ΔTgPL1 bradyzoite to tachyzoite stage transition. Future genome-wide expression analyses will elucidate the extent of the development and/or reactivation defect present in ΔTgPL1.

TgPL1 has homology to patatin like phospholipases (PLPs) (17), which may suggest a mechanism for this modulation. PLPs typically have lipid hydrolase activity, most notably phospholipase A_2 activity, which results in lysophospholipid and fatty acid production (31).

Myristic and palmitic acids, which are abundant in *T. gondii,* have been found to suppress production of TNFα in macrophage cells (32). However, TgPL1 lacks one of the catalytic residues that is necessary for PLA_2 activity in other homologs (17) and has been shown to not have PLA_2 activity (18). Because the other active site residues are conserved, TgPL1 may be involved in binding phospholipids. Lipid binding activity would allow TgPL1 to sequester molecules that could lead to cytokine production, or perhaps to act as a coenzyme that delivers phospholipids to other PLA_2 enzymes.

Plant patatin changes location from within vesicles to the cytoplasm in response to stress (5), but the timing and mechanism of this localization change has not been elucidated. TgPL1 is mostly within the parasite 1 day after macrophage activation, but after 5 days in macrophage activation conditions, TgPL1 is largely localized to the PV (18). Similarly, after 5 days in bradyzoite development conditions, TgPL1 is mostly found in the PV and co-localizes with DBA (Fig. 1). This delayed response may indicate that new protein synthesis occurs, so we examined if TgPL1 initiates at different methionines in the tachyzoite and bradyzoite stages. These studies indicate that the mechanism of TgPL1 localization change is not due to differences in translation start site as TgPL1 begins from one of the first two-initiator methionines in both tachyzoites and bradyzoites. The lack of TgPL1 expression when these two codons were mutagenized could be due to a non-optimal sequence context for the third ATG. The optimal start codon sequence context for *T. gondii* is GNCAAAATG g (30). The sequence context around the third ATG is TTCTGTATGT, which has only one of the preferred *T. gondii* base pairs in those positions. The second ATG has the best sequence context (GACATGATGA), which has optimal residues at 3 of the designated positions. Alternatively, the M1-2 mutant may be mislocalized and/or misfolded and then degraded by the parasite. Regardless, here we have shown that the open

reading frame of TgPL1 does not change between tachyzoites and bradyzoites. It may be that a subset of *T. gondii* vesicles are delivered to the PV space under stress conditions. We have seen partial co-localization of TgPL1 with some of the plant-like vacuole markers (data not shown), but none of the resident plant-like vacuole proteins we have examined so far change location in response to stress. It is possible that the partial co-localization of plant-like vacuole markers with TgPL1 in tachyzoites is due to shared compartmentalization during early trafficking, but that TgPL1 localizes to an uncharacterized vesicle, distinct from the plant-like vacuole. We plan to characterize TgPL1 trafficking in the future. Understanding the mechanism of the TgPL1 localization change in bradyzoites will undoubtedly uncover interesting cell biology.

This study identifies a role for the *T. gondii* gene *TgPL1* in development of TE. We show that a ΔTgPL1 mutant is able to develop viable cysts in the brains of C57BL/6 mice similar to WT parasites. In contrast to WT-infected mice that succumb to TE by 11 weeks, the ΔTgPL1-infected mice survive past 12 weeks and maintain viable cysts. This phenotype correlates with the loss of IFNγ, TNFα, IL-6, and MCP-1 in WT-infected mice but maintenance of these cytokines in ΔTgPL1-infected animals. Further studies will elucidate the mechanism by which TgPL1 alters cytokine production during chronic infection.

Materials and methods

T. gondii strains and cell culture

The parental wild type *T. gondii* strain was Pru in which the HPT gene was replaced with firefly luciferase under the control of the tubulin promoter (18). The ΔTgPL1 mutant and the genetically complemented strains were generated as previously described (18). Parasites were passaged in

confluent human foreskin fibroblasts (HFFs) in Dulbecco's Modified Eagle's Medium supplemented with 10% FBS, 2 mM L-glutamine, and 1% penicillin-streptomycin.

Plasmid construction

The plasmid with a hemagglutinin tagged version of TgPL1 (pTgPL1-SacHA) was constructed as described (19). A fragment containing the three in frame start codons of *TgPL1* was digested from pEndoTgPL1HA (17) using StuI and SacI and subcloned into pBSII SK+ using SacI and NotI. The first two in frame start codons were mutagenized to isoleucines using site directed mutagenesis with the primers 5'-TCCCTTAAAAACGAACATCATCAAGGGTAACAGCGTGG-3' and its reverse complement. The third in frame start codon was removed using the primers 5'-CTGTTCTCCTTCTGTATCGACACACGCTCCAGT-3' and its reverse complement. These mutagenized fragments were then subcloned into a version of pTgPL1-SacHA that lacked the dihydrofolate reductase (DHFR) gene. DHFR gene from pDHFR-TSC3 (20) was reintroduced by blunt ligation into the EcoRI site. The construct where the first two start codons were mutagenized is called pTgPL1HAM12QC and the construct where the third start codons was mutagenized is called pTgPL1HAM3QC.

Mouse infections

In 4 independent experiments, 10-12 week old C57BL/6 mice were intraperitoneally infected with 10^3 tachyzoites for each parasite strain tested. Plaque assays were performed in HFFs immediately after inoculation to confirm parasite counts and viability. Experiments with more than 2-fold differences in plaques between strains were discarded. Surviving mice were

sacrificed at 4, 6, 8 and 12 weeks post infection to determine cyst burden as previously described (17). *T. gondii* mouse bioassays were performed by withholding food from IFN-$\gamma^{-/-}$ mice overnight then feeding each mouse half of a freshly harvested brain from chronically infected mice. Mice were sacrificed if paralysis, tremors or severe head tilt, balance and coordination problems were apparent.

For TgPL1 localization from in vivo bradyzoites, 10-12 week old C57BL/6 mice were intraperitoneally infected with 2 x 10^3 tachyzoites expressing TgPL1-HA. After 22 days, mice were sacrificed and their brains were removed, ground with a mortar and pestle, and the bradyzoite cysts purified with a Percoll gradient (21). Purified cysts were stained for IFA as described below.

Serum cytokine levels

Serum samples were obtained by tail bleed at 4 and 6 weeks post infection in 2 independent experiments or 8 weeks post infection 3 independent experiments. Levels of IL-12p70, IFNγ, TNFα, MCP-1, IL-6 and IL-10 in serum were measured using BD™ Cytometric Bead Array (CBA) Mouse Inflammation Kit (BD Biosciences, San Jose, CA).

Bradyzoite differentiation

Human foreskin fibroblasts (HFFs) were seeded in 25 cm^2 tissue culture flasks or on glass coverslips in 24 well tissue culture plates and grown in 10% FBS, 2 mM L-glutamine, and 1% penicillin-streptomycin in Dulbecco's Modified Eagle Medium (DMEM). The confluent HFFs were infected with 4x10^6 tachyzoites for the 25 cm^2 tissue culture flasks or 10^5 tachyzoites for the 24-well plates. The parasites were allowed to invade for 3 hours. After invasion, the medium was

replaced with bradyzoite development medium (0.5% FBS, 0.5% penicillin-streptomycin, and 21mM HEPES in RPMI 1640 without bicarbonate pH 8.0). Parasites were grown in bradyzoite development medium for 5 days and harvested as indicated. For reactivation studies, bradyzoites were syringe passed through first a 27-gauge and then a 30-gauge needle before passage onto HFF cells and growth under tachyzoite conditions for 24, 48 or 72 hours.

TgPL1 mRNA analysis

RNA was extracted from tachyzoites and bradyzoites using TRIzol and treated with Invitrogen Amplification grade DNase I prior to cDNA synthesis using random hexamers and SuperScript™ III (Invitrogen, Carlsbad, CA). The predicted intron splice junction in bradyzoites was confirmed by PCR of cDNA with primers 5′-GCTCTGCCACATTCTCGTTC-3′ and 5′-TTGCCTCTTCGTCCATAGGC-3′. For qPCR, primer efficiencies (*E*) for alpha-tubulin 1A, BAG1, and TgPL1 were calculated using the slopes of a 1:10 dilution series (neat through 10^4) and the formula $E = 10^{[-1/\text{slope}]}$. Efficiencies were 1.93, 1.98, and 2.04 respectively. The reactions used Bio-Rad iTaq Universal SYBR Green Supermix and 300nm primers, and were analyzed on an Applied Biosystems StepOnePlus Real-Time PCR system with an extension temperature of 60 °C for 60 seconds. Relative expression was calculated using the $2^{(-\Delta\Delta Ct)}$ method. Three biological replicates were used. Each biological replicate was conducted in duplicate on each plate and ran twice.

Primer sequences were as follows: Tub1A F 5'-GACGACGCCTTCAACACCTTCTTT-3', Tub1A Rev 5'-AGTTGTTCGCAGCATCCTCTTTCC-3', BAG1 F 5'-GATGACGTAACCATAGAAGTCGACAAC-3', BAG1 Rev-5'-GCAAAATAACCGGACACTCGCTCAGTC-3', TgPL1 F 5'-

CCGTGAACTGAAGTGGGACG -3', and TgPL1 Rev 5'-AAAACCTCCACAGGCTCTCGC-3'.

Western analysis

Protein samples were harvested from parasites grown in a single 25 cm^2 tissue culture flasks for tachyzoites and three 25 cm^2 tissue culture flasks grown in the bradyzoite condition as above. Lysates were separated on 10% polyacrylamide gels, transferred to polyvinylidene fluoride (PVDF) membrane and incubated with mouse anti-HA, or rabbit anti-SAG1, anti-BAG1 or anti-β-tubulin antibodies to detect the indicated protein. Horseradish peroxidase conjugated donkey anti-mouse and donkey anti-rabbit secondary antibodies were used (Jackson labs, Bar Harbor, ME). Membranes were incubated with ECL Plus detection reagent (GE Healthcare) and visualized by exposure to film.

Immunofluorescence Assay

T. gondii expressing an HA tagged TgPL1 was used for all experiments. Tachyzoites were grown in HFFs on glass coverslips for 24 hours and bradyzoites were grown under bradyzoite development conditions for 5 days before they were washed with PBS and fixed in 3% formaldehyde. Blocking, permeablization, and staining were performed as previously described (19). Mouse anti-HA monoclonal 16B12 (MMS-101P-200, Covance, Princeton, NJ) was used to detect TgPL1, and co-stained with rabbit anti-GRA4, rabbit anti-GRA-7, rabbit anti-BAG-1 or biotinylated *Dolichos bifluorous* agglutinin. AlexaFluor 488-conjugated donkey anti-mouse was used to visualize the HA, while AlexaFluor 633-conjugated goat anti-rabbit, or streptavidin were used to visualize the co-stains (Invitrogen, Carlsbad, CA). No fluorescence signal was seen with

any of the secondary antibodies alone (data not shown). Coverslips were mounted onto slides by using VectaShield mounting medium containing 4,6-diamidino-2-phenylindole (DAPI) (Vector Labs, Burlingame, CA). Serial image stacks (0.2 micron Z-increment) were taken at 100x magnification (PlanApo oil immersion 1.4 na) using a motorized Zeiss Axioplan III equipped with a rear-mounted excitation filter wheel, a triple pass (DAPI/FITC/Texas Red) emission cube, differential interference contrast optics, and a Hamamatsu ORCA-AG CCD camera operated by OpenLabs 4.0 software (Improvision, Lexington, MA). Fluorescence images were deconvolved by a constrained iterative algorithm, pseudocoloured, and merged using the Volocity software package (Perkin Elmer, Downers Grove, IL).

Determination of Brain Inflammatory Foci

In 2 independent experiments, three C57BL/6 mice were infected with 10^3 parasites of each strain (6 total mice per strain) and allowed to establish a chronic infection for 8 weeks. Brains were perfused with saline, followed by 4% paraformaldehyde before removal and fixation overnight in 4% paraformaldehyde. Coronal samples of 5 micron thickness were taken every 100 microns, providing 36 brain sections per animal. Sections were stained with hematoxylin and eosin, examined by light microscopy on the 4x objective and aggregates of 10 or more inflammatory cells were enumerated.

References

1. **Park WD, Blackwood C, Mignery GA, Hermodson MA, Lister RM**. 1983. Analysis of the Heterogeneity of the 40,000 Molecular Weight Tuber Glycoprotein of Potatoes by Immunological Methods and by NH(2)-Terminal Sequence Analysis. *Plant Physiol*. 71: 156-60.

2. **Sonnewald U, Studer D, Rocha-Sosa M**. 1989. Immunocytochemical localization of patatin, the major glycoprotein in potato (Solanum tuberosum L.) tubers. *Planta*. 178: 176-183.

3. **Senda K, Yoshioka H, Doke N, Kawakita K**. 1996. A cytosolic phospholipase A2 from potato tissues appears to be patatin. *Plant Cell Physiol*. 37: 347-53.

4. **Kawakita K, Senda K, Doke N**. 1993. Factors, affecting in vitro activation of potato phospholipase A2. *Plant Sci*. 92: 183-190.

5. **Laxalt AM, Munnik T**. 2002. Phospholipid signalling in plant defence. *Curr Opin Plant Biol*. 5: 332-8.

6. **La Camera S, Geoffroy P, Samaha H, Ndiaye A, Rahim G, Legrand M, Heitz T**. 2005. A pathogen-inducible patatin-like lipid acyl hydrolase facilitates fungal and bacterial host colonization in Arabidopsis. *Plant J*. 44: 810-25.

7. **Sonnewald U, von Schaewen A, Willmitzer L**. 1990. Expression of mutant patatin protein in transgenic tobacco plants: role of glycans and intracellular location. *Plant Cell*. 2: 345-55.

8. **Sitkiewicz I, Stockbauer KE, Musser JM**. 2007. Secreted bacterial phospholipase A2 enzymes: better living through phospholipolysis. *Trends Microbiol*. 15: 63-9.

9. **Banerji S, Flieger A**. 2004. Patatin-like proteins: a new family of lipolytic enzymes present in bacteria? *Microbiology*. 150: 522-525.

10. **Jacobs L, Remington JS, Melton ML**. 1960. The resistance of the encysted form of Toxoplasma gondii. *J Parasitol*. 46: 11-21.

11. **Denkers EY, Kim L, Butcher BA**. 2003. In the belly of the beast: subversion of macrophage proinflammatory signalling cascades during Toxoplasma gondii infection. *Cell Microbiol*. 5: 75-83.

12. **Lang C, Groß U, Lüder CGK**. 2007. Subversion of innate and adaptive immune responses by Toxoplasma gondii. *Parasitol Res*. 100: 191-203.

13. **Courret N, Darche S, Sonigo P, Milon G, Buzoni-Gâtel D, Tardieux I**. 2006. CD11c- and CD11b-expressing mouse leukocytes transport single Toxoplasma gondii tachyzoites to the brain. *Blood*. 107: 309-16.

14. **Lambert H, Vutova PP, Adams WC, Lore K, Barragan A**. 2009. The Toxoplasma gondii-shuttling function of dendritic cells Is linked to the parasite genotype. *Infect. Immun.*. 77: 1679-1688.

15. **Black M, Boothroyd J**. 2000. Lytic cycle of Toxoplasma gondii. *Microbiology and Mol. Bio. Rev*. 64: 607-623.

16. **Weiss LM, Dubey JP**. 2009. Toxoplasmosis: A history of clinical observations. *Int. J. Parasitol*. 39: 895-901.

17. **Mordue DG, Scott-Weathers CF, Tobin CM, Knoll LJ**. 2007. A patatin-like protein protects Toxoplasma gondii from degradation in activated macrophages. *Mol. Micro*. 63: 482-496.

18. **Tobin CM, Knoll LJ**. 2012. A patatin-like protein protects Toxoplasma gondii from degradation in a nitric oxide-dependent manner. *Infect Immun*. 80: 55-61.

19. **Tobin C, Pollard A, Knoll L**. 2010. Toxoplasma gondii cyst wall formation in activated bone marrow-derived macrophages and bradyzoite conditions. *JoVE*. 42:

20. **Donald RG, Roos DS**. 1993. Stable molecular transformation of Toxoplasma gondii: a selectable dihydrofolate reductase-thymidylate synthase marker based on drug-resistance mutations in malaria. *Proc Natl Acad Sci USA*. 90: 11703-7.

21. **Blewett DA, Miller JK, Harding J**. 1983. Simple technique for the direct isolation of toxoplasma tissue cysts from fetal ovine brain. *Vet Rec*. 112: 98-100.

22. **Suzuki Y, Joh K, Orellana MA, Conley FK, Remington JS**. 1991. A gene(s) within the H-2D region determines the development of toxoplasmic encephalitis in mice. *Immunology*. 74: 732-9.

23. **Suzuki Y, Orellana MA, Schreiber RD, Remington JS**. 1988. Interferon-gamma: the major mediator of resistance against Toxoplasma gondii. *Science*. 240: 516-8.

24. **Gazzinelli RT, Eltoum I, Wynn TA, Sher A**. 1993. Acute cerebral toxoplasmosis is induced by in vivo neutralization of TNF-alpha and correlates with the down-regulated expression of inducible nitric oxide synthase and other markers of macrophage activation. *J Immunol*. 151: 3672-81.

25. **Suzuki Y, Rani S, Liesenfeld O, Kojima T, Lim S, Nguyen TA, Dalrymple SA, Murray R, Remington JS**. 1997. Impaired resistance to the development of toxoplasmic encephalitis in interleukin-6-deficient mice. *Infect. Immun*. 65: 2339-45.

26. **Wen X, Kudo T, Payne L, Wang X, Rodgers L, Suzuki Y**. 2010. Predominant interferon-gamma-mediated expression of CXCL9, CXCL10, and CCL5 proteins in the brain during chronic infection with Toxoplasma gondii in BALB/c mice resistant to development of toxoplasmic encephalitis. *J Interferon Cytokine Res*. 30: 653-60.

27. **Robben PM, LaRegina M, Kuziel WA, Sibley LD**. 2005. Recruitment of Gr-1+ monocytes is essential for control of acute toxoplasmosis. *J Exp Med*. 201: 1761-9.

28. **Yap G, Pesin M, Sher A**. 2000. Cutting edge: IL-12 is required for the maintenance of IFN-gamma production in T cells mediating chronic resistance to the intracellular pathogen, Toxoplasma gondii. *J Immunol*. 165: 628-31.

29. **Wilson EH, Hunter CA**. 2004. The role of astrocytes in the immunopathogenesis of toxoplasmic encephalitis. *Int. J. Parasitol*. 34: 543-8.

30. **Seeber F**. 1997. Consensus sequence of translational initiation sites from Toxoplasma gondii genes. *Parasitol Res*. 83: 309-311.

31. **Dessen A, Tang J, Schmidt H, Stahl M, Clark JD, Seehra J, Somers WS**. 1999. Crystal structure of human cytosolic phospholipase A2 reveals a novel topology and catalytic mechanism. *Cell*. 97: 349-60.

32. **Debierre-Grockiego F, Rabi K, Schmidt J, Geyer H, Geyer R, Schwarz RT**. 2007. Fatty acids isolated from Toxoplasma gondii reduce glycosylphosphatidylinositol-induced tumor necrosis factor alpha production through inhibition of the NF-kappaB signaling pathway. *Infect. Immun*. 75: 2886-93.

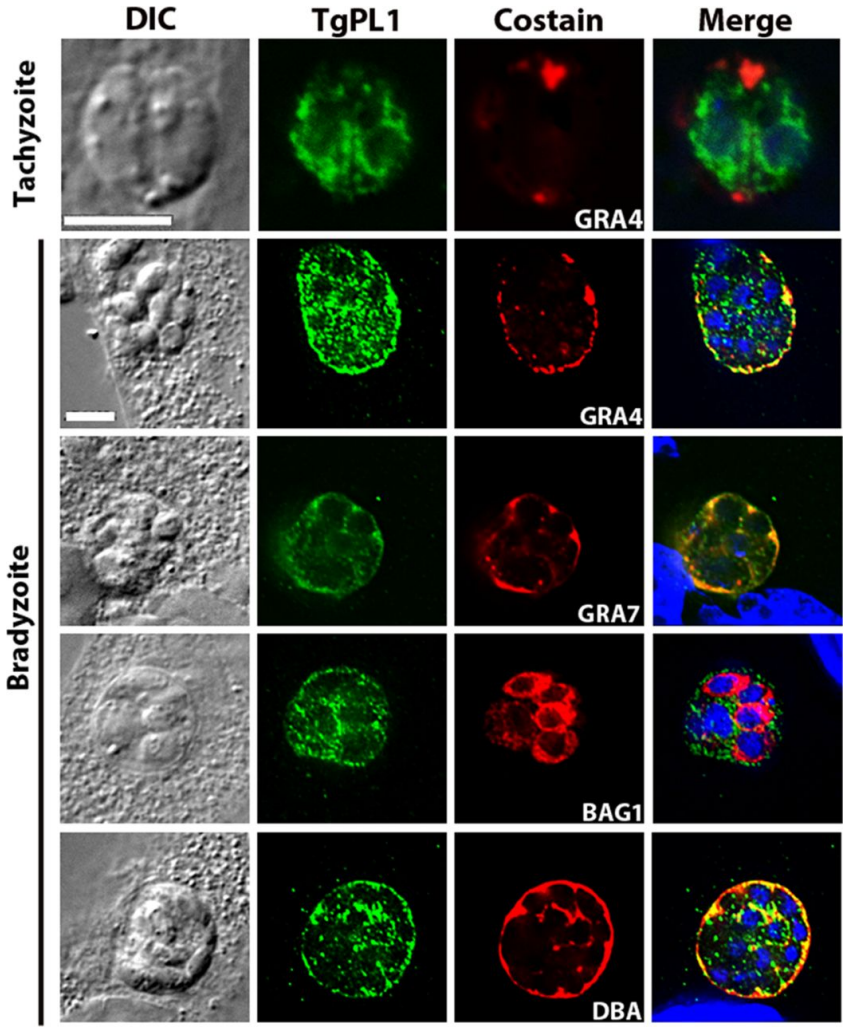

Figure 1.TgPL1 localizes within the parasite in tachyzoites but on the cyst wall and PV space in bradyzoites.

Tachyzoites were grown on coverslips containing confluent HFFs for 24 hours before fixation. Bradyzoites were grown in confluent HFFs on coverslips under low CO_2 and high pH for 5 days. Parasites were stained for HA-tagged TgPL1 (green) and co-stained for dense granule proteins GRA4 and GRA7, a cytoplasmic bradyzoite-specific heat shock protein BAG1, or *Dolichos biflorus* agglutinin (DBA) as a marker of the bradyzoite cyst wall DBA (all co-stains in red). Nuclei were stained with 4,6-diamidino-2-phenylindole (DAPI, blue in merge). DIC, differential interference contrast. Scale bar = 5 mm. The scale is identical for all bradyzoite images.

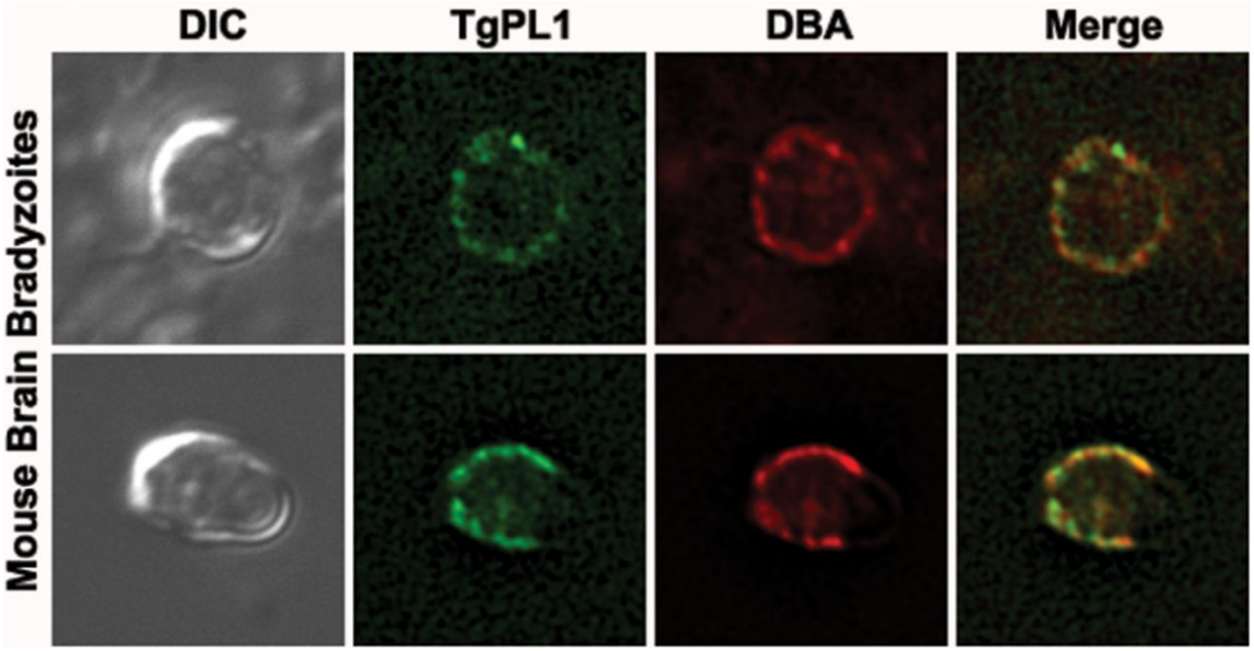

Figure 2. TgPL1 localizes to the cyst wall and PV space in bradyzoite cysts from mouse brains.

C57BL/6 mice were infected with HA-tagged TgPL1 containing parasites for 22 days. Bradyzoite cysts from the brains were partially purified by percoll gradient. Cysts were incubated with mouse anti-HA antibody and AlexaFluor 488 conjugated donkey anti-mouse to detect TgPL1 (green) and biotinylated DBA and AlexaFluor 633 conjugated streptavidin to visualize the cyst (red). DIC, differential interference contrast.

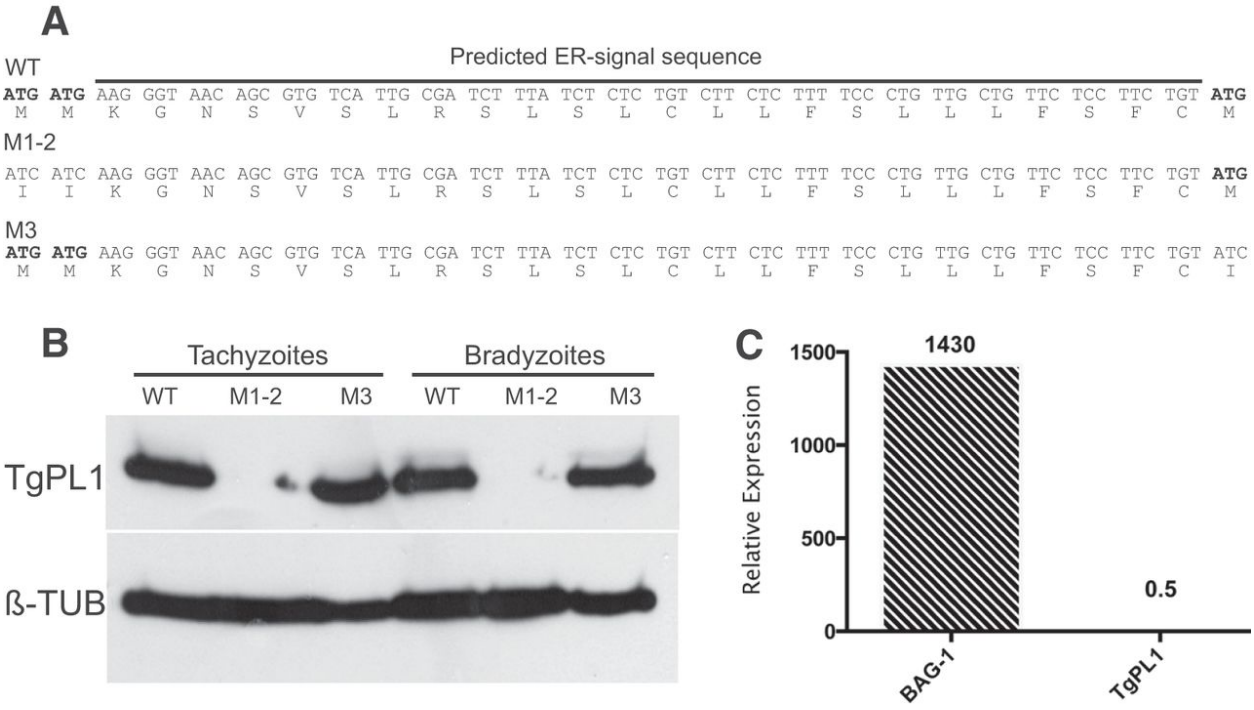

Figure 3. TgPL1 translates from the one of the first two ATG codons.

(A) The genomic region encompassing the potential start codons. Start codons are in bold and a predicted ER signal peptide is labeled with a black bar. The top line is the wild type sequence (WT) with all three potential methionines. The middle line is the M1-2 construct, which lacks the first two start codons. The bottom line is the M3 construct, which lacks the third start codon. (B) Clones of WT, M1-2, and M3 were grown in tachyzoite conditions or bradyzoite conditions for 3 days. Parasites were assessed for protein expression by western analysis with anti-HA (TgPL1) or anti-ß-tubulin (ß-TUB). No TgPL1 protein was present when the first two methionines were mutated (M1-2), even on long exposures (data not shown). (C) Relative Expression of BAG1 and TgPL1 normalized against Tubulin 1A using the $2^{(-_{\Delta\Delta}Ct)}$ method between tachyzoites and bradyzoites. BAG1 was used to determine the switch efficiency. A relative expression value of greater than 1 indicates higher expression in bradyzoites than tachyzoites. Three biological replicates and two technical replicates were performed.

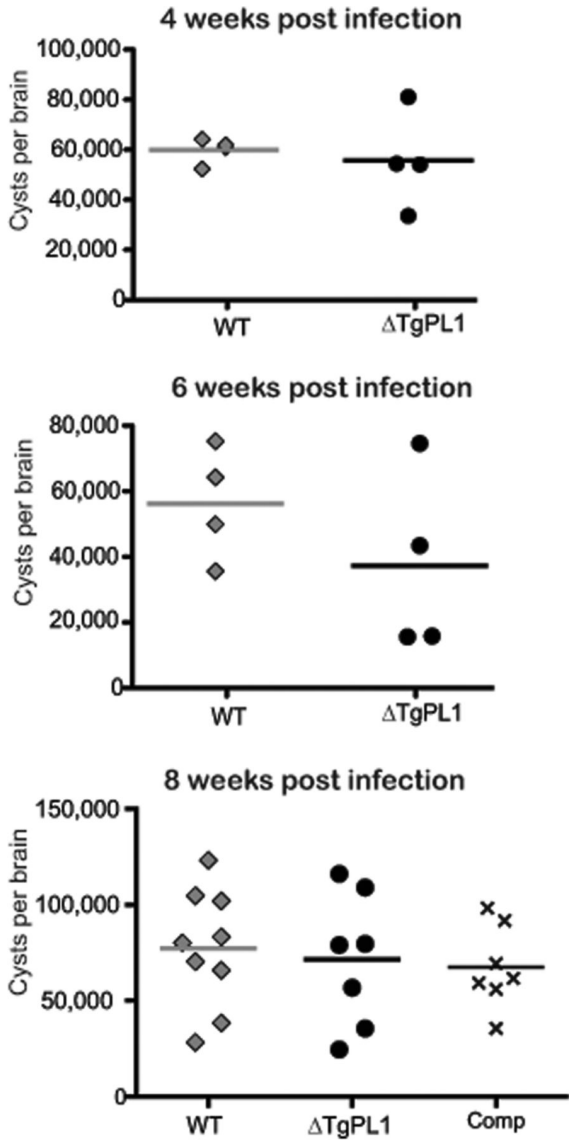

Figure 4. ΔTgPL1 does not have a reduced cyst numbers in vivo.

C57BL/6 mice were infected with 1,000 tachyzoites of wild type (WT, medium grey diamonds), ΔTgPL1 (black circles) or complemented ΔTgPL1 (comp, black X). Mice were sacrificed at 4, 6, 8 or 12 weeks post infection and cyst burdens were assessed by fluorescence microscopy. Each symbol represents cyst counts from an individual mouse and horizontal bars indicate the mean of each group. No significant differences in cyst numbers were seen between WT, ΔTgPL1 or complement infected mice.

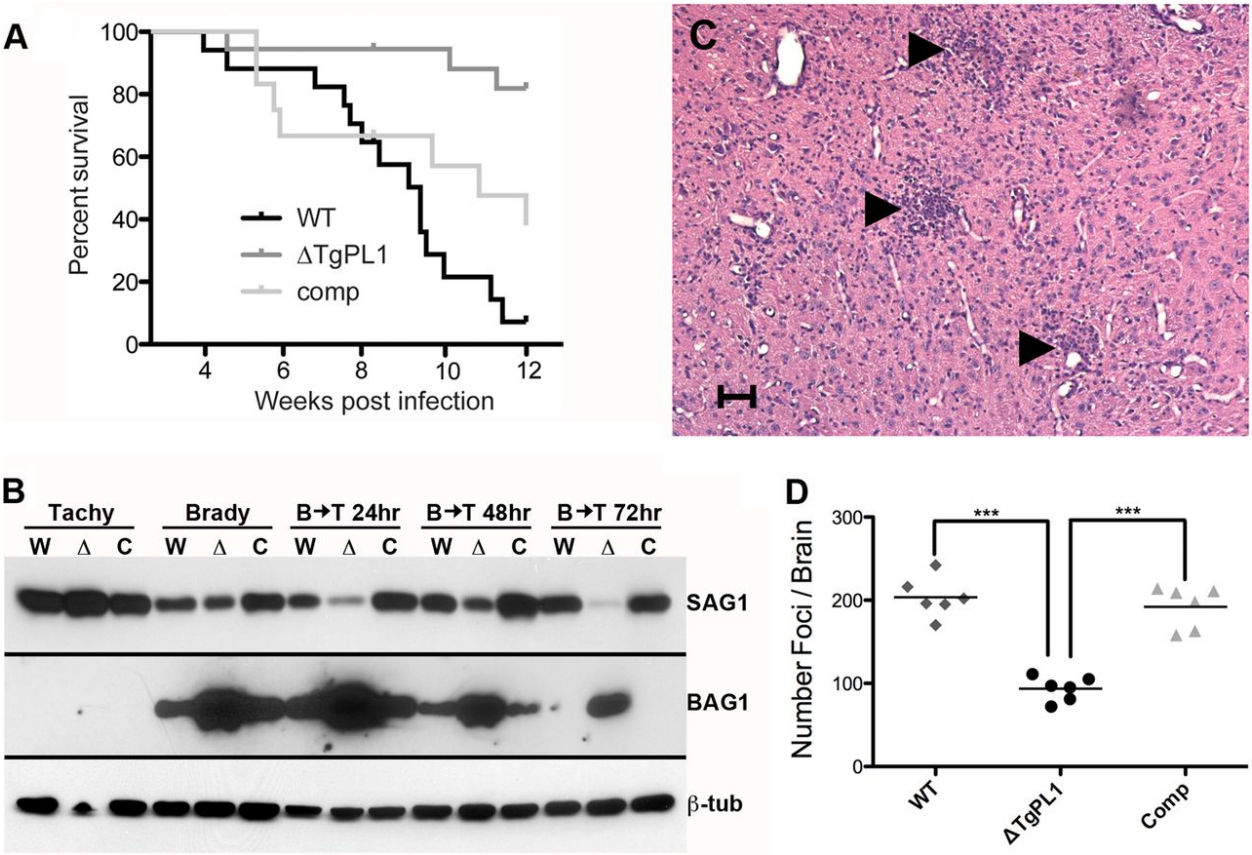

Figure 5. ΔTgPL1-infected mice have delayed TE and reduced brain inflammatory foci.

(A) C57BL/6 mice were infected with 1,000 tachyzoites and monitored for survival. This graph is a compilation of 4 independent experiments, with 17 total mice infected with wild type (WT, medium grey), 18 mice infected with ΔTgPL1 (black), and 12 mice infected with complemented ΔTgPL1 parasites (comp, light gray). For statistical analysis, Log-rank (Mantel-Cox) values for WT vs. ΔTgPL1 were $p<0.0001$, for ΔTgPL1 vs. comp were $p=0.0147$ and differences were not significant for WT vs. comp. (B) WT (W), ΔTgPL1 (Δ) or complemented ΔTgPL1 (C) parasites were grown as tachyzoites (Tachy) or bradyzoites for 5 days (Brady). Bradyzoites were syringed lysed and grown under tachyzoite conditions for 24 (BèT 24 hr), 48 (BèT 48 hr), or 72 (BèT 72 hr) hours. Parasites were assessed for protein expression by western analysis with anti-SAG1 (SAG1), anti-BAG1 (BAG1) or anti-ß-tubulin (ß-tub) as a loading control. Shown is a

representative immunoblot from three independent experiments. (C) Example section of a wild type infected brain at 8 weeks post infection. Sections were stained with hematoxylin and eosin, then scanned using light microscopy to identify aggregates of 10 or more inflammatory cells. Black arrows indicate example foci. Scale bar = 50μm. (D) Three C57BL/6 mice from two independent experiments (6 total mice per strain) were infected with either wild type (WT, medium grey diamonds), TgPL1 (black circles) or complemented parasites (comp, light gray triangles) and allowed to establish a chronic infection for 8 weeks. After fixation, 5 micron sections were taken every 100 microns, providing 36 total sections per animal. Each symbol represents the total number of inflammatory loci counted in the 36 sections (Number of Foci / Brain) for each individual mouse. Significance was analyzed by One way ANOVA. *** $p<0.0001$.

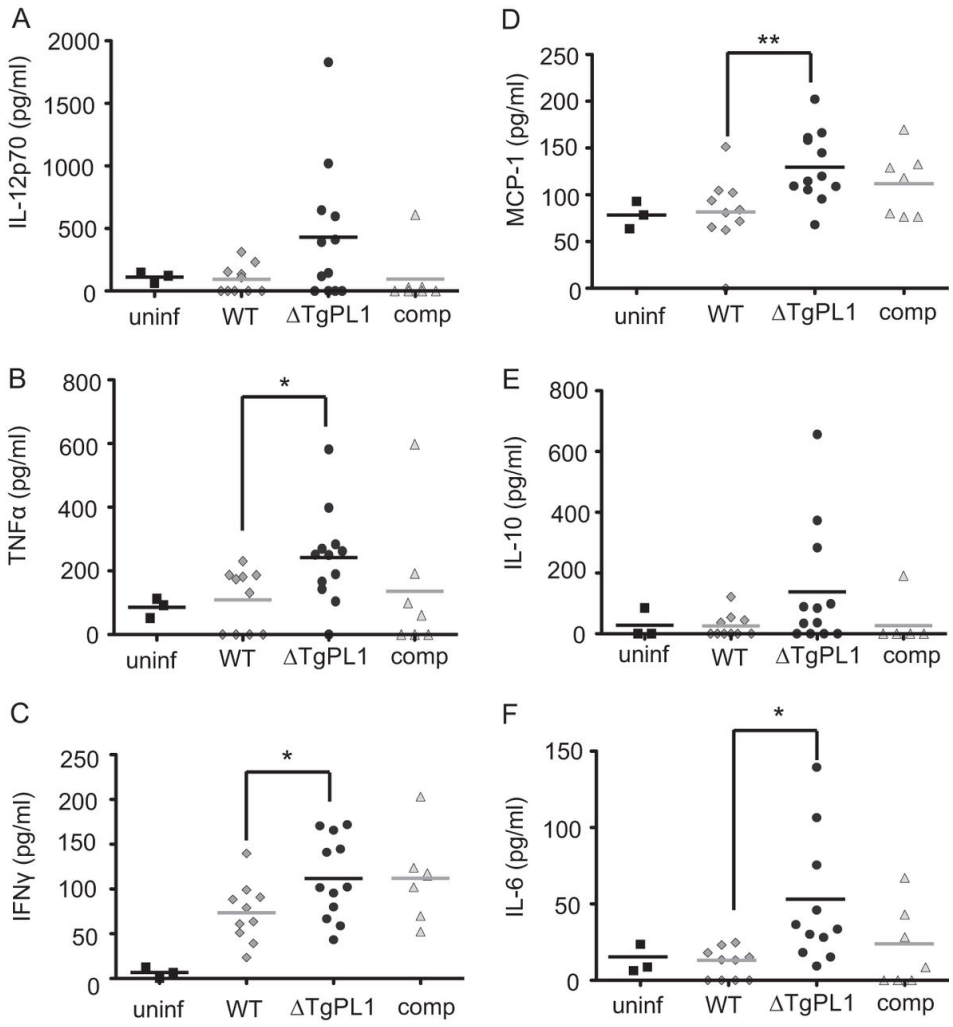

Figure 6. ΔTgPL1 infected mice have higher cytokine levels at 8 weeks post infection.

This graph is a compilation of 3 independent experiments, with 3 uninfected age-matched control mice (uninf, black squares), 10 total mice infected with wild type (WT, medium grey diamonds), 12 mice infected with ΔTgPL1 (black circles), and 7 mice infected with complemented ΔTgPL1 parasites (comp, light gray triangles). Serum was collected at 8 weeks post infection and serum cytokine levels were assessed by cytometric bead array for the interleukin-12 heterodimer (IL-12p70, panel A), TNFα (panel B), IFN-γ (panel C), MCP-1 (panel D), IL-10 (panel E) and IL-6 (panel F). Each symbol represents cytokine levels from an individual mouse. * indicates a p-value <0.05 and ** indicates a p-value <0.01.

Appendix B

The role of CCCH zinc fingers in T. gondii differentiation

Kelly J. Pittman[1], Emily R. Wilson, and Laura J. Knoll

Department of Medical Microbiology and Immunology

University of Wisconsin-Madison, Madison, WI

Summary

Analysis of the *T. gondii* transcriptome revealed a group of RNA binding CCCH zinc-fingers that are more abundant during chronic infection compared to acute infection time points. Out of 37 known CCCH zinc-fingers in the *T. gondii* genome, 5 of them were shown to be 5-fold or greater in abundance between acute and chronic infection. In *Trypanosoma brucei* CCCH zinc finger proteins are involved in life cycle regulation. The goal of this project is to determine whether these CCCH zinc fingers that are more abundant during chronic *T. gondii* infection are essential for differentiation from the rapidly replicating tachyzoite, prominent in acute infection, to the encysted bradyzoite during chronic infection. To address this, deletion mutants of the six CCCH zinc-fingers were attempted for the purpose of testing the ability of the parasite to differentiate in both tissue culture and mice. Generation of a strain of *T. gondii* that lacks the ability to persist long term in a host would be a crucial step in vaccine development and subsequent decrease of life long *T. gondii* infections in humans.

Introduction

T. gondii is a obligate intracellular eukaryotic parasite that has the ability to infect any nucleated cell in warm blooded animals. The success of the parasite is largely due to the ability to establish a long-term infection that remains transmissible if infected host tissue is consumed. Differentiation from the fast growing acute form, the tachyzoite, to the slow growing encysted bradyzoite is critical to the establishment of a long-term chronic infection. . Formation of cysts containing bradyzoites occurs within cells of the central nervous system and striated muscle (1). Bradyzoite cysts can persist for the lifetime of the host and are infectious if consumed. *T. gondii* infection is typically asymptomatic, but does present issues in the immune compromised and

unborn fetuses when acquired congenitally. The most common routes of exposure to *T. gondii* are ingestion of undercooked meat containing bradyzoite cysts and consumption of uncooked food contaminated with environmentally stable oocysts (2). During differentiation the parasite is adapting to pressure from the host immune system and is undergoing major morphological and metabolic changes to adapt to a new environment. Studies have identified in vitro elements responsible these changes, but few components necessary for long term in vivo survival have been conducted. *T. gondii* resides in the brain and central nervous system primarily during chronic infection, therefore we sought out to characterize both host and pathogen responses at the onset of infection in the brain, and at the peak of chronic infection.

CCCH zinc fingers are a class of single-stranded RNA binding proteins (3). Members of CCCH class of zinc fingers are involved in RNA destabilization resulting in RNA degradation (4, 5). Post-transcriptional regulation of mRNA is extremely important for parasite survival from host-to-host and tissue-to-tissue. This has been studied in the context of mRNA splicing, reviewed in (6). Little is known about destabilization and degradation of mRNA and its role during differentiation in the host. The hypothesis would be that turn over of stage specific mRNAs would be essential for successful differentiation of the parasite. The ultimate goal of this project is to elucidate essential genes necessary for long-term infection of the parasite due to development of encysted bradyzoites. Producing an attenuated strain of *T. gondii* that is defective in its ability to persist in the host could result in a safe vaccine for both humans and livestock. CCCH zinc fingers are good candidates for development of a non-persistent *T. gondii* strain because they have been implicated in differentiation of *Trypanosoma brucei*, another eukaryotic parasite that is the causative agent of sleeping sickness (7).

From this analysis, multiple *T. gondii* CCCH zinc finger proteins were identified as highly abundant during chronic infection when compared to acute time points. To address whether these CCCH zinc fingers were critical for establishment and maintenance of a chronic *T. gondii* infection, knockout plasmids targeting the most abundantly expressed CCCH zinc fingers were produced and generation of knockout parasites were attempted.

Results

Generation of knockout plasmids. Knockout constructs for TgME49_062970, TgME49_111100, TgME49_224630, and TgME49_269310 as well as a complementation construct for TgME49_062970 were generated as described in the materials and methods. TgME49_224630 and TgME49_269310 were designed for concurrent electroporations with the CRISPR/CAS plasmids. The 20-nucleotide guide RNA region in the CRISPR/CAS plasmids were individually modified to target the translation start site of TgME49_224630 and TgME49_269310. Electroporations for knockout of TgME49_224630 and TgME49_269310 were done as described, except the CRISPR/CAS plasmids and corresponding knockout plasmids were mixed at a 5:1 ratio in Cytomix prior to electroporation. All plasmids were cloned successfully with the exception of TgME49_269310. The 5' upstream flank could never be properly ligated into the pBC-CAT/HPT backbone that contained the 1038 bp downstream of TgME49_269310. A summary of the plasmids produced for this project can be found in Table 2.

TgME49_062970

TgME49_062970 has a conserved CCCH zinc finger domain towards the C-terminus of the amino acid sequence. In the RNAseq data set it had a 34-fold increase during chronic infection

time points (Table 1). The goal of this project was to elucidate the potential role of TgME49_062970 during establishment and maintenance of a chronic infection in the host. A knockout (Figure 2), a complementation (Figure 3), and a CRISPR/CAS plasmid (Figure 7) targeted to the translation start site were constructed for these studies. As summarized in Table 2, knockout of TgME49_062970 was attempted four times: Twice with the knockout vector in a TgME49 background, once with the knockout vector in a KU80 background, and once with the knockout vector in combination with a CRISPR/CAS plasmid targeted to the translation start site of the gene.

With each attempt, 2 electroporations were performed with the desired plasmid along with a third electroporation that contained no DNA. Drug selection with the corresponding positive selectable marker began 24 hours post electroporation. After each attempt in the TgME49 background, the parasites in the no DNA control died after 3-4 passages, approximately 10 days, after selection with 20μM of chloramphenicol. At this point, negative selection was performed with 34mg/mL of 6-Thioxanthine for 3-4 passages. Serial dilutions were performed to isolate single colonies for screening. Screening was done using southern blot analysis with a P^{32} labeled probe targeting the 3' UTR of TgME49_062970. A representative film was chosen to depict the present of a random insertion of the knockout plasmid as well as presence of the wild-type TgME49_062970 gene (red arrow, Figure 1A).

TgME49_111100

TgME49_111100 has a conserved CCCH zinc finger domain at the N-terminus of the amino acid sequence. In the RNAseq data set it had a 6-fold increase during chronic infection time points (Table 1). The goal of this project was to elucidate the potential role of TgME49_111100 during

establishment and maintenance of a chronic infection in the host. A knockout (Figure 4) plasmid was constructed as described in the materials and methods. As summarized in Table 2, knockout of TgME49_111100 was attempted three times: Twice with the knockout vector in a TgME49 background and once with the knockout vector in a KU80 background. With each attempt, 2 electroporations were performed with the desired plasmid along with a third electroporation that contained no DNA. Drug selection with the corresponding positive selectable marker began 24 hours post electroporation. After each attempt in the TgME49 background, the parasites in the no DNA control died after 3-4 passages, approximately 10 days, after selection with 20μM of chloramphenicol. At this point, negative selection was performed with 34mg/mL of 6-Thioxanthine for 3-4 passages. Serial dilutions were performed to isolate single colonies for screening. Screening was done using southern blot analysis with a P^{32} labeled probe targeting the 3' UTR of TgME49_111100. A representative film was chosen to depict the present of a random insertion of the knockout plasmid as well as presence of the wild-type TgME49_111100 gene (red arrow, Figure 1B).

TgME49_224630

TgME49_224630 has a conserved zinc finger domain at the N-terminus of the amino acid sequence. In the RNAseq data set it had a 169-fold increase during chronic infection time points (Table 1). The goal of this project was to elucidate the potential role of TgME49_224630 during establishment and maintenance of a chronic infection in the host. A knockout (Figure 5) plasmid was constructed as described in the materials and methods. This plasmid has a CAT as a positive selectable marker and UPT as a negative selectable marker. Insertion of CAT into the *T. gondii* genome gives rise to chloramphenicol resistance. UPT knockout parasites, which have resistance

to FUDR, were used as the parental strain so that negative selection could be used. A corresponding CRISPR/CAS plasmid (Figure 7) was also designed to target the translation start site of TgME49_224630 to use in combination with the knockout plasmid. As summarized in Table 2, knockout of TgME49_224630 was attempted once in the TGME49ΔHPT ΔUPT background using the CRISPR/CAS plasmid and knockout plasmid at a 5:1 ratio. Screening is still in progress.

TgME49_269310

TgME49_269310 has no annotated conserved CCCH zinc finger domain, but the N-terminus of the amino acid sequence aligns to CCCH zinc finger proteins in other organisms. In the RNAseq data set it had a 142-fold increase during chronic infection time points (ToxoDB.org). The goal of this project was to elucidate the potential role of TgME49_269310 during establishment and maintenance of a chronic infection in the host. A knockout (Figure 6) plasmid was constructed as described in the materials and methods. This plasmid has CAT as a positive selectable marker and UPT as a negative selectable marker. Insertion of CAT into the *T. gondii* genome gives rise to chloramphenicol resistance. UPT knockout parasites, which have resistance to FUDR, were used as the parental strain so that negative selection could be used. A corresponding CRISPR/CAS plasmid (Figure 7) was also designed to target the translation start site of TgME49_269310 for use in combination with the knockout plasmid. As summarized in Table 2, a knockout of this gene was never attempted because the 5' flank was never successfully cloned into the knockout plasmid.

Discussion

Successful generation of a *T. gondii* CCCH zinc finger knockout was not achieved. One reason could be that these CCCH zinc fingers, although showing low levels of expression during acute infection, could be essential during growth and maintenance of the tachyzoite stage of the parasite. Tachyzoites are used to generate gene knockouts and therefore genes that are essential to the tachyzoite are difficult to eliminate. Also, bradyzoite specific genes may be less accessible, i.e. bound in histones, during the tachyzoite stage. One way to address this would be to apply stress conditions, such as high pH media and low CO_2 conditions, to the parasites overnight prior to electroporation. This would potentially initiate expression of bradyzoite specific genes, but not long enough to cause full differentiation to the bradyzoite form. This short exposure to stress would be critical to success as these CCCH zinc fingers are potentially critical during the bradyzoite stage.

Materials and Methods

qPCR of *T. gondii* CCCH zing fingers. Sequences for TGME49_224630, TGME49_069270, and TGME49_111100 were obtained from ToxoDB.org. Sequences were run through BLASTp to confirm presence of CCCH zinc finger motifs. cDNA was generated from the same RNA samples used for RNA sequencing with Invitrogen Superscript III Reverse Transcriptase cDNA synthesis kit. All CCCH zinc fingers were normalized to the *T. gondii* house keeping gene tub1A. Efficiencies were determined using in vitro bradyzoite cDNA. RNA was extracted from 5 day bradyzoites grown under low CO_2 and high pH conditions using TRIzol. cDNA was generated using the Invitrogen Superscript III Reverse Transcriptase cDNA synthesis kit. Efficiencies were calculated using the slopes of a 1:10 dilution series (neat through 10^4) and the formula $E = 10^{[-1/\text{slope}]}$. Efficiencies for tub1A, TGME49_224630, TGME49_069270, and

TGME49_111100 were 1.96, 1.89, 2.14, and 2.04 (Between 90-107% efficient). Quantitative PCR was performed using Bio-Rad iTaq Universal SYBR Green Supermix on an Applied Biosystems StepOnePlus Real-Time PCR system. Primers were used at a 300nm concentration and an extension temperature of 60 °C for 60 seconds. Relative quantification was calculated using Pfaffl's method (8). Three biological replicates were used and conducted in duplicate. Wells with only one melt curve and temperature were used, and duplicate Ct values were all at or below a 0.25 difference in cycle threshold value.

Electroporation of *T. gondii* 50μg-75μg of plasmid was linearized and purified using phenol/chloroform prior to electroporation. Linearized DNA was used for two separate electroporations, 25μg each, along with a third no DNA control. Approximately $1x10^7$ type II strain TgME49ΔHPT-luciferase parasites were suspended in Cytomix prior to electroporations. 24 hours after electroporation of the parasites, fresh media was added with chloramphenicol at a concentration of 20μM, or 1 μM pyrimethamine for the complementation construct. After the no DNA control died from chloramphenicol selection, the negative selectable drug was added for another 4 passages. The selectable

drug used was either 6-thioxanthine, final concentration of 34 mg/mL, or FUDR, final concentration 10μM, depending on the presence of HPT or UPT in the knockout plasmid. Parasites were then isolated into single colonies by diluting them to 60 parasites/mL and adding100μL to each well in a 96 well plate. At 10 days post-infection wells containing single colonies were identified, transferred to 24 and 6 well plates, and grown until large vacuoles were present. DNA was then extracted for either PCR or southern blot analysis to determine presence or absence of the gene of interest.

TgME49_062970 knockout plasmid construction. A TgME49_062970 knockout construct

was generated by PCR amplification, using *T. gondii* genomic DNA, of approximately 3.3 kb upstream of the predicted translation start site and 3.8 kb downstream of the predicted poly-A addition site using Phusion Polymerase (Thermo). Upstream primers were Forward 5' -CTCGAGTGTGAACCCCCACAAGCAAGC-3', which adds a 5' XhoI cut site, and Reverse 5'-AAGCTTCCATACTTCCCCGCAAAGGCA-3', which adds a HindIII 3' cut site to the 3.3kb fragment. Downstream primers were Forward 5'- ACTAGTGGAAGGGGGAGCACCAGTTTG-3', which adds a 5' SpeI cut site to the fragment, and Reverse 5'-GCGGCCGCTCGCTGTCGGAGGAAGTGAGG-3', which adds a NotI restriction site to the 3' end of the fragment. PCR products were cloned into the pCR-TOPO vector (Invitrogen). They were then sequenced using M13 Forward and M13 Reverse primers to ensure incorporation of the proper PCR fragment. The 5' fragment was subcloned using XhoI and HindIII restriction enzymes into pBC-CAT/HPT, which contains the CAT gene from pT/230 and the HPT gene from pminiHXGPRT-l (9, 10). The 3' fragment was then subcloned into the resulting plasmid with SpeI and NotI, creating a 062970-KO construct (Figure 2).

TgME49_062970 complementation plasmid construction. A TgME49_062970 complementation construct was created containing the 2.5kb TgME49_062970 coding sequence. This was PCR amplified from a cDNA template synthesized from bradyzoite RNA using Phusion polymerase and primers 5'-ATGCATTGCCCCCCTTTGCTTACCGA-3',which adds a NsiI site to the 5' end of the coding sequence, and reverse primer 5'-GGTTAATTAAGGCGCGTAGTCTGGGACGTCGTATGGGTA CCACCACAGAGGGTTGTCCG-3'. The reverse primer contains a PacI site from 5'-GGTTAATTAAGG-3' followed by an HA-tag from 5' –

CGCGTAGTCTGGGACGTCGTATGGGTA-3', and then the 3' end of the TgME49_062970 coding sequence, 5'- CCACCACAGAGGGTTGTCCG-3'.

The PCR product was cloned into pCR-TOPO and digested with PacI and NciI, from pCR-TOPO, then subcloned into PacI and NciI digested pBC SK+ (Stratagene) with dihydrofolate reductase from DHFR-TS creating a TgME49_062970 complementation plasmid (11) (Figure 2).

TgME49_111100 plasmid construction. The TgME49_111100 knockout construct was generated by PCR amplification, using *T. gondii* genomic DNA, of approximately 3.1 kb upstream of the predicted translation start site and 1.9 kb downstream of the predicted poly-A addition site using Phusion Polymerase. Upstream primers were Forward 5' -GGTACCGAGGAGGAAGTGAAGACG -3', which adds a 5' KpnI cut site to the fragment, and Reverse 5'-AAGCTTGAGCGGTAGACACGAGAC -3', which adds a HindIII 3' cut site to the 3.1kb fragment. Downstream primers were Forward 5'- TCTAGAGGGACCTTAGATCCTTGGCA-3', which adds a 5' XbaI cut site to the fragment, and Reverse 5'-GCGGCCGCTCGCTGTCGGAGGAAGTGAGG-3', which adds a NotI restriction site to the 3' end of the fragment. PCR products were cloned into the pCR-TOPO vector and sequenced using M13 Forward and M13 Reverse primers to ensure incorporation of the proper PCR fragment. The 5' fragment was subcloned using KpnI and HindIII restriction enzymes into pBC-CAT/HPT. The 3' fragment was then subcloned into the resulting plasmid with XbaI and NotI, creating a 111100-KO construct (Figure 3).

TgME49_224630 plasmid construction. The TgME49_224630 knockout construct was generated by PCR amplification, using *T. gondii* genomic DNA, of approximately 1040 bp upstream of the predicted translation start site and 712 bp downstream of the predicted poly-A addition site using Phusion Polymerase. Upstream primers were Forward

5’ -TTTGCGGCCGCCGGAGACAACTGTCCCCCAA -3’, which adds a 5’ NotI cut site to the fragment, and Reverse 5’-TTTACTAGTAGGGATCAGCGTGAAAGGGG -3’, which adds a SpeI 3’ cut site to the 1040 bp fragment. Downstream primers were Forward 5’- ATAGAGCTCCGTTTCGTGTGAGCGTCCC-3’, which adds a 5’ SacI cut site to the fragment, and Reverse 5’-TTAGGTACCGCTGACCCCGTTCACCTCTG -3’, which adds a KpnI restriction site to the 3’ end of the fragment. PCR products were cloned into the pCR-TOPO vector and sequenced using M13 Forward and M13 Reverse primers to ensure incorporation of the proper PCR fragment. The 5' fragment was subcloned using NotI and SpeI restriction enzymes into pBC-CAT/UPT, which contains the cat gene from pT/230 and the UPT gene from *p*ΔUPRT/HXGPRT (9, 12). The 3' fragment was then subcloned into the resulting plasmid with XbaI and NotI, creating a 224630-KO construct (Figure 4).

The 224630-KO construct is designed for simultaneous use with the corresponding 224630 CRISPR/CAS plasmid (Figure 6). The CRISPR/CAS technology was previously adapted for use in *T. gondii* (13). The CRISPR/CAS plasmid contains the CAS9 protein responsible for the double-stranded DNA breaks, driven under the *T. gondii* α-tubulin promoter. The plasmid also has a guide RNA region under the *T. gondii* U6 promoter. The guide RNA region must be altered for gene specificity of CAS9 double stranded DNA breaks as described in Sibley et al. David Sibley graciously provided the *T. gondii* CRISPR/CAS plasmid. The guide RNA region was altered using the Q5 site directed mutagenesis kit (New England BioLabs) according to manufactures protocol. The forward primer was as follows, 5’-GAACCGAATATGCACCTTACGTTTTAGAGCTAGAAATAGC-3’. The 20 nucleotides on the 5’ end of the primer correspond to the guide RNA. The guide RNA targets the translation start site of TgME49_224630 for cleavage by CAS9. The reverse primer was as follows, 5’-

AACTTGACATCCCCATTTAC-3'.

TgME49_269310 plasmid construction. The TgME49_269310 knockout construct was generated by PCR amplification, using *T. gondii* genomic DNA, of approximately 1093 bp upstream of the predicted translation start site and 1038 bp downstream of the predicted poly-A addition site using Phusion Polymerase. Upstream primers were, forward 5' -TATTCTAGAGAGTTCTTGATAGGTGCTCC -3', which adds a 5' XbaI cut site to the fragment, and reverse 5'-AATACTAGTCGTTTGTCGTATTGAGTGTCTTCG -3', which adds a SpeI 3' cut site to the 1038 bp fragment. Downstream primers were forward 5'-ATAGGGCCCGTGGGTACACAGTATTCTTGG -3', which adds a 5' ApaI cut site to the fragment, and reverse 5'-TAAGGTACCAGGTGATTCACTGGCTCG -3', which adds a KpnI restriction site to the 3' end of the fragment. PCR products were cloned into the pCR-TOPO vector and sequenced using M13 Forward and M13 Reverse primers to ensure incorporation of the proper PCR fragment. The 5' fragment was subcloned using NotI and SpeI restriction enzymes into pBC-CAT/UPT. The 3' fragment was then subcloned into the resulting plasmid with XbaI and NotI, creating a 269310-KO construct (Figure 5).

The 269310-KO construct was also designed for simultaneous use with the corresponding 224630 CRISPR/CAS plasmid, as described above (Figure 6). The guide RNA region was altered using the Q5 site directed mutagenesis kit (New England BioLabs) according to manufactures protocol. The forward primer was as follows, 5'-TGATAACGCCTTTGCATGTAGTTTTAGAGCTAGAAATAGC-3'. The 20 nucleotides on the 5' end of the primer correspond to the guide RNA. The guide RNA targets the translation start site of TgME49_269310 for cleavage by CAS9. The reverse primer was as follows, 5'-AACTTGACATCCCCATTTAC-3'.

References

1. **Dubey JP, Lindsay DS, Speer CA.** 1998. Structures of Toxoplasma gondii tachyzoites, bradyzoites, and sporozoites and biology and development of tissue cysts. Clin Microbiol Rev **11:**267-299.
2. **Jones JL, Dubey JP.** 2012. Foodborne toxoplasmosis. Clin Infect Dis **55:**845-851.
3. **Auweter SD, Oberstrass FC, Allain FH.** 2006. Sequence-specific binding of single-stranded RNA: is there a code for recognition? Nucleic Acids Res **34:**4943-4959.
4. **Blackshear PJ.** 2002. Tristetraprolin and other CCCH tandem zinc-finger proteins in the regulation of mRNA turnover. Biochemical Society transactions **30:**945-952.
5. **Lai WS, Carballo E, Thorn JM, Kennington EA, Blackshear PJ.** 2000. Interactions of CCCH zinc finger proteins with mRNA. Binding of tristetraprolin-related zinc finger proteins to Au-rich elements and destabilization of mRNA. J Biol Chem **275:**17827-17837.
6. **Suvorova ES, White MW.** 2014. Transcript maturation in apicomplexan parasites. Curr Opin Microbiol **20:**82-87.
7. **Hendriks EF, Robinson DR, Hinkins M, Matthews KR.** 2001. A novel CCCH protein which modulates differentiation of Trypanosoma brucei to its procyclic form. The EMBO journal **20:**6700-6711.
8. **Pfaffl MW.** 2001. A new mathematical model for relative quantification in real-time RT-PCR. Nucleic Acids Res **29:**e45.
9. **Soldati D, Boothroyd JC.** 1995. A selector of transcription initiation in the protozoan parasite Toxoplasma gondii. Molecular and cellular biology **15:**87-93.
10. **Donald RG, Carter D, Ullman B, Roos DS.** 1996. Insertional tagging, cloning, and expression of the Toxoplasma gondii hypoxanthine-xanthine-guanine phosphoribosyltransferase gene. Use as a selectable marker for stable transformation. J Biol Chem **271:**14010-14019.
11. **Donald RG, Roos DS.** 1993. Stable molecular transformation of Toxoplasma gondii: a selectable dihydrofolate reductase-thymidylate synthase marker based on drug-resistance mutations in malaria. Proc Natl Acad Sci U S A **90:**11703-11707.
12. **Donald RG, Roos DS.** 1998. Gene knock-outs and allelic replacements in Toxoplasma gondii: HXGPRT as a selectable marker for hit-and-run mutagenesis. Mol Biochem Parasitol **91:**295-305.
13. **Shen B, Brown KM, Lee TD, Sibley LD.** 2014. Efficient gene disruption in diverse strains of Toxoplasma gondii using CRISPR/CAS9. mBio **5:**e01114-01114.

Table 1. Comparison of fold changes between acute and chronic infection for *T. gondii* CCCH zinc fingers.

gene ID	RNAseq fold change (Chronic vs Acute)	qPCR fold change (normalized to tub1A)
TGME49_224630	169	53
TGME49_262970	34	79
TGME49_311100	5.7	6.1

Fold change of *T. gondii* specific CCCH zinc fingers were determined between acute and chronic samples using RNAseq and qPCR techniques. The first column is the gene ID found on ToxoDB.org. The second column is the fold change of the normalized FPKM values between chronic and acute infection samples. The third column is the fold change between chronic and acute samples as determined by the ΔΔCT method. The CCCH zinc finger transcript levels were normalized to *T. gondii* tub1A transcripts.

Table 2. Summary and description of constructs.

name	(+) selectable drug	(-) selectable drug	# of attempts	Strain (number of attempts)	In combination with CRISPR/CAS (number of attempts)	Outcome
TgME49_062970 knockout	chloramphenicol	6-TX	4	TGME49ΔHPT(3) KU80 (1)	Yes(1)	Random insertion
TgME49_111100 knockout	chloramphenicol	6-TX	3	TGME49ΔHPT (2) KU80 (1)	No	Random insertion
TgME49_312480 knockout (UPT)	none	FUDR	1	TGME49ΔHPT (1)	Yes(1)	Knockout generated
TgME49_224630 knockout	chloramphenicol	FUDR	1	TGME49ΔHPT ΔUPT (1)	Yes(1)	In progress/ screening
TgME49_269310 knockout	chloramphenicol	FUDR	0	N/A	No	N/A
TgME49_062970 complementation	pyrimethamine	none	1	TGME49ΔHPT (1)	No	Parasites not viable

The first column is the name assigned to the plasmid, which includes whether the plasmid was used for generation of a knockout or for complementation of the gene of interest. The second column lists the positive selectable drug marker used for selection of parasites that successfully incorporated the construct into the genome. The third column lists the negative selectable drug marker used to screen parasites that have undergone double homologous recombination, as opposed to a single recombination event, of the target plasmid. The fourth column summarizes

the number of times the knockout or complementation of the gene of interest was attempted. The fifth column lists the strain of *T. gondii* used for the experiment followed by the number of attempts in parentheses. The sixth column signifies whether the construct was used in combination with the corresponding CRISPR/CAS plasmid, which would produce double stranded DNA breaks in the gene of interest. The seventh column describes the overall outcome of the attempts.

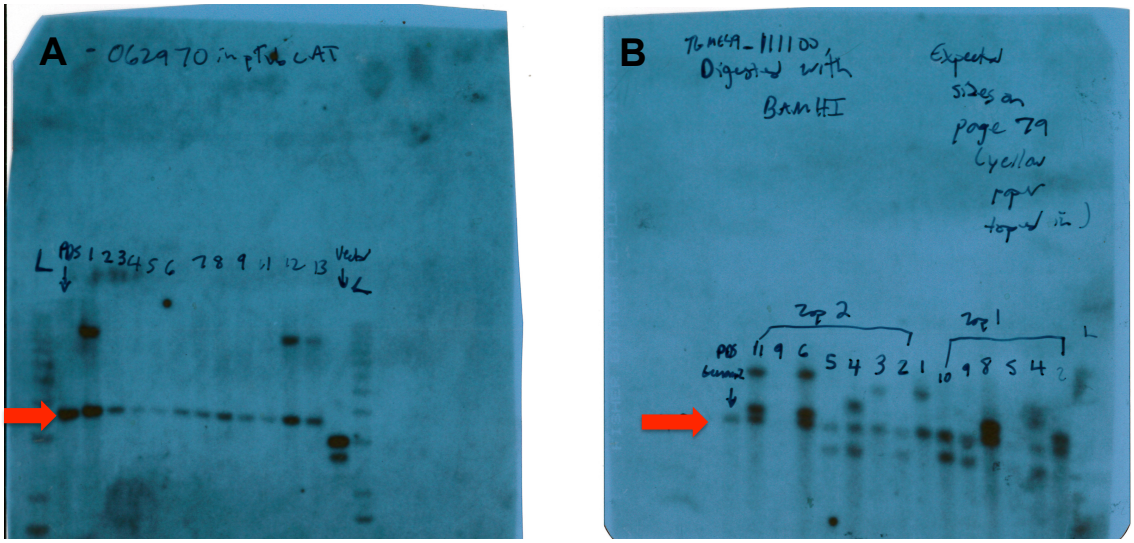

Figure 1. Southern Blot analysis of TgME49_Δ062970 and Δ111100 clones

(A) Representative film from a southern blot analysis of TgME49_062970 and (B) TgME49_111100 clones obtained from screening after electroporated parasites were treated with positive and negative drugs. Approximately 1µg of DNA was extracted from individual clones (generated from single colonies), digested with NaeI (Δ062970 clones) or BamHI (Δ 111100 clones) and ran out on a 1% agarose gel. DNA from the gel was transferred overnight onto a Nytran SPC membrane. A probe for each target was synthesized using a random primed DNA labeling kit (Roche). Red arrows indicate size of wild type bands as determined from the wild type PDS-Luc control DNA.

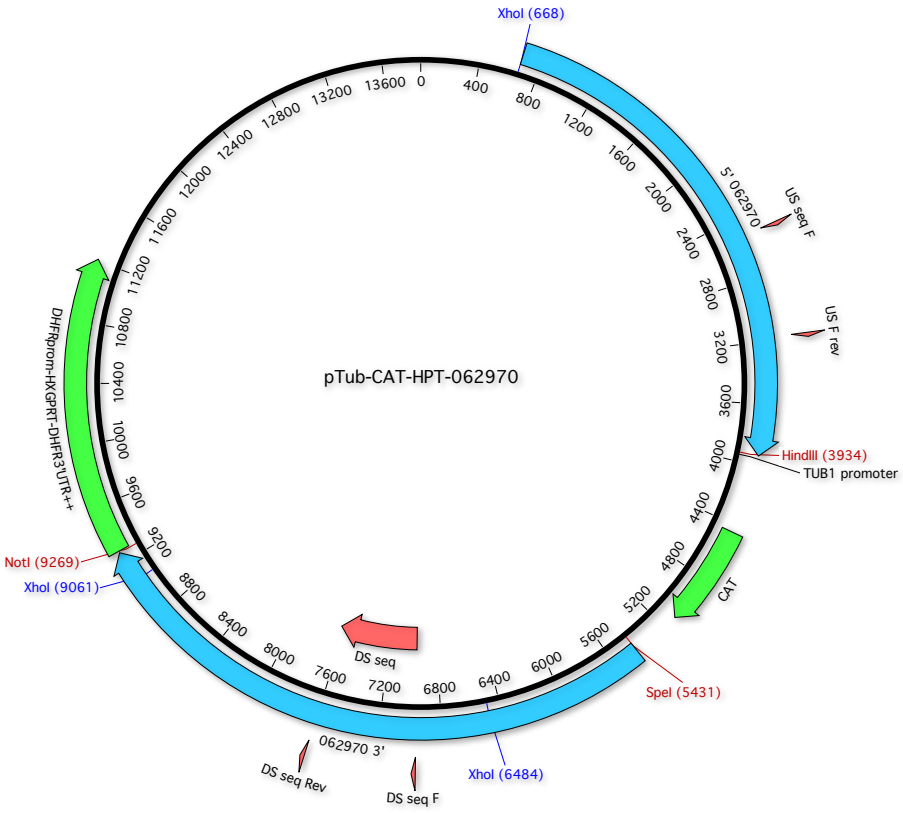

Figure 2. TgME49_062970 knockout construct.

The knockout vector was generated using backbone plasmid pBC TubCATΔHPT. The *T. gondii* tub1A promoter drives the positive selectable gene CAT, which encodes for chloramphenicol resistance (small green arrow). The negative selectable gene, HXGPRT, encodes for 6-Thioxanthene drug resistance (large green arrow). The *T. gondii* parental strain used for electroporations must be in a ΔHXGPRT background. The plasmid is altered to include approximately 3kb of both the upstream and downstream regions of TgME49_062970, depicted as light blue arrows. Restriction enzymes XhoI and HindIII were used to clone the upstream 5' flank into the backbone vector while SpeI and NotI were used for the downstream 3' flank.

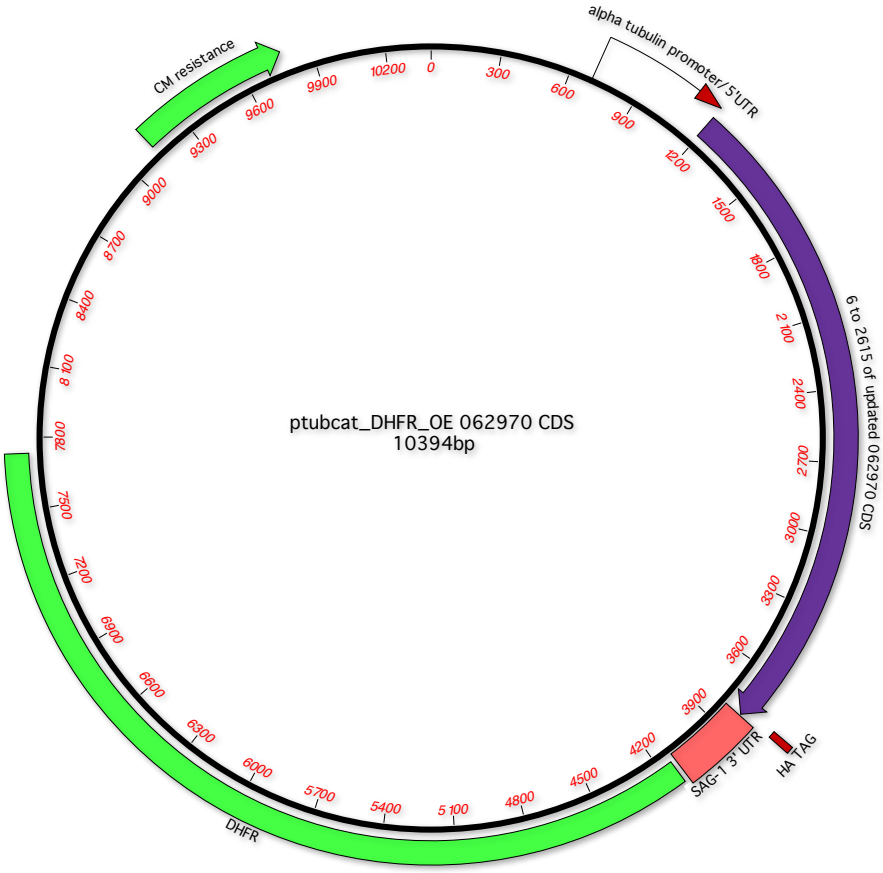

Figure 3. TgME49_062970 complementation construct.

The complementation construct was generated using the backbone plasmid pBC TubCAT DHFR. The *T. gondii* tub1A promoter drives the positive selectable gene CAT, which was excised out and replaced with the coding sequence of TgME49_062970 followed by an HA-tag. The positive selectable gene, DHFR, encodes for pyrimethamine drug resistance (large green block). Any parental strain of *T. gondii* may be used. The plasmid was altered using restriction enzymes NsiI and PacI.

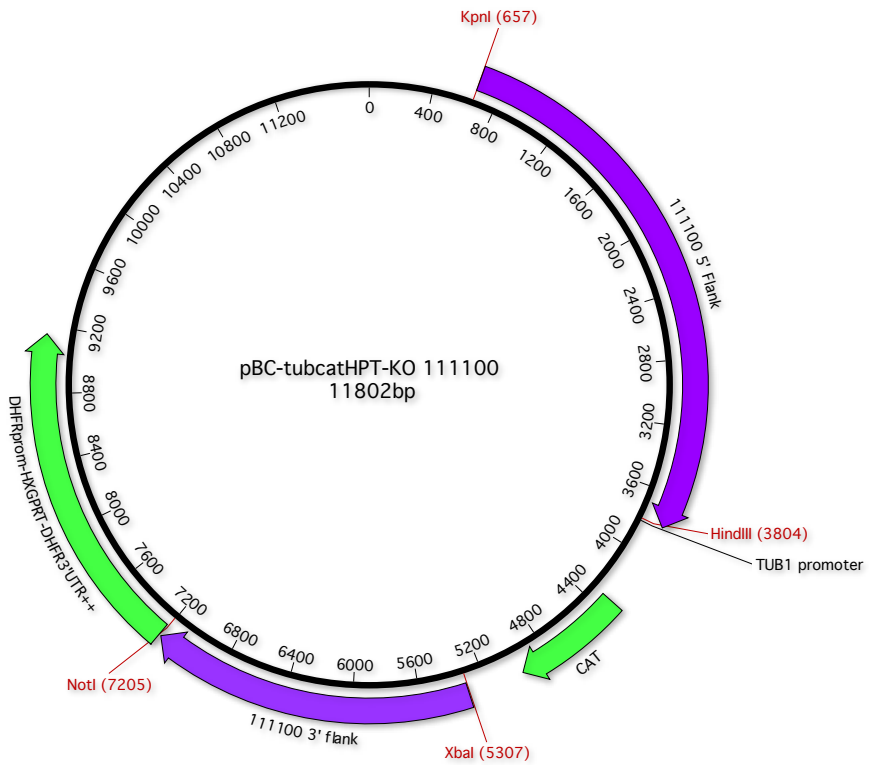

Figure 4. TgME49_111100 knockout construct.

The knockout vector was generated using backbone plasmid pBC TubCATΔHPT. The *T. gondii* tub1A promoter drives the positive selectable gene CAT, which encodes for chloramphenicol resistance (small green arrow). The negative selectable gene, HXGPRT, encodes for 6-Thioxanthene drug resistance (large green arrow). The *T. gondii* parental strain used for electroporations must be in a ΔHXGPRT background. The plasmid is altered to include approximately 2-3kb of both the upstream and downstream regions of TgME49_111100, depicted as purple arrows. Restriction enzymes KpnI and HindIII were used to clone the upstream 5' flank into the backbone vector while XbaI and NotI were used for the downstream 3' flank.

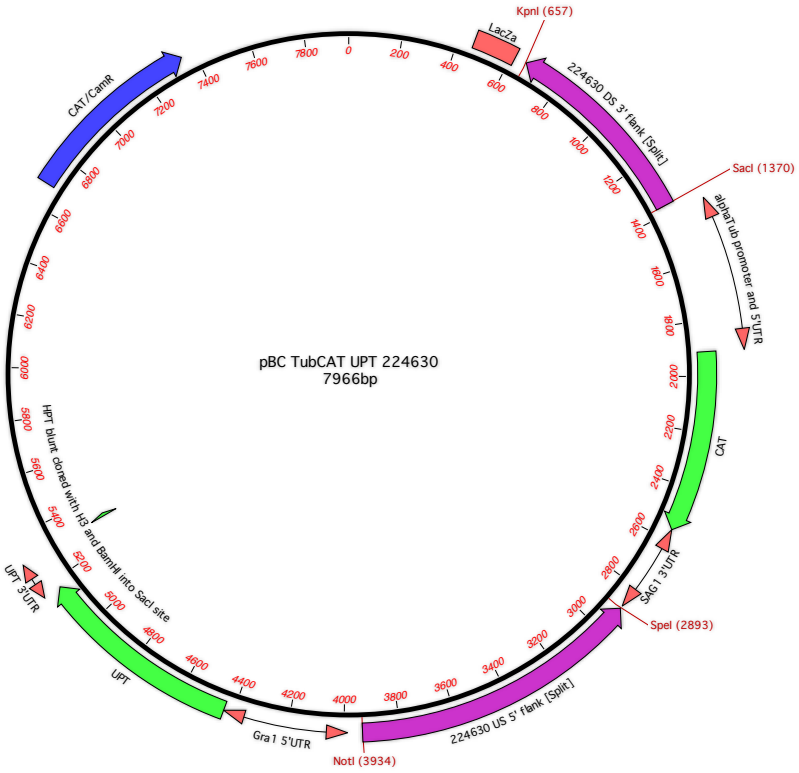

Figure 5. TgME49_224630 knockout construct.

The knockout vector was generated using backbone plasmid pBC TubCATΔUPT. The *T. gondii* tub1A promoter drives the positive selectable gene CAT, which encodes for chloramphenicol resistance (small green arrow). The negative selectable gene, UPT, encodes for FUDR drug resistance (large green arrow). The *T. gondii* parental strain used for electroporations must be in a ΔUPT background. The plasmid is altered to include approximately 1kb of both the upstream and downstream regions of TgME49_224630, depicted as pink arrows. Restriction enzymes NotI and SpeI were used to clone the upstream 5' flank into the backbone vector while SacI and KpnI were used for the downstream 3' flank.

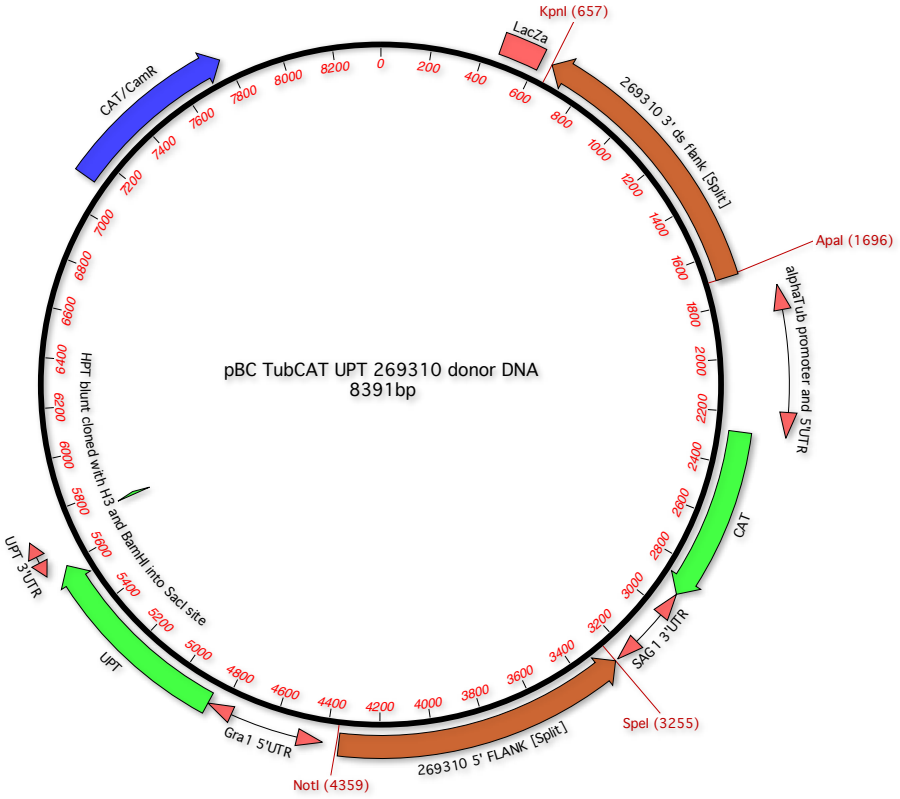

Figure 6. TgME49_269310 knockout construct.

The knockout vector was generated using backbone plasmid pBC TubCATΔUPT. The *T. gondii* tub1A promoter drives the positive selectable gene CAT, which encodes for chloramphenicol resistance (small green arrow). The negative selectable gene, UPT, encodes for FUDR drug resistance (large green arrow). The *T. gondii* parental strain used for electroporations must be in a ΔUPT background. The plasmid is altered to include approximately 1kb of both the upstream and downstream regions of TgME49_269310, depicted as orange arrows. Restriction enzymes NotI and SpeI were used to clone the upstream 5' flank into the backbone vector while ApaI and KpnI were used for the downstream 3' flank.

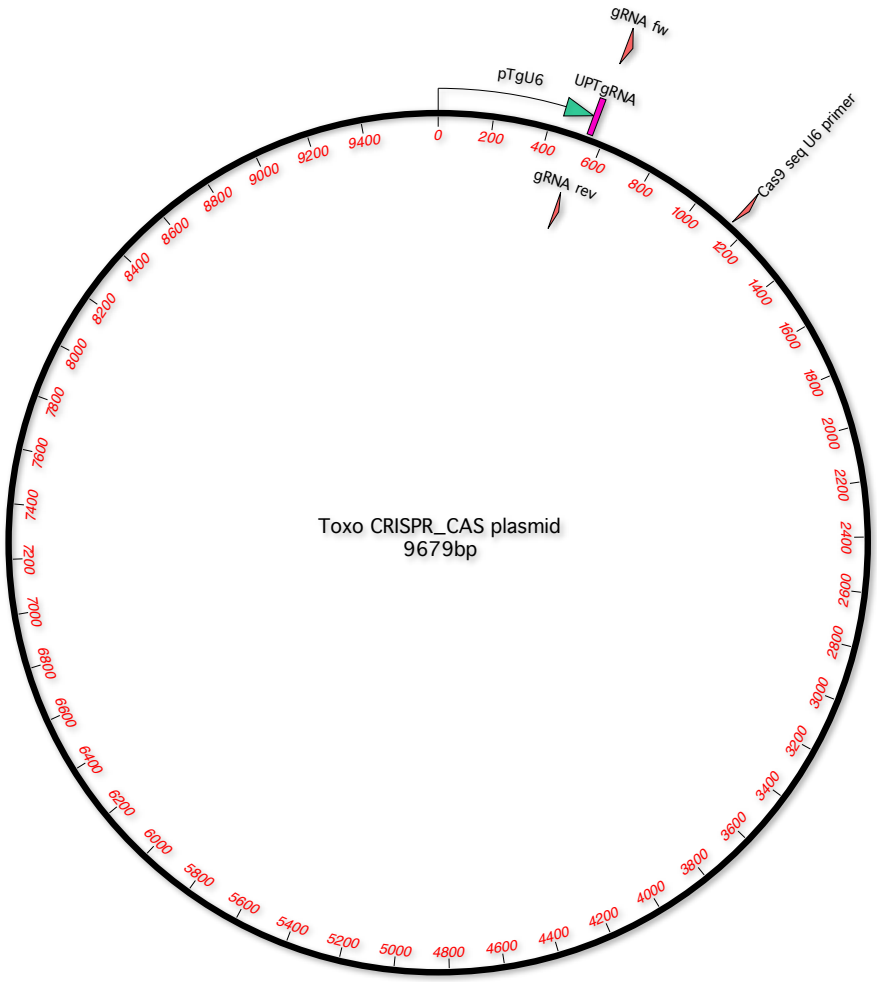

Figure 7. CRISPR/CAS9 plasmid for targeted double-stranded DNA breaks in *T. gondii*. This plasmid was graciously provided by David Sibley and is optimized for use in *T. gondii*. Briefly, the *T. gondii* SAG1 promoter drives expression of CAS9 (not depicted above, but in the backbone of the vector). The *T. gondii* U6 promoter drives the expression of the UPT guide RNA, which will complex with CAS9 and initiate double stranded DNA breaks in the *T. gondii* genome. The UPT guide RNA can be altered for targeting any gene of interest using the Q5 site directed mutagenesis kit.